

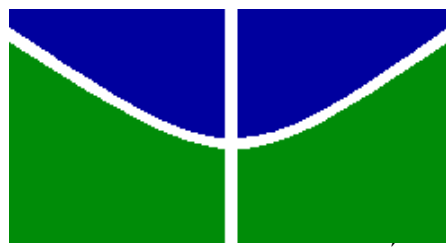


Universidade de Brasília
Faculdade de Medicina
Programa de Pós-graduação em
Patologia Molecular

**ANÁLISE DA VIA DE BIOSSÍNTESE
DE SIDERÓFORO EM
*PARACOCCIDIOIDES BRASILIENSIS***

Candidata: Marielle Garcia Silva
Orientadora: Profa. Dra. Célia Maria de Almeida Soares

Brasília, DF
2019



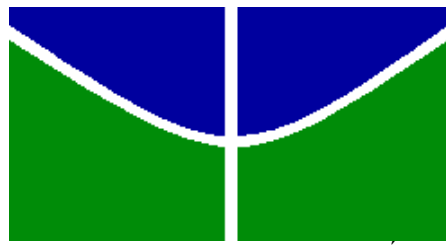
UNIVERSIDADE DE BRASÍLIA
FACULDADE DE MEDICINA
PROGRAMA DE PÓS-GRADUAÇÃO EM PATOLOGIA MOLECULAR

Tese de Doutorado

Análise da via de biossíntese de sideróforo em *Paracoccidioides brasiliensis*

Candidata: Marielle Garcia Silva
Orientadora: Prof^a. Dr^a. Célia Maria de Almeida Soares

Brasília, DF
Fevereiro de 2019



UNIVERSIDADE DE BRASÍLIA
FACULDADE DE MEDICINA
PROGRAMA DE PÓS-GRADUAÇÃO EM PATOLOGIA MOLECULAR

Tese de Doutorado

Análise da via de biossíntese de sideróforo em *Paracoccidioides brasiliensis*

Tese de Doutorado apresentada ao Programa de Pós-Graduação em Patologia Molecular da Universidade de Brasília para obtenção do Título de Doutor.

Candidata: Marielle Garcia Silva

Orientadora: Dra. Célia Maria de Almeida Soares

Brasília, DF
Fevereiro de 2019

Programa de Pós-Graduação em Patologia Molecular da Universidade de Brasília

BANCA EXAMINADORA DA TESE DE DOUTORADO

Candidata: Marielle Garcia Silva

Orientadora: Doutora Célia Maria de Almeida Soares

Membros:

Presidente: Profa. Dra. Célia Maria de Almeida Soares.

Instituto de Ciências Biológicas, Universidade Federal de Goiás.

Membro 1: Profa. Dra. Maristela Pereira.

Instituto de Ciências Biológicas, Universidade Federal de Goiás.

Membro 2: Profa. Dra. Ana Flávia Parente.

Instituto de Biologia, Universidade de Brasília.

Membro 3: Prof. Dr. Jaime Martins Santana.

Instituto de Biologia, Universidade de Brasília.

Membro Suplente: Prof. Dr. Mariana Vieira Tomazett,

Instituto de Ciências Biológicas, Universidade Federal de Goiás.

Data: 28 de fevereiro de 2019.

AGRADECIMENTOS

A Deus, pela oportunidade da vida e pela capacidade de vivê-la!

À minha orientadora, Professora Dr. Célia Maria de Almeida Soares, pela oportunidade concedida à mim de fazer parte deste grupo de pesquisa. Agradeço pela orientação e pelo estímulo para meu desenvolvimento profissional e pessoal. Obrigada pela oportunidade e por não medir esforços para oferecer os subsídios necessários para o desenvolvimento dos trabalhos!

Aos professores do Laboratório de Biologia Molecular, da Universidade Federal de Goiás, Maristela Pereira, Mirelle Garcia, Alexandre Bailão, Clayton Borges, Juliana Parente, que sempre estão dispostos a auxiliar!

Aos professores da pós-graduação em Patologia Molecular da Universidade de Brasília, pelas excelentes disciplinas ministradas. Obrigada pela contribuição no desenvolvimento profissional. Estendo meus agradecimentos aos funcionários da secretaria do Programa de Pós-graduação em Patologia Molecular, pela agilidade e disponibilidade em ajudar.

Agradeço aos meus pais, Lucelha Garcia e José Cunha (*in memorian*), por ter me concedido a vida e por não medirem esforços para me oferecer estudo de qualidade. Vocês sempre serão meu exemplo à seguir!

À minha irmã, Mirelle Garcia, que sempre me deu força e incentivo para seguir em frente até chegar ao final de cada etapa iniciada. Agradeço pela ajuda científica nunca negada! Ao meu cunhado, Alexandre Bailão, pelo apoio e incentivo!

Ao meu noivo, Matuzalem Kleyton, por me ajudar e me apoiar nos momentos mais difíceis já enfrentados. Obrigada pela compreensão, paciência ... e principalmente, pelo estímulo!

Agradeço aos meus amigos “de Brasília” Ju, Dani e Noja, pelo companheirismo durante todos estes anos de idas e vindas de Brasília. Espero que nossa amizade não acabe

junto com o finalizar de mais um ciclo em nossas vidas. Agradeço a Deus por ter colocado anjos como vocês na minha vida!

Agradeço aos amigos do LBM Lavínia, Krebs, Raísa, Amanda, Thaynara, Sam, Igor, Petito, Pedrosa por cada momento de descontração e apoio oferecido nos momentos mais difíceis. Vocês são demais!

A todos os colegas do LBM pela boa convivência, muito obrigada!

A Patrícia Lima, Luciana Casaletti e Elisa Flávia por estes vários anos de convívio, pelo saber profissional e amizade!

A todos os membros da minha família pelo apoio incondicional e palavras de incentivo!

Ao CNPq, pela concessão da bolsa de doutorado. Ao demais órgãos financiadores de pesquisa CAPES, FINEP e FAPEG.

Enfim, agradeço a todos que de alguma forma contribuíram para o desenvolvimento e finalização deste trabalho! Muito Obrigada!

SUMÁRIO

CAPÍTULO 1

1. INTRODUÇÃO.....	11
1.1 Complexo <i>Paracoccidioides</i>	11
1.2 Paracoccidioidomicose – PCM.....	14
1.3 Ferro e sua homeostase.....	16
1.4 Captação de ferro durante a infecção.....	19
1.5 <i>Paracoccidioides</i> e absorção de ferro	25

2. JUSTIFICATIVA.....	26
------------------------------	-----------

3. OBJETIVOS.....	27
3.1 Objetivo geral.....	27
3.2 Objetivos específicos.....	27

CAPÍTULO 2

Siderophores biosynthesis in <i>Paracoccidioides brasiliensis</i> : molecular characterization of SidA and SidH.....	29
---	----

CAPÍTULO 3

CONSIDERAÇÕES FINAIS.....	64
----------------------------------	-----------

PERSPECTIVAS	65
---------------------------	-----------

REFERÊNCIAS.....	66
-------------------------	-----------

ANEXO

Artigo.....	77
-------------	----

RESUMO

O complexo *Paracoccidioides* é constituído por fungos patogênicos termodimórficos, causadores da paracoccidioidomicose (PCM), micose sistêmica endêmica da América Latina. O ferro é um nutriente essencial para todos eucariotos e procariotos. No entanto, o excesso de ferro ou o seu armazenamento incorreto dentro da célula é deletério devido à produção de espécies reativas de oxigênio. O controle da homeostase do ferro é de grande importância na interação patógeno-hospedeiro, pois ambos competem por este micronutriente. Como o ferro é essencial para o sucesso da infecção, os fungos desenvolveram mecanismos de captação de alta afinidade para lidar com as condições de privação de ferro impostas pelo hospedeiro. A produção de sideróforos é um dos mecanismos que os patógenos fúngicos utilizam para aquisição de ferro. Estudos anteriores mostraram que *Paracoccidioides* apresenta genes ortólogos que codificam as enzimas necessárias para a biossíntese e transporte de sideróforos do tipo hidroxamato e que, durante a privação de ferro, esses genes são induzidos. Além disso, foi visto que *Paracoccidioides* é capaz de usar sideróforos como fonte de ferro. No presente trabalho observamos a indução de transportadores de sideróforos (MirB, MirC e Sit1) e a repressão de SidA em nível de RNA e proteína, quando *Paracoccidioides brasiliensis* foi cultivado na presença do xenosideróforo ferrioxamina B (FOB). Além disso, a atividade de SidA de *Paracoccidioides brasiliensis* também foi reduzida na presença de FOB. As enzimas da via de biossíntese de sideróforos, SidA e SidH, estão localizadas principalmente no citoplasma e na parede celular, respectivamente. Com base nesses resultados concluímos que o fungo bloqueia a síntese de sideróforos e utiliza FOB presente no ambiente como fonte de ferro.

Palavras-chave: ferro, sideróforos, SidA, SidH

ABSTRACT

The *Paracoccidioides* complex comprises thermomorphic pathogenic fungi, which cause paracoccidioidomycosis (PCM), a systemic mycosis endemic in Latin America. Iron is an essential nutrient for all eukaryotes and prokaryotes. However, iron excess or its incorrect storage inside the cell is deleterious due to the production of reactive oxygen species. The control of iron homeostasis is of great importance in the host-pathogen interaction, since both compete for this micronutrient. As iron is essential for the success of the infection, fungi have developed high affinity uptake mechanisms to cope with the iron deprivation conditions imposed by the host. The production of siderophores is one of the mechanisms that fungal pathogens use to acquire iron. Previous studies have shown that *Paracoccidioides* present orthologous genes that encode the enzymes required for the biosynthesis and transport of siderophores of the hydroxamate type and that, during iron deprivation, these genes are induced. In addition, it has been seen that *Paracoccidioides* is able to use siderophores as source of iron. In the present work we observed the induction of siderophore transporters (MirB, MirC and Sit1) and repression SidA at RNA and protein levels, when *Paracoccidioides brasiliensis* was cultivated in presence of the xenosiderophore ferrioxamine B (FOB). In addition, the activity of SidA was also reduced in the presence of FOB. The enzymes of the siderophores biosynthesis pathway, SidA and SidH, are mainly located in the cytoplasm and cell wall, respectively. Based on these results, we concluded that the fungus blocks siderophores synthesis and uses FOB present in the environment as iron source.

Key-words: iron, siderophore, SidA, SidH



Capítulo 1

1. Introdução

1.1. Complexo *Paracoccidioides*

O complexo *Paracoccidioides* é constituído por fungos patogênicos causadores da paracoccidioidomicose (PCM). Por apresentarem a capacidade de modificar sua morfologia, estes patógenos pertencem ao grupo dos fungos dimórficos, causadores da maioria das infecções sistêmicas em humanos. A temperatura é o estímulo mais evidente no dimorfismo de *Paracoccidioides* spp., por isso são chamados de fungos termodimórficos. Quando exposto à temperatura ambiente (18-23 °C) apresentam-se em forma de micélio e em temperaturas que variam entre 35 a 37 °C, apresentam-se como leveduras (BAGAGLI et al., 2006; BRUMMER et al., 1993; SAN-BLAS; NINO-VEGA; ITURRIAGA, 2002). O micélio de *Paracoccidioides* apresenta hifas hialinas, septadas, com conídios intercalares e terminais, enquanto as leveduras são arredondadas com múltiplos brotamentos com aspectos semelhantes a uma “roda de leme” (LACAZ et al., 2002; MENDES et al., 2017). A forma de conídios de *Paracoccidioides* pode ser induzida quando na presença de estresses ambientais, principalmente nutricionais (BUSTAMANTE-SIMON et al., 1985). Os conídios e o micélio são as formas infectivas, ao passo que as leveduras são a forma parasitária (BRUMMER et al., 1993; MCEWEN et al., 1987). Dessa forma, para o sucesso da infecção, o fungo, após infecção, deve transitar da forma filamentosa para forma leveduriforme. Quando não há diferenciação os isolados são considerados avirulentos (BORBA; SCHAFFER, 2002; ROONEY; KLEIN, 2002).

Paracoccidioides spp. foi identificado pela primeira vez em 1908 por Adolpho Lutz, em pacientes que apresentavam lesões na mucosa bucal (RESTREPO M, 1985). Durante muitos anos as espécies causadores da PCM foram descritas apenas como *Paracoccidioides brasiliensis*. Entretanto, com os avanços das ferramentas de biologia molecular, bioinformática e com a melhoria das técnicas de microscopia, *P. brasiliensis* foi reclassificado e atualmente é descrito como um complexo de espécies (TURISSINI et al., 2017a). Todas as espécies que atualmente constituem o gênero *Paracoccidioides* são incluídas no filo Ascomycota, ordem Onygenales e família Ajellomycetaceae. Nesta classificação são também descritas outras espécies de fungos como *Lacazia loboi*, *Blastomyces dermatitidis*, *Histoplasma capsulatum*, *Emmonsia parva* (DUKIK et al., 2017; UTEREINER; SCOTT; SIGLER, 2016).

A primeira classificação filogenética do gênero *Paracoccidioides* data de 2006, sendo realizada por Matute e colaboradores. Empregando técnicas de polimorfismo genético, uma redistribuição das espécies dentro do gênero foi sugerida. A espécie filogenética descrita como S1 seria composta por 38 isolados pertencentes ao Brasil, Venezuela, Peru e Argentina, já PS2 seria constituída por 6 isolados sendo 5 brasileiros e 1 venezuelano e PS3 teria 21 isolados colombianos. Dois anos depois, utilizando a metodologia de reconhecimento de espécies filogenéticas por concordância genealógica (GCPSR), foi demonstrado que o isolado *Pb01* é filogeneticamente diferente das outras espécies filogenéticas S1, PS2 e PS3 (CARRERO et al., 2008).

Em 2009, uma nova espécie foi sugerida dentro do gênero *Paracoccidioides*, denominada como *Pb01-like* ou *Paracoccidioides lutzii*, uma homenagem ao descobridor destes fungos (TEIXEIRA et al., 2009). Análises da distribuição geográfica das espécies revelaram que *P. lutzii* é endêmico da região Centro-Oeste brasileira, mais especificamente, nos estados do Mato Grosso e Goiás. Uma sobreposição geográfica é observada entre o *Pb01-like* e a espécie filogenética S1, sugerindo que sejam simpátricas visto que ambos os isolados vêm do estado de Goiás. O isolado *Pb18* também pertencente a S1 compartilha uma sobreposição no estado do Mato Grosso com *P. lutzii* (Figura 1)(TEIXEIRA et al., 2009).



Figura 1. Distribuição geográfica de espécies filogenéticas do gênero *Paracoccidioides*. Os isolados *Pb01-like* são encontrados quase que exclusivamente na Região Centro-Oeste do Brasil, principalmente nos estados de Mato Grosso e Goiás. A

espécie filogenética S1 é encontrada parcialmente na mesma região (Teixeira et al., 2009).

Em função de todas as análises de biologia molecular e de distribuição geográfica foi proposta uma divisão do gênero *Paracoccidioides* em duas espécies biológicas distintas descritas como *P. brasiliensis* e *P. lutzii* (BOCCA et al., 2013; SALGADO-SALAZAR; JONES; MCEWEN, 2010; TEIXEIRA et al., 2009; THEODORO et al., 2012). Alguns anos depois, sugeriu-se novamente uma reclassificação das espécies filogenéticas do complexo *P. brasiliensis*, sendo a nova espécie filogenética descrita como PS4 englobando isolados clínicos provenientes da Venezuela (BOCCA et al., 2013; TEIXEIRA et al., 2014). Em 2017, Turissini e colaboradores, utilizando-se de análises morfológicas, dados de distribuição geográfica das espécies e técnicas moleculares sugeriram um reclassificação completa das espécies filogenéticas dentro do complexo *Paracoccidioides*. Portanto, *P. brasiliensis* é empregado para descrever as espécies filogenéticas encontradas em S1, *P. restrepoensis* para PS3, *P. americana* para PS2 e *P. venezuelensis* para PS4, além da espécie já descrita como *P. lutzii* (TEIXEIRA et al., 2009). Atualmente esta é a classificação filogenética empregada para descrever as espécies deste complexo (TURISSINI et al., 2017a).

Estudos sugerem que fungos do complexo *Paracoccidioides* vivam saprobioticamente na natureza, pois já foram isolados da água, solo e plantas (RESTREPO; MCEWEN; CASTAÑEDA, 2001; TERÇARIOLI et al., 2007). Em seu nicho ecológico natural o micro-organismo se encontra na forma de micélio ou conídio. A partir do manuseio do solo pelo homem, propágulos micelianos e/ou conídios podem ser dispersos no ar e, consequentemente, serem inalados atingindo o parênquima pulmonar. Caso não haja a eliminação do fungo pelo sistema imunológico do hospedeiro, o fungo transita de micélio/conídio para leveduras, estabelecendo a infecção (ARANTES et al., 2013; BAGAGLI et al., 2008; BENARD, 2008). Além do homem, *Paracoccidioides* spp. já foi identificado em outros organismos, como tatus (BAGAGLI et al., 2003; CORREDOR et al., 2005; SANO et al., 1999), cachorro (RICCI et al., 2004; RODRIGUES DE FARIAS et al., 2011; THEODORO et al., 2012), preguiça (TREJO-CHÁVEZ et al., 2011) e em pinguins (GARCIA et al., 1993). Estes organismos não devem ser considerados reservas naturais do fungo e sim hospedeiros acidentais, pois podem ser acometidos com a doença (CONTI-DIAZ, 2007).

1.2. Paracoccidioidomicose - PCM

A doença causada pelos fungos do gênero *Paracoccidioides* é denominada de Paracoccidioidomicose (PCM) (MCEWEN et al., 1987). A PCM é uma doença inflamatória granulomatosa podendo ser uni ou multifocal (FORTES et al., 2010; MARQUES, 2012). Os pulmões são o sítio de infecção primário e, após o estabelecimento da infecção, as leveduras podem ser transportadas pelas vias hematogênica e linfática para os órgãos como linfonodos, boca, pele, fígado e baço (MENDES et al., 2017; SHIKANAI-YASUDA et al., 2017). A PCM tem elevada incidência em adultos do sexo masculino (SHIKANAI-YASUDA et al., 2006). Esse perfil se dá pela maior quantidade de homens em atividades laborais associadas ao manejo do solo e pela resistência natural feminina proveniente do hormônio β -estradiol o qual impede a transição morfológica do fungo (ARISTIZABAL; CLEMONS; STEVENS, 1998; SALAZAR; RESTREPO; STEVENS, 1988; SHANKAR et al., 2011). Além disso, comorbidades com neoplasias, HIV e tuberculose, bem como o uso de álcool e tabaco são fatores de risco para a PCM (SHIKANAI-YASUDA et al., 2017).

Clinicamente a PCM é classificada como aguda ou crônica. Na forma aguda (Figura 2) a evolução da doença é rápida, com disseminação para vários órgãos, apresentando frequentemente hepatoesplenomegalia, linfadenomegalia e lesões cutâneas. É predominante em crianças e adolescentes, correspondendo de 5 a 25% de todo quantitativo da PCM. Por outro lado, a forma crônica (Figura 3) é de progressão lenta, unifocal ou disseminada que, em sua forma mais grave, pode levar a insuficiência respiratória e síndromes neurológicas. Possui maior prevalência em adultos chegando a atingir de 76 a 96% dos pacientes (MENDES et al., 2017; SHIKANAI-YASUDA et al., 2017).

A visualização direta do fungo nos espécimes clínicos é patognomônico para o diagnóstico da PCM. Além disso, o médico assistente conta com os exames de imagem e métodos moleculares para o auxiliar no diagnóstico diferencial (LACAZ et al., 2002; SHIKANAI-YASUDA et al., 2017). Após a confirmação diagnóstica a conduta terapêutica é realizada com antifúngicos, tais como azóis, sulfamídicos e a anfotericina B (que pode ser administrada individualmente ou em associação com itraconazol, sulfametoxazol e trimetroprim) (SHIKANAI-YASUDA et al., 2017). Métodos de prevenção a PCM com imunização (TRAVASSOS; TABORDA, 2012), de diagnóstico (SYLVESTRE et al., 2018a, 2018b) e de tratamento farmacológico (SILVA et al., 2018a, 2018b) vêm sendo estudados em grande escala buscando maior sobrevida dos pacientes.



Figura 2. Forma aguda da PCM. A imagem à esquerda mostra uma criança do sexo feminino com um abscesso linfático. A imagem à direita evidencia lesões ulcerativas papulonodulares causadas por disseminação hematogênica (SHIKANAI-YASUDA et al., 2006)



Figura 3. Forma crônica da PCM. A imagem à esquerda mostra um adulto do sexo masculino com envolvimento perioral e mentoniano. A imagem à direita evidencia uma lesão vegetativa com bordas irregulares na região perianal (SHIKANAI-YASUDA et al., 2006)

Em estudo retrospectivo de 1996 a 2006, Prado e colaboradores (2009) verificaram que dentre os óbitos por fungos em paciente imunodeficientes, a PCM representou 51% das mortes por micoses, totalizando 1.853 casos. As taxas mais elevadas de hospitalização e mortalidade relacionadas a PCM se concentra principalmente nas regiões Centro-Oeste e Sudeste do Brasil (MARTINEZ, 2017). No estado do Paraná, estudos demonstraram que a taxa de mortalidade anual média foi de 3,48 casos/milhão de habitantes e no Rio de Janeiro a taxa de incidência de paracoccidioidomicose aguda foi de 8,25 casos/milhão de habitantes (BITTENCOURT; OLIVEIRA; COUTINHO, 2005; VALLE et al., 2017). Em regiões endêmicas essa média está em cerca de 9,4/100.000

habitantes/ano, uma vez que já foram registrados 40 casos/100.000 habitantes/ano durante um surto (VIEIRA et al., 2014).

1.3. Ferro e sua homeostase

A disponibilidade de ferro é crucial para sobrevivência de todos os organismos vivos, incluindo fungos, bactérias, plantas, animais e seres humanos. Essa essencialidade é explicada pelo fato de o ferro servir como cofator para várias hemoproteínas e proteínas não-heme contendo ferro, como enzimas. Este metal é importante para o transporte de oxigênio (através da hemoglobina), para produzir energia (através da transferência de elétrons na cadeia respiratória mitocondrial) e para vários processos metabólicos (replicação e reparo do DNA, regulação da expressão gênica, ciclo do ácido tricarboxílico, entre outros). Com suas propriedades redox, o ferro está disponível em dois estados de oxidação, íon ferroso (Fe^{+2}) e íon férrico (Fe^{+3}). Apesar de ser um dos elementos mais abundantes da crosta terrestre, sua biodisponibilidade é baixa sendo a deficiência de ferro o distúrbio nutricional mais comum no mundo (WHO, 2001). Por outro lado, o excesso de ferro ou seu armazenamento incorreto dentro da célula é deletério. A forma reduzida (Fe^{+2}) catalisa a produção de espécies reativas de oxigênio por meio da reação de Fenton (HALLIWELL; GUTTERIDGE, 1984). Devido suas propriedades químicas o Fe^{+2} é espontaneamente oxidado para forma Fe^{+3} na presença de oxigênio. No ambiente, o ferro está presente na forma Fe^{+3} e, por ser pouco solúvel em pH neutro, sua biodisponibilidade é baixa (KOSMAN, 2003). Diante da dualidade de efeitos advindos do ferro (importante para crescimento reprodutivo e citotóxico), a manutenção da homeostase deste micronutriente é essencial para o desenvolvimento do organismo. Essa manutenção depende de estratégias reguladas que resultem no controle da captação, utilização e armazenamento do ferro.

Em mamíferos, o descontrole da homeostase de ferro está associado a várias doenças, como anemia, causada pela deficiência de ferro resultante da alteração na aquisição ou distribuição, e danos oxidativos nos tecidos, causados pelo excesso de ferro obtido da absorção excessiva ou utilização incorreta. Para atingir a homeostase de ferro estes organismos utilizam mecanismos tanto em nível sistêmico como celular. A concentração de ferro no plasma é regulada pelo hormônio hepcidina e pelo transportador ferroportina (Figura 4), presente na membrana plasmática de enterócitos, macrófagos, hepatócitos (HENTZE et al., 2010). A absorção de ferro livre da dieta ocorre pelo transportador de metal divalente 1 (DMT1) presente na membrana dos enterócitos duodenais (GUNSHIN et al., 1997), enquanto a absorção de ferro ligado ao grupo heme

ocorre independentemente (QIU et al., 2006). Como o ferro da dieta está presente na forma oxidada, precisa ser reduzido pela ferro redutase DcytB para depois ser absorvido. Após absorção, o ferro pode ser armazenado ou liberado dos enterócitos duodenais para a circulação sistêmica por meio da ferroportina. Os hepatócitos, além de armazenarem ferro, secretam hepcidina, hormônio peptídico catiônico de 25 aminoácidos que é secretado na urina. Este hormônio se liga à ferroportina na superfície das células liberadoras de ferro promovendo sua fosforilação e internalização, que leva à degradação lisossômica. Dessa forma, a inativação da ferroportina causa retenção de ferro intracelular e promove o controle de ferro no plasma (DOMENICO et al., 2017; HENTZE et al., 2010; NEMETH et al., 2004; PARK et al., 2001). No plasma, esse metal é transportado, na forma Fe^{+3} , ligado à transferrina. Essa ligação à transferrina mantém o Fe^{+3} em uma forma solúvel, facilita o transporte até as células alvo e previne a formação de radicais livres. Nas células alvo, o receptor de transferrina auxilia na aquisição do ferro ligado à esta glicoproteína (Figura 4) (HENTZE et al., 2010).

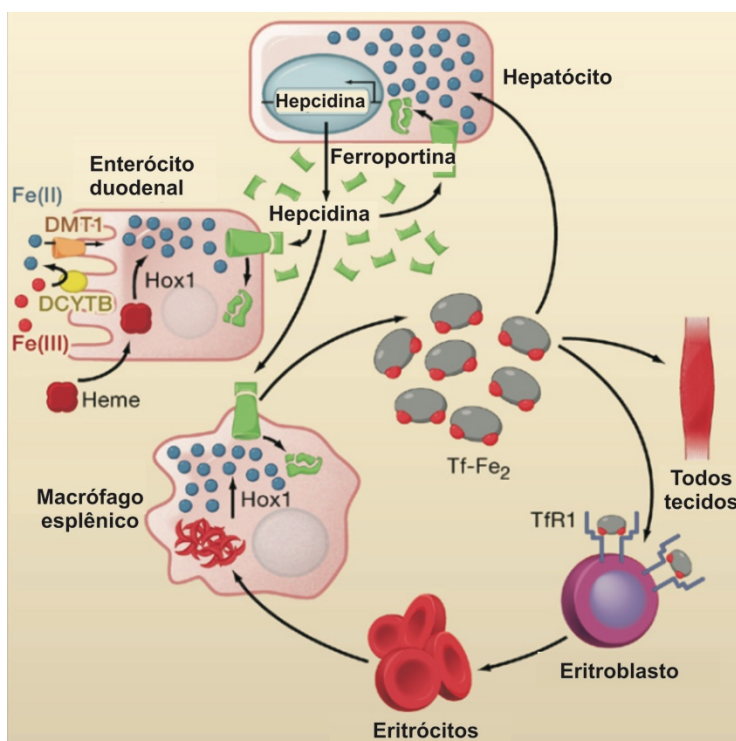


Figura 4. Homeostase de ferro em mamíferos. Regulação sistêmica de ferro quando há sobrecarga deste micronutriente no ambiente. DcytB: ferro redutase. DMT1: transportador de metal divalente 1. Tf-F₂: transferrina ligada ao ferro. TfR1: receptor de transferrina. HOX1: hemoxigenase 1. Adaptado de Hentze et al., 2010.

Durante o processo infeccioso o hospedeiro sequestra o ferro impedindo que este metal fique disponível para o patógeno. O primeiro trabalho que sugeriu este efeito foi

realizado em 1944, quando pesquisadores observaram que ao adicionar claras de ovos a culturas de vários micro-organismos o crescimento microbiano era prejudicado e que essa inibição era restaurada quando suplementavam a cultura com ferro (SCHADE; CAROLINE, 1944). A partir deste achado, vários trabalhos demonstraram o papel do ferro na imunidade do hospedeiro. Esse mecanismo de restrição de ferro aos micro-organismos invasores com intuito de reduzir a proliferação microbiana é chamado de imunidade nutricional (CASSAT; SKAAR, 2013; WEINBERG, 1975), o qual também acontece para outros minerais, como zinco e manganês (KEHL-FIE; SKAAR, 2010). As moléculas responsáveis pelo sequestro de ferro variam de acordo com o tecido no qual o micro-organismo está presente. No epitélio mucoso, as moléculas responsáveis são lactoferrina e lipocalina-2; no plasma e fluido extracelular, transferrina, interleucina-6, hepcidina e ferroportina e, nos fagócitos, lactoferrina, lipocalina-2 e Nramp-1 (*natural resistance-associated macrophage protein 1*) (GANZ, 2018).

O hormônio hepcidina, produzido pelo fígado, controla o nível de ferro no plasma através da regulação da absorção da dieta, liberação do estoque de ferro dos hepatócitos e sequestro de macrófagos (NICOLAS et al., 2001). Este hormônio é regulado por infecção (inflamação) e pelo estoque de ferro. A infecção de robalo-branco pelo agente patogênico *Streptococcus iniae* levou ao aumento de 4500 vezes a expressão de RNAm da hepcidina no fígado (SHIKE et al., 2002). Em pacientes com anemia da inflamação, resultante de infecções crônicas ou doenças inflamatórias graves, foi observado um aumento de 100 vezes na excreção de hepcidina na urina. Em pacientes com distúrbios inflamatórios menos graves esse aumento foi menor. Além disso, também foi observado aumento de 100 vezes da hepcidina urinária em pacientes com sobrecarga de ferro em função de transfusões para anemia falciforme ou mielodisplasia (NEMETH et al., 2003). Nicolas e colaboradores (2002), com objetivo de avaliar o papel da hepcidina durante processos inflamatórios, que estão relacionados ao aumento do sequestro de ferro e à diminuição da absorção intestinal, induziram o processo inflamatório em camundongos selvagens e em camundongos deficientes em hepcidina através da administração de terebintina. Foi observado indução da hepcidina e redução do ferro sérico nos camundongos selvagens. Já em camundongos deficientes em hepcidina não houve alteração do nível de ferro, comprovando que esta resposta é dependente de hepcidina. O aumento deste hormônio durante o processo inflamatório é causado por citocinas, principalmente a interleucina-6 (IL-6) (HENNIGAR; MCCLUN, 2016; NEMETH et al., 2004; NICOLAS et al., 2002). Em muitos modelos de infecção e inflamação esta citocina desempenha importante papel no combate à proliferação do microrganismo (NEMETH

et al., 2004; RODRIGUEZ et al., 2014), mas em alguns modelos outras citocinas podem assumir parcialmente este efeito estimulatório sobre a hepcidina (GARDENGHI et al., 2014). Todo este processo de sequestro de ferro, na tentativa de impedir o processo infeccioso, tem como consequência a anemia da inflamação e é responsável pela disponibilidade limitada deste metal para as células progenitoras eritróides (eritropoiese restrita ao ferro) (GANZ; NEMETH, 2009; THEURL et al., 2009). A Figura 5 apresenta o mecanismo de sequestro de ferro pelo hospedeiro.

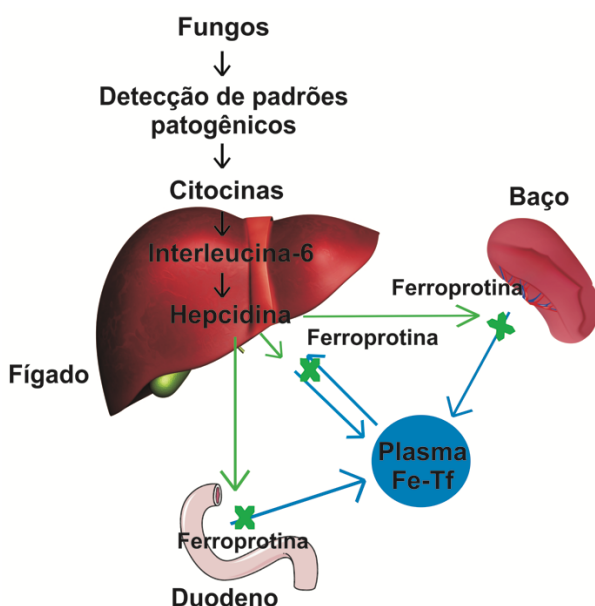


Figura 5. Mecanismo geral de limitação de ferro pelo hospedeiro. Regulador inflamatório, via reguladora de ferro e fluxo de ferro. Modificado de Ganz et al., 2018.

A restrição de ferro também ocorre quando os patógenos são fagocitados. Citocinas pró-inflamatórias promovem a redução da expressão do receptor de transferrina na superfície dos fagócitos e induzem a expressão de Nramp-1 (APPELBERG, 2006). Nramp-1 é um transportador de íons metálicos divalentes, que durante a fagocitose, transporta o ferro do fagossomo para o citosol. Neste compartimento o ferro é armazenado pela ferritina (GRUENHEID et al., 1997). A perda da função deste transportador reduz a resposta inflamatória à infecção e, consequentemente, reduz a proteção contra os efeitos patológicos do microrganismo invasor (VALDEZ et al., 2009).

1.4. Captação de ferro durante a infecção

Diante da condição de limitação de nutriente imposta pelo hospedeiro, microrganismos patogênicos desenvolveram mecanismos especializados para obter ferro durante infecções. Três diferentes mecanismos para aquisição de ferro já foram

identificados: redução de Fe⁺³ para Fe⁺² (também conhecido como via redutiva), captação e degradação do heme e absorção de Fe⁺³ mediada por quelantes específicos (sideróforos). Dentre estes mecanismos, a captação de ferro mediada por sideróforos e a via redutiva são destacados como sistemas de captação de ferro de alta afinidade. Já a captação e degradação do heme representa uma fonte especial de ferro normalmente encontrada no hospedeiro (HAAS; EISENDLE; TURGEON, 2008).

Em pH fisiológico e em presença de oxigênio os íons Fe⁺³ são insolúveis. Dessa forma, para melhor absorção do metal, é necessária a redução para Fe⁺² para que o ferro torne-se solúvel. A redução do Fe⁺³ ocorre pela ação de redutases férricas presentes na superfície celular. Após redução, o Fe⁺² pode ser transportado diretamente para dentro da célula ou passa por um processo de re-oxidação (Fe⁺² para Fe⁺³) conhecido como ferroxidação (KOSMAN, 2003). O Fe⁺³ derivado de uma reação de ferroxidase é ligado a uma permease de ferro de alta afinidade que está associada à membrana plasmática fúngica por uma ferroxidase (KWOK; SEVERANCE; KOSMAN, 2006; ZIEGLER et al., 2011). Em *Cryptococcus neoformans* (JUNG et al., 2009) e *Candida albicans* (KNIGHT et al., 2005) foi observado que a deleção de genes relacionados à via redutiva promoveu redução de virulência.

A maior parte do ferro no corpo humano está ligado à hemoglobina, nos eritrócitos. Dessa forma, fungos patogênicos desenvolveram mecanismos para utilizar o ferro complexado à hemoglobina. Primeiramente, a hemoglobina é internalizada em vesículas endocíticas com o auxílio de receptores de superfície. Nas vesículas, o Fe⁺² é liberado após a extração e degradação do grupo heme por uma heme oxigenasse (PENDRAK et al., 2004; WEISSMAN et al., 2008; WEISSMAN; KORNITZER, 2004). Em *Candida tropicalis* foi realizado um estudo com o objetivo de avaliar a atividade hemolítica e a expressão gênica da heme oxigenase após o crescimento na privação de ferro e na presença de hemoglobina e eritrócitos. Foi observado um aumento da atividade hemolítica e da expressão gênica quando *C. tropicalis* foi cultivada na presença de hemoglobina ou eritrócitos. Com estes dados os autores sugeriram que a hemoglobina tem efeito positivo na produção do fator hemolítico e da expressão gênica relacionada à captação de ferro (FRANÇA; FURLANETO-MAIA; FURLANETO, 2017). Em condições em que a única fonte de ferro é a hemoglobina, foi observado o crescimento de *Histoplasma capsulatum* e *C. neoformans* mostrando que estes dois patógenos também são capazes de utilizar o grupo heme como fonte de ferro (FOSTER, 2002; JUNG et al., 2008).

A síntese e captação de sideróforos é outro mecanismo não redutivo de captação de ferro de alta afinidade utilizada por fungos patogênicos. Estas moléculas são compostos de baixo peso molecular que apresentam alta afinidade por íons férricos (NEILANDS, 1993). A alta afinidade permite estes compostos competir com a transferrina do hospedeiro por Fe^{+3} (HISSEN et al., 2004). Sideróforos, do grego “portadores de ferro”, solubilizam o Fe^{+3} extracelular e o fornecem para a célula. Na maioria dos fungos, também funcionam como moléculas armazenadoras de ferro (MATZANKE et al., 1987). Estes compostos podem ser classificados, dependendo da natureza química dos motivos que doam os ligantes de oxigênio para o ferro, em três grupos principais: carboxilatos, catecós e hidroxamatos (MIETHKE; MARAHIEL, 2007). A maioria dos sideróforos fúngicos pertencem ao grupo dos hidroxamatos. As exceções são os sideróforos produzidos por *Mucorales* e *Penicillium biali* que pertencem ao grupo dos carboxilatos e catecós, respectivamente (CAPON et al., 2007; THIEKEN; WINKELMANN, 1992). Sideróforos hidroxamato, derivados do aminoácido ornitina, podem ser agrupados em quatro famílias: coprógenos, fusarininas, ferricromos e ácido rodotorúlico (HAAS; EISENDLE; TURGEON, 2008). A Figura 6 apresenta os sideróforos representativos de cada família (HAAS, 2014). O processo desde à síntese até a captação do complexo sideróforo- Fe^{+3} ocorre na seguinte sequência: síntese, secreção, ligação ao Fe^{+3} e captação por transportadores presentes na membrana celular (WINKELMANN, 2002).

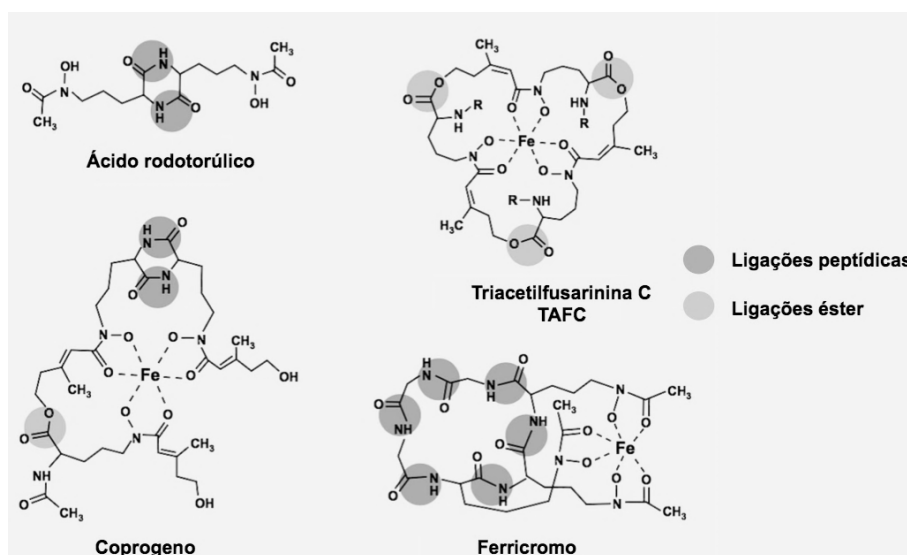


Figura 6. Representação química de sideróforos do tipo hidroxamato. TAFC é formada por ligações éster, enquanto ácido rodotoúlico e ferricromos apresentam somente ligações peptídicas entre os grupos hidroxamatos. Caprogenos apresentam ambos os tipos de ligações. Adaptado de Haas et al, 2008.

A via de biossíntese de sideróforos é bem caracterizada em *Aspergillus fumigatus* (BLATZER et al., 2011). Este fungo produz quatro sideróforos, sendo dois extracelulares pertencentes à família das fusarininas e dois intracelulares da família dos ferricromos. Fusarinina C (FsC) e seu derivado triacetilfusarinina (TAFC), representantes das fusarininas, são produzidos para absorção de ferro. Ferricrocina (FC) é sintetizada para distribuição e armazenamento de ferro em hifas e hidroxiferricrocina (HFC), para armazenamento do metal em conídios (SCHRETTL et al., 2007). A via biossintética de sideróforos do tipo hidroxamato em *A. fumigatus* é apresentada na Figura 7. A síntese inicia com a enzima L-ornitina N⁵-monooxigenase (SidA), que promove a hidroxilação da ornitina. Ortólogos ao SidA já foram identificados em outros microrganismos, como *Histoplasma capsulatum* (HWANG et al., 2008), *A. nidulans* (EISENDLE et al., 2003), *Aureobasidium pullulans* (CHI et al., 2012) e *Magnaporthe grisea* (HOF et al., 2009). SidA e enzimas biossintéticas de sideróforos de bactérias, como lisina-hidroxilase IucD de *Escherichia coli* e ornitina N⁵-monooxigenase PvdA de *Pseudomonas aeruginosa*, apresentam semelhança significativas (HERRERO; LORENZO; NEILANDS, 1988; VISCA; CIERVO; ORST, 1994). A atividade da L-ornitina monooxigenase depende da presença de oxigênio, FAD e NADPH como co-fatores (MEI; BUDDET; LEONG, 1993).

Após hidroxilação da ornitina, ocorre a formação do grupo hidroxamato. Esta etapa consiste na adição de um grupo acil na hidroxiornitina e é catalisada pela ação de duas transacilases. Para formação de sideróforos do tipo fusarinina, a transacilase SidF transfere anidromevalonil para N⁵-hidroxiornitina. O anidromevalonil é obtido a partir do mevalonato pela ação de duas enzimas SidI (acil-CoA sintetase) e SidH (enoil-CoA hidratase), que promovem a ligação da coenzima A ao mevalonato (CoA) e a desidratação do mevalonil-CoA, respectivamente. Dessa forma, existe uma ligação entre as vias de síntese de ergosterol e de sideróforo. Sideróforos intracelulares do tipo ferricromo são formados a partir de duas enzimas, SidL e SidC. SidL, uma transacilase, catalisa a adição de acetil-CoA à N⁵-hidroxiornitina. Após a formação do grupo hidroxamato, ocorre a união destes grupos pela ação de peptídeo sintetasas não ribossômicas (NRPSs; SidD e SidC). SidD promove a união através de ligações éster e SidC através de ligações peptídicas, formando assim fusarinina C e ferricrocina, respectivamente. A partir da fusarinina C SidG promove a formação de triacetilfusarinina C (TAFC) e, por uma etapa ainda desconhecida, também ocorre a formação de hidroxiferricrocina (HFC) a partir da ferricrocina (Figura 7). Estes genes (*sidA*, *sidD*, *sidG*, *sidF*, *sidC* e *sidL*) relacionados a síntese de sideróforos, em *A. fumigatus*, estão localizados em diferentes locais nos cromossomos 1, 2 e 3 (KHAN; SINGH; SRIVASTAVA, 2017).

Em *A. fumigatus* foi observado que a linhagem mutante $\Delta sidA$ foi incapaz de sintetizar os sideróforos TAFC e ferricrocina. Em adição, o crescimento desta linhagem foi igual ao do tipo selvagem em meio rico, mas em meio com restrição de ferro ou contendo soro humano a 10% foi incapaz de crescer. Em modelo murino de aspergilose invasiva, a linhagem mutante $\Delta sidA$ demonstrou ser desprovida de virulência, indicando a importância de *sidA* durante a infecção (HISSEN et al., 2005). Redução da virulência também foi observada em mutantes para $\Delta sidF$, $\Delta sidC$, $\Delta sidD$, $\Delta sidG$, $\Delta sidH$ e $\Delta sidI$ (SCHRETTL et al., 2007; YASMIN et al., 2011). Em *H. capsulatum*, resultados similares foram observados. A deleção do ortólogo de *sidA*, *sidI*, resultou na diminuição do crescimento em condições de baixas concentrações de ferro e perda de produção de sideróforos. Além disso, apresentaram comprometimento da virulência em camundongos (HWANG et al., 2008). Dessa forma, em condições de restrição de ferro, a deficiência na produção de sideróforos reduz o crescimento e a virulência do patógeno (SCHRETTL et al., 2007).

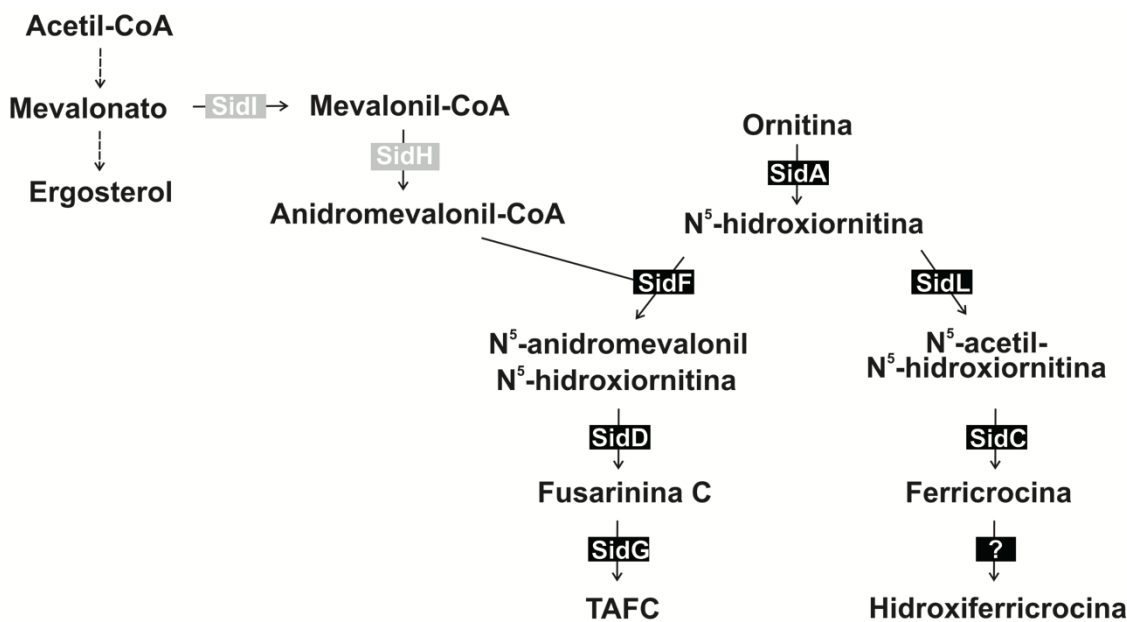


Figura 7. Via de biossíntese de sideróforos em *A. fumigatus*. Enzimas destacadas em cinza representam a conexão entre a via de síntese do ergosterol e a de sideróforo. Adaptado de Yasmin et al, 2012

Após ligação ao ferro, o complexo ferro-sideróforo liga-se a transportadores específicos na membrana celular fúngica para ser transportado para o citosol. Estes transportadores geralmente pertencem à subfamília SIT (*Siderophore-iron transporter*) e superfamília MFS (*Major facilitator superfamily*) (PAO; PAULSEN; SAIER, 1998). Mesmo em espécies fúngicas que não produzem sideróforos, como *Saccharomyces*

cerevisiae, *Candida* spp e *C. neoformans*, estes transportadores são sintetizados (HAAS; EISENDLE; TURGEON, 2008; JUNG et al., 2008; NEVITT; THIELE, 2011; PHILPOTT; PROTCHENKO, 2008). Estudos tem mostrado que cada microrganismo possui quantidade variável de transportadores e que cada transportador apresenta especificidade de substrato variável. *S. cerevisiae* possui quatro transportadores com especificidade para quatro tipos de sideróforos. Já *C. albicans* produz somente um transportador com especificidade ampla (ARDON et al., 2001). *C. glabrata* também produz um único transportador, Sit1, que é essencial para a sobrevivência do fungo em macrófagos (NEVITT; THIELE, 2011). *A. nidulans* tem pelo menos três transportadores (MirA, MirB e MirC) com diversas especificidades de substrato (HAAS et al., 2003). A habilidade de utilizar diferentes tipos de sideróforos, até mesmo xenosideróforos, pode ser reflexo da expressão de vários transportadores pelo microrganismo. *A. nidulans*, além de transportar os sideróforos nativos (ferricrocina e TAFC) também é capaz de captar xenosideróforos (enterobactina e ferrioxamina B) (OBEREGGER; SCHOESEER; ZADRA, 2001).

A utilização da terapia de quelação de ferro com deferoxamina aumenta o risco de desenvolvimento de murcomicose, causada por fungos do gênero *Rhizopus* (BOELAERT et al., 1994). Apesar de atuar como quelante de ferro em relação ao hospedeiro, a deferoxamina é utilizada como xenosideróforo por *Rhizopus*. Fungos pertencentes à este gênero são capazes de remover o ferro do quelante (BOELAERT et al., 1993; LOCHT; BOELAERT; SCHNEIDER, 1994). Assim, a administração de deferoxamina piora a sobrevivência de animais com mucormicose (ABE et al., 1990; BOELAERT et al., 1994; LOCHT; BOELAERT; SCHNEIDER, 1994).

Após captação, as ligações do complexo ferro-sideróforo em *A. fumigatus* e *A. nidulans* são hidrolisadas no citosol. EstA, EstB e SidJ são esterases específicas para enterobactina, TAFC e FSC, respectivamente, que melhoram a hidrólise, mas não são essenciais (GRUNDLINGER et al., 2013; KRAGL et al., 2007; OBEREGGER et al., 2002). Em mutantes para EstB foi observada redução do crescimento, da transferência de ferro de TAFC para o metabolismo e para o sideróforo intracelular FC (KRAGL et al., 2007). Em *S. cerevisiae*, ferricromos e ferrioxamina B acumulam-se no citoplasma e vacúolos, respectivamente (FROISSARD et al., 2007; MOORE; KIM; PHILPOTT, 2003).

1.5. *Paracoccidioides* e absorção de ferro

Ferro, assim como para outros organismos, também é importante para o desenvolvimento de fungos do gênero *Paracoccidioides*. Estudos mostraram que este micronutriente é essencial para o dimorfismo (CANO et al., 1994) e que a sobrevivência de leveduras é suprimida em monócitos humanos tratados com o quelante de ferro deferoxamina (DIAS-MELICIO et al., 2005). Por outro lado, a susceptibilidade de camundongos à infecção por *Paracoccidioides* sp. é aumentada quando estes animais são tratados com ferro exógeno (PARENTE et al., 2011). Análise proteômica mostrou que, em condições de restrição de ferro, ocorre um remodelamento do metabolismo fúngico, relacionado principalmente à produção de energia. Assim, em resposta à falta de ferro, o fungo aumenta a atividade glicolítica para compensar a diminuição das vias aeróbicas, que são dependentes de ferro. Este remodelamento pode ser uma estratégia de sobrevivência utilizada por *Paracoccidioides* sp. em ambientes de restrição de ferro, como durante a infecção no hospedeiro. A alteração das enzimas envolvidas nos processos energéticos observadas em nível proteômico também foram detectadas em nível transcripcional em leveduras de *Paracoccidioides* sp. recuperadas de baços de camundongos (PARENTE et al., 2011).

Para adquirir ferro em condições de escassez do metal, fungos do gênero *Paracoccidioides* podem utilizar a via redutiva (Fe^{+3} para Fe^{+2}) e a via de captação de sideróforos. Desta forma, esses fungos são capazes de sintetizar e utilizar sideróforos como fonte de ferro (BAILÃO et al., 2015; SILVA-BAILÃO et al., 2014; SILVA et al., 2011). Trabalho realizado por nosso grupo demonstrou que *Paracoccidioides* spp. possui todos genes ortólogos necessários para síntese (*sidA*, *sidF*, *sidC*, *sidD*, *sidH* e *sidI*) e captação (*sit1*, *mirB* e *mirC*) de sideróforos do tipo hidroxamato (SILVA-BAILÃO et al., 2014; SILVA et al., 2011). A expressão destes genes é induzida sob restrição de ferro, e em tal condição, os sideróforos hidroxamatos são produzidos (PARENTE et al., 2011; SILVA-BAILÃO et al., 2014). A expressão de *sidA* também foi aumentada durante infecção em macrófagos, evidenciando a restrição de ferro pelo hospedeiro. Além do ácido dimerúmico extracelular, *Paracoccidioides* spp. também é capaz de utilizar ferrioxamina B (FOB) como fonte de ferro. Exposição a este xenosideróforo aumenta a sobrevivência do fungo após a fagocitose por macrófagos ativados (SILVA-BAILÃO et al., 2014).

2. JUSTIFICATIVA

A PCM é uma micose sistêmica, causada por fungos pertencentes ao complexo *Paracoccidioides*, com alta incidência no Brasil e que afeta principalmente trabalhadores rurais. A capacidade do fungo de provocar a infecção está relacionada tanto à biologia do próprio fungo quanto a de seu hospedeiro humano. Desta forma, conhecer como o agente etiológico age para causar a infecção é a base para entender a interação patógeno-hospedeiro. Durante o processo infeccioso o hospedeiro restringe os micronutrientes na tentativa de impedir a evolução da infecção. Entre estes micronutrientes está o ferro que é importante para vários processos biológicos da célula. Em *Paracoccidioides* spp., estudos já mostraram a necessidade deste micronutriente para o seu desenvolvimento. Além disso, já foi apresentado que fungos pertencentes à este complexo possuem mecanismos, como produção de sideróforos e via redutiva de captação de ferro, para tentar driblar a condição de restrição de nutriente imposta pelo hospedeiro. Foi observado também que, além de produzir sideróforos, conseguem utilizar xenosideróforos presentes no ambiente que apresenta restrição de ferro. Dessa forma, é importante saber como o fungo se comporta na presença de moléculas que irão auxiliar à sua sobrevivência em ambiente com restrição de ferro. As informações obtidas poderão auxiliar no melhoramento do tratamento da doença.

3. OBJETIVOS

3.1 Objetivo Geral

Analisar a expressão de sideróforos em *P. brasiliensis* na presença do xenosideróforo ferrioxamina B (FOB).

3.2 Objetivos Específicos

- Avaliar a expressão dos genes transportadores (*sit1*, *mirB* e *mirC*) e das enzimas da via de biossíntese de sideróforos (*sidA* e *sidH*);
- Produzir proteína recombinante e anticorpos para SidA e SidH;
- Avaliar a expressão, em nível proteico, de SidA e SidH;
- Determinar a localização celular de SidA e SidH por microscopia eletrônica de transmissão;
- Analisar a estrutura molecular das proteínas SidA e SidH;
- Verificar, em nível proteômico, a expressão proteínas relacionadas à síntese de sideróforos.



Capítulo 2

Siderophores biosynthesis in *Paracoccidioides brasiliensis*: molecular characterization of SidA and SidH

Marielle Garcia Silva^{a,b}, Lucas Nojosa Oliveira^{a,b}, Mirelle Garcia Silva Bailão^a, Juliana Santana de Curcio^a, Aparecido Ferreira de Souza^a, Raisa Melo de Lima^a, Sônia Nair Bão^c, Alexandre Melo Bailão^a, Maristela Pereira^a, Célia Maria de Almeida Soares^{a,*}

^aLaboratório de Biologia Molecular, Instituto de Ciências Biológicas, ICB II, Campus II, Universidade Federal de Goiás, Goiânia, Goiás, Brazil;

^bPrograma de Pós-graduação em Patologia Molecular, Faculdade de Medicina, Universidade de Brasília, 70910-900, Brasília, Distrito Federal, Brazil;

^cLaboratório do Microscopia, Departamento de Biologia Celular, Instituto de Ciências Biológicas, Universidade de Brasília, Brasília, Distrito Federal, Brazil

*Corresponding author

Célia Maria de Almeida Soares
Laboratório de Biologia Molecular
Instituto de Ciências Biológicas II
Câmpus Samambaia
Universidade Federal de Goiás
74690-900, Goiânia, Goiás – Brazil
Tel/Fax: +55 62 3521 1110
E-mail address: cmasoares@gmail.com

Key-words: Iron, siderophore, SidA, SidH

Abstract

Iron is an essential nutrient for all eukaryotes and prokaryotes. Since iron is essential for the success of the infection, fungi have developed high affinity uptake mechanisms for this metal to deal with the iron deprivation conditions imposed by the host. Siderophore production is one of the mechanisms that fungal pathogens use for acquisition of iron. Previous studies showed that *Paracoccidioides* present orthologue genes encoding all enzymes necessary for the biosynthesis and transport of hydroxamate type siderophores and that during iron deprivation these genes are induced. In addition, it has been seen that *Paracoccidioides* is able to use siderophores as source of iron. Here we observe, in presence of the xenosiderophore ferrioxamine B (FOB), induction of siderophores transporters (*mirB*, *mirC* and *sitI*) and repression SidA at RNA and protein levels. In addition, the activity of SidA from *Paracoccidioides brasiliensis* was also reduced in the presence of FOB. The enzymes of the siderophore biosynthesis pathway, SidA and SidH, are mainly located in the cytoplasm and cell wall, respectively. Based on these results we suggest that the fungus blocks siderophores synthesis and uses FOB present in the environment as iron source.

Introduction

Iron is an essential nutrient for growth and development of all living organisms. Due to its redox properties, this metal occurs in either of two oxidation states, ferrous ion (Fe^{+2}) and ferric ion (Fe^{+3}), which are influenced by pH and oxygen¹. In the presence of oxygen, Fe^{+2} spontaneously converts to Fe^{+3} ². Iron is indispensable for a variety of cellular processes such as respiration, the tricarboxylic acid cycle, biosynthesis of amino acids, deoxyribonucleotides, lipids and sterols. However, the excess or incorrect storage of this metal inside the cell is harmful since the reduced form (Fe^{+2}) catalyzes the production of reactive oxygen species (ROS) through the Fenton/Haber Weiss reaction^{3,4}. In this way, the maintenance of the homeostasis of this micronutrient, that is the balance between the sufficient supply of iron and the prevention of the toxicity, is essential. This is achieved by a fine tuned regulation of iron acquisition, use and storage.

In mammals, iron from diet is absorbed in the duodenal enterocytes⁵ and transported in the blood plasma bound to the glycoprotein transferrin, which has two high-affinity binding sites for Fe^{+3} . Macrophages, hepatocytes and erythroid precursors acquire

iron through the transferrin receptor. Iron that is not used in cellular processes is stored in macrophages and hepatocytes bound to proteins, such as ferritin⁶.

Since iron is essential for both the host and the pathogen, a battle between both for the acquisition of the metal is established during the infectious processes. Multiple mechanisms of the host innate immunity restrict the availability of iron in extracellular fluid and plasma to the invasive microrganisms in an attempt to prevent infection^{7,8}. Iron scarcity is also a strategy to counteract the development of intracellular pathogens. Macrophages, in response to inflammatory signs, decrease the expression of transferrin receptor and stimulate the expression of Nramp1, which transports iron from the macrophages to the cytosol^{9,10}. In the cytosol this metal is stored by ferritin.

To overcome the low availability of iron imposed by the host, microorganisms developed high affinity mechanisms for iron absorption¹¹. In fungal pathogens these mechanisms include: the reduction of Fe⁺³ to Fe⁺², the acquisition of the iron bound to the heme group and the solubilization of Fe⁺³ promoted by siderophores¹²⁻¹⁴. The first mechanism begins with extracellular reduction of Fe⁺³ to Fe⁺² by metalloreductases. After reduction, Fe⁺² is absorbed by a high affinity capture system independent of siderophore¹⁵⁻¹⁷. The use of haemoglobin/haemin as an iron source by *Candida albicans* has been widely investigated and depends on the function of proteins that share the same domain, called CFEM^{18,19}. Initially, the extracellular haemin is captured by Csa2, a secreted dimeric protein that acts as a haemophore^{20,21}. Csa2 interacts with Rbt5, another CFEM-protein present on the cell surface and promotes haemin exchange between them. Rbt5 delivers the haemin molecule to Pga7, a CFEM-protein located more internally in the cell membrane¹⁹. The haemin internalization event is concluded by the endocytic action of the ESCRT pathway and the removal of Fe³⁺ is performed by a heme oxygenase called HMX1^{22,23}. Increased hemolytic activity and gene expression of heme oxygenase was observed when *Candida tropicalis* was cultured in the presence of hemoglobin or erythrocytes. Based on these results, the authors suggested that hemoglobin has a positive effect on hemolytic factor production and gene expression related to iron uptake²⁴.

The non-reductive iron uptake is characterized by the use of siderophores, which are low molecular weight compounds binding Fe⁺³ with high affinity, solubilizing the extracellular iron for subsequent uptake²⁵. The high affinity for iron allows siderophores to compete with host transferrin for Fe⁺³²⁶. The siderophore biosynthesis pathway is well described in *Aspergillus fumigatus*. The first enzyme of hydroxamate siderophore biosynthesis pathway is L-ornithine N⁵-monooxygenase (SidA), which promotes the hydroxylation of ornithine. Transacylases and transacetylases (SidF and SidL,

respectively) promote the formation of the hydroxamate group by transferring an anhydromevalonyl or acyl group to hydroxyornithine. The attachment of the hydroxamate groups via peptide (ferricrocin -FC) and ester (fusarinine C – FSC) linkages is performed by non-ribosomal peptide synthetases, SidC and SidD, respectively. The acetyl transferase SidG promotes the formation of triacetylfusarinine C (TAFC) from FSC²⁷⁻²⁹. *A. fumigatus* also produces hydroxyferricrocin (HFC), which functions as an iron storage molecule in conidia²⁹. The pathways for the biosynthesis of siderophores and ergosterol are connected by two enzymes, acyl-CoA ligase (SidI) and enoyl-CoA hydratase (SidH)³⁰. The internalization of siderophore-iron complex is mediated by transporters (SIT – siderophore iron transporter) located on the cell surface. Sit, MirA, MirB and MirC are some of these carriers. The *Candida glabrata* genome encodes a single siderophore transporter, Sit1, which is essential for the survival of this fungus in macrophages and responsible for the transport of ferrichrome, a hydroxamate siderophore³¹. *Aspergillus nidulans*, on the other hand, has at least three SIT transporters (MirA, MirB and MirC) with diverse substrate specificities. MirA carries the bacterial siderophore enterobactin, while MirB transports the native siderophore TAFC^{32,33}.

Studies have shown that siderophore biosynthesis is essential for virulence in pathogenic fungi. The *A. fumigatus* ΔsidA strain is devoid of virulence in a murine model of aspergillosis²⁸ while ΔsidF, ΔsidC, ΔsidD, ΔsidG, ΔsidH and sidI strains were partially virulent^{29,30}. Similar results were observed in *Histoplasma capsulatum*. Deletion of sidI, sidA ortholog, promoted decreased fungal growth within macrophages and compromised virulence in mice³⁴.

Siderophores are also produced by fungi of the *Paracoccidioides* genus that cause paracoccidioidomycosis (PCM), a systemic mycosis³⁵. The disease is restricted to Latin America³⁶ and the country with the highest rates of PCM is Brazil³⁷. *Paracoccidioides* genus includes thermodimorphic species which grow as mycelia in the environment and as yeast cells in host tissues³⁵. After inhalation of conidia or mycelial propagules, these reach the pulmonary alveoli of the host and differentiate into yeast, thus initiating the infectious process³⁸.

Fungi of the *Paracoccidioides* genus can use the reductive (Fe⁺³ to Fe⁺²) and siderophore uptake pathways to acquire iron under conditions of metal shortage. In this way, those fungi are able to synthesize and use siderophores as a source of iron³⁹⁻⁴¹. We have previously demonstrated that *Paracoccidioides* spp. present genes orthologous to those related to hydroxamate siderophore production (sidA, sidF, sidC, sidD, SidH and sidI) as well as siderophore uptake (sit1, mirB and mirC)^{39,41}. All of them are up-

regulated under iron restriction and, in such condition, hydroxamate siderophores are produced^{39,42}. Expression of *sidA* is also induced during macrophage infection, evidencing iron restriction by the host. Besides the extracellular siderophore dimerumic acid, *Paracoccidioides* spp. is also able to utilize ferrioxamine B (FOB) as an iron source. Exposure to this xenosiderophore increases fungus survival after phagocytosis by activated macrophages³⁹.

Considering those findings, we sought to investigate the adaptation of *P. brasiliensis* after FOB exposure and observed: the induction of siderophores transporters; the repression SidA at RNA and protein levels; the reduced SidA activity in the presence of FOB. We also observed that SidA and SidH proteins are mainly located in the cytoplasm and cell wall, respectively. With these results we concluded that the fungus blocks siderophores synthesis and uses FOB present in the environment as iron source.

Materials and Methods

Strains and Culture Conditions

Yeast cells of *P. brasiliensis*, *Pb18* (ATCC32069) were used in all the experiments. Cells were maintained in brain heart infusion (BHI) solid medium added of 4% (w/v) glucose for 4 days, at 36 °C. For experiments, cells were grown in liquid BHI for 72 hours at 36°C, 150 rpm, in order to reach the exponential growth phase (10^7 cells/mL). Afterward, the cells were centrifuged at 1200 x g for 10 minutes at 4°C and washed twice with phosphate buffered saline solution 1X (PBS 1X; 1.4 mM KH₂PO₄, 8 mM Na₂HPO₄, 140 mM NaCl, 2.7 mM KCl; pH 7.4). Yeasts were then incubated in McVeigh/Morton liquid medium (MMcM) [4% (w/v) glucose, 0.15% (w/v) KH₂PO₄, 0.05% (w/v) MgSO₄.7H₂O, 0.015% (w/v) CaCl₂.2H₂O, 0.2% (w/v) (NH₄)₂SO₄, 0.2% (w/v) L-asparagine, 0.02% (w/v) L-cystine, 1% (v/v) of vitamin supplement (0.006% [w/v] thiamine, 0.006% [w/v] niacin B3, 0.006% [w/v] Ca⁺² pantothenate, 0.001% [w/v] inositol B7, 0.0001% [w/v] biotin B8, 0.001% [w/v] riboflavin, 0.01% [w/v] folic acid B9, 0.01% [w/v] choline chloride, 0.01% [w/v] pyridoxine) and 0.1% (v/v) of trace elements supplement (0.0057% [w/v] H₃BO₃, 0.0081% MnSO₄.14H₂O, 0.0036% [w/v] (NH₄)₆Mo₇O₂₄.4H₂O, 0.0157% [w/v] CuSO₄.H₂O, 0.0792% [w/v] ZnSO₄.7H₂O)⁴³ containing 50 μM of bathophenanthroline-disulfonic acid (BPS; Sigma-Aldrich, Germany), a ferrous iron-specific chelator, for 24 hours at 36°C with shaking at 150 rpm. Cells were centrifuged and washed twice with PBS 1X and cell viability was determined

using trypan blue. A total of 10^7 cells/mL were transferred for MMcM medium containing 50 μ M of BPS or 10 μ M of ferrioxamine B (FOB)³⁹. FOB was prepared by incubating equal molar amounts of deferoxamine mesylate (Sigma-Aldrich, MO, USA) and FeCl₃ together in 1 M Tris pH 7.4 for 30 minutes at room temperature. Yeast cells were incubated at 36°C for 6 and 24 hours, 150 rpm. After the culture period, the cells were collected and used for microscopy experiments and RNA and protein extraction. For culture in MMcM medium all the glassware was acid treated to remove residual traces of iron⁴⁴.

RNA extraction and quantitative real time PCR (RT-qPCR)

Total RNA extraction was accomplished using TRIzol (TRI Reagent, Sigma-Aldrich, St. Louis, MO) and mechanical cell rupture (Mini-Beadbeater – Biospec Products Inc., Bartlesville, OK). RNAs were reverse-transcribed using Super-Script III First-Strand Synthesis SuperMix (Invitrogen, Life Technologies) and cDNAs were submitted to qRT-PCR in the QuantStudio5 real-time PCR system (Applied Biosystems Inc.). The specificity of each primer pair was confirmed by visualization of a single PCR product following agarose gel electrophoresis and melting curve analysis after qRT-PCR. SYBER green PCR master mix was used in the reaction mixture (Applied Biosystems, Foster City, CA). The sequences of forward and reverse oligonucleotides used are listed in Supplementary Table 1. The annealing temperature for all oligonucleotides pairs was 62 °C. For each cDNA sample, the reaction was performed in triplicate. The data were normalized with the transcript for a 28 kDa ribonucleoprotein (GenBank XP_015701336). The relative expression levels of transcripts of interest were calculated using the standard curve method for relative quantification⁴⁵. This standard curve was generated by gathering an aliquot from each cDNA sample, which was serially diluted 1:5 to 1:125. Statistical analysis was performed using the Student's *t*-test and *P* values of 0.05 or less were considered statistically significant.

Protein Extraction

Yeast cells were centrifuged at 10,000 x g for 5 minutes, washed twice with 1X PBS followed by the addition of Tris-Ca buffer (20 mM Tris-HCl pH 8.8; 2 mM CaCl₂). Glass beads (425-600 μ m) were added to the cell suspension and the mixture was submitted to vigorous mixing in a bead beater apparatus (BioSpec) for 5 cycles with

intervals of 30 seconds on ice. The cell lysate was centrifuged at 10,000 x g for 15 minutes at 4 °C and the protein concentration in the supernatant was determined using Bradford reagent ⁴⁶. Bovine serum albumin was used as a standard. The integrity of the proteins was verified using a 12% SDS-PAGE.

Heterologous Expression of Recombinant SidA and SidH

Oligonucleotides used for amplification of the transcript encoding SidA and SidH were SidA-Forward (5'- GGTTCCGCGTGGATCCCATGGAGACCGTTTATCAAGAA - 3'), SidA-Reverse (5'- GTCGACCCGGGAATTCCTATAGTCGTGCGTAATTCT - 3'), SidH-Forward (5'- GGTTCCGCGTGGATCCCATGGCTCCTCGGACACTC - 3') and SidH-Reverse (5'- GTCGACCCGGGAATTCTCAAAGCTTACTATCAACCC - 3'). Underlined regions correspond to *Bam*HI and *Eco*RI restriction sites. The PCR product was subcloned into the *Bam*HI/*Eco*RI sites of pGEX-4T3 vector (GE Healthcare Life Sciences). Transformation of *Escherichia coli* Rosetta (DE3) was carried out using standard procedures. For protein expression, transformed cells were cultured in LB medium supplemented with ampicillin (100 µg/mL) for 16 hours at 37 °C. Culture was diluted 100-fold in fresh LB medium with ampicillin and cultured at 37 °C with shaking at 150 rpm until O.D₆₀₀ of 0.4 - 0.6. The induction of the recombinant protein was performed by addition of Isopropyl β-D-1-thiogalactopyranoside (IPTG; Sigma-Aldrich, St Louis, MO, USA) at a final concentration of 1 mM for 2 hours. Bacteria were collected by centrifugation. The size and identity of the recombinant proteins SidA and SidH was evaluated using SDS-PAGE and in-gel protein digestion ⁴⁷ followed by LC-MS/MS⁴⁸.

Polyclonal antibodies production

SidA and SidH recombinant proteins were used in the production of specific mouse and rabbit polyclonal antibodies, respectively. The preimmune sera were obtained and stored at -20 °C. SidA and SidH were extracted from the SDS-PAGE, which was disrupted with the assistance of glass grinder, and subsequently injected into mouse and rabbit, respectively, three times at 15 days intervals. The obtained sera were sampled and stored at -20 °C.

Immunoblotting

A total of 40 µg of the protein extract, obtained after cultivation in BPS and FOB, was loaded on 12% SDS-PAGE. After separation, proteins were stained with Coomassie Blue R or transferred to Hybond ECL membrane (GE Healthcare). Following transference, the membranes were incubated with blocking buffer (BF) [PBS 1X, 10% (w/v) non-fat milk and 0.1% (v/v) Tween 20] for 2 hours to block non-specific sites. Blocked membranes were incubated with anti-SidA and anti-SidH polyclonal antibodies diluted 1:150 and 1:1000 respectively, in BF for 1 hour 30 minutes. After incubation, the membranes were washed with BF and incubated with secondary antibodies: peroxidase conjugated anti-mouse (1:1000) for SidA and phosphatase conjugated anti-rabbit (1:20000) for SidH. The reaction was developed using the ECL reagent (GE Healthcare Life Sciences) and a Chemiluminescent Film (Lumi-Film Chemiluminescent, Roche Diagnostics Germany) for SidA. SidH was developed by using 5-bromo-4-chloro-3-indolylphosphate–nitroblue tetrazolium (BCIP-NBT). The pixel intensity of the bands was analyzed using the ImageJ 1.51 software. The pixel intensity was generated and expressed as arbitrary units.

Immunolocalization

Yeast cells of *P. brasiliensis* were fixed for localization analysis by Transmission Electron Microscopy (TEM). Cells were fixed in 2% (v/v) glutaraldehyde, 2% (w/v) paraformaldehyde, and 3% (w/v) sucrose in 0.1 M sodium cacodylate buffer pH 7.2. After fixation, the samples were washed three-times with 0.1 M sodium cacodylate buffer pH 7.2. Free aldehyde groups were removed with 50 mM ammonium chloride for 1 h. Block staining was performed in solution containing 2% (w/v) uranyl acetate in 15% (v/v) acetone. After dehydration with increasing acetone concentration scales (30, 50, 70, 90%), samples were embedded in LR Gold resin (Electron Microscopy Sciences, Washington, PA). The samples were embedded in acetone/LR Gold resin (2:1) overnight, acetone/LR Gold resin (1:1) for 6 hours, acetone/LR Gold (1:2) overnight and lastly in pure LR Gold resin submitted to UV light for 48 hours at -20 °C. For immunolocalization, the samples were ultrathin sliced in sections (50 to 70 nm) and incubated for 1 hour with the polyclonal antibodies generated against SidA and SidH and for 1 hour at room temperature with the labeled secondary antibodies mouse/rabbit IgG, Au-conjugated (10 nm average particle size; 1:20 dilution; Electron Microscopy Sciences). The grids were

stained with uranyl acetate and lead citrate, and observed with a Jeol 1011 transmission electron microscope (Jeol, Tokyo, Japan).

L-ornithine-N⁵-oxygenase enzymatic assay

The enzymatic activity of L-ornithine-N⁵-oxygenase (SidA) was evaluated as previously described by Zhou, Haas and Marzluf (1998) with few modifications. Briefly, *P. brasiliensis* yeast cells were collected and suspended in 0.5 mM potassium phosphate buffer (pH 8.0). The suspension was transferred for tubes containing glass beads (425-600 µm) and submitted to vigorous mixing in a bead beater apparatus (BioSpec) for 5 cycles with intervals of 30 seconds on ice. The samples were centrifuged 10,000 x g for 15 minutes and the protein concentration in supernatants was determined with Bradford reagent. To measure the enzymatic activity of SidA, equal amounts of proteins (50 µg) of both conditions, yeast cells incubated with BPS or FOB, were used. The reaction mixture containing 40 µL of 0.5 mM potassium phosphate pH 8.0, 10 µL 10 mM NADPH, 2 µL 0.5 mM FAD, 50 µg cell extract, 30 µL 10 mM L-ornithine and water, was incubated at 30 °C for 2 hours and added of 100 µl of 0.2 M perchloric acid to stop the reaction. For control, the same amount of perchloric acid was added to one sample before incubation. The samples were centrifuged and the supernatants were used to determine the absorbance at 340 nm.

Protein Molecular Modeling

The amino acid sequence of the *P. brasiliensis* SidA (PADG_00097) was modeled by using I-Tasser algorithm ⁵¹. TM-score analysis, which evaluates the similarity of the main template used in the modeling, was carried out. Analysis of function prediction were performed with the COFACTOR ⁵² and COACH ⁵³, algorithms which evaluate functional regions and protein-binding sites, both available on the ZhangLab server (<https://zhanglab.ccmb.med.umich.edu/>). To predict protonation states of the model, the PDB2PQR server and pH 7 were used. Pymol visualizer program was used to perform the structural analysis ⁵⁴.

The molecular dynamics (MD) simulation was performed by the GROMACS 4.5.5 package, using the AMBER force field (ff99SB-ILDM) in the presence of solvent TIP3P ⁵⁵. The protein was subjected to the simulation of 100 nanoseconds, temperature

of 300 K, pressure of 1 atm and time interval of 2 fentoseconds, without restriction of the conformation, according to the protocol of Costa and collaborators (2015).

The analysis of cluster RMSD (root-mean-square deviation of atomic positions), RMSF (root-mean-square fluctuation) and energies related to the simulation of molecular dynamics were performed with the software of the GROMACS package. The quality and the Ramachandran diagram of the final molecular dynamics model were performed with the MolProbity server⁵⁷.

Protein Digestion for nano-ESI-UPLC-MS^E acquisition

A total of 150 µg of cytoplasmic protein was prepared for nanoUPLC-MS^E analysis, as previously described^{58,59}. Briefly, ammonium bicarbonate pH 8.5 at 50 mM and 35 µL of 0.2% (v/v) RapiGEST (Waters Corporation, MA, USA) were sequentially added to the samples. The solution was vortexed and then incubated in dry bath at 80 °C for 15 minutes. After incubation, the samples were centrifuged and the disulphide bonds were reduced by treating proteins with 2.5 µL of 100 mM D-L-dithiothreitol (DTT), for 30 minutes at 60 °C. The cysteine residues were alkylated by addition of 2.5 µL of 300 mM iodoacetamide (GE Healthcare, NJ, USA) followed by incubation in the dark at room temperature for 30 minutes. Digestion was performed with 30 µL of trypsin (Promega, Madison, WI, USA) 0.05 µg/µL in 50 mM ammonium bicarbonate for 16 hours at 37 °C. The hydrolysis of RapiGEST was performed by addition of 30 µL of 5% (v/v) trifluoroacetic acid (Sigma-Aldrich, MO, USA) and the mixture was incubated for 90 minutes at 37°C. The samples were centrifuged at 20,000 x g for 30 minutes at 4°C and the supernatants were transferred to microfuge tubes and dried in a *speed vacuum* (Eppendorf, Hamburg, Germany). The peptides were resuspended in 30 µL of ultrapure water and subsequently purified in ZipTip C18 Pipette Tips (Millipore, MA, USA) and dried in a *speed vacuum*. The peptides obtained were suspended in 80 µL of a solution containing 20 mM of ammonium formate and 200 fmol/µL of PHB (MassPREP™ protein). After solubilization, peptides were transferred to a Waters Total Recovery vial (Waters Corporation, MA, USA).

For separation of tryptic peptides, Nanoscale LC was performed using a ACQUITY UPLC® M-Class system (Waters Corporation, MA, USA) equipped with a XBridge® Peptide 5 µm BEH130 C18 300 µm x 50 mm precolumn; Trap, 2D Symmetry® 5 µm BEH100 C18, 180 µm x 20 mm column and Peptide CSHTM BEH130 C18 1.7 µm, 100 µm x 100 mm analytical reversed-phase column (Waters Corporation, MA, USA).

The peptides were separated using a gradient of 11.4%, 14.7%, 17.4%, 20.7% and 50% of acetonitrile, with a flow rate of 0.5 µL/minutes. The lock mass was used for calibration of the apparatus, using a constant flow rate of 0.5 µL/minutes at a concentration of 200 fmol protein GFB ([Glu1]-Fibrinopeptide B human (Sigma-Aldrich, MO, USA – MW 785.84261). The spectrometer Synapt G1 MSTM (Waters Corporation, MA, USA) equipped with a nanoelectrospray source and two mass analyzers: a quadrupole and a time-of-flight (TOF) operating in TOF V-mode, was utilized for mass spectrometry analysis. Data were obtained using the instrument in the MS^E mode, which switches the low energy (6 V) and elevated energy (40 V) acquisition modes every 0.4 s. Samples were analyzed from three replicates.

Data processing and protein identification

For analysis of the data obtained from the LC-MS^E, the ProteinLynx Global Server version 3.0.2 (Waters, Manchester, UK) was employed. The data were subjected to automatic background subtraction, deisotoping and charge state deconvolution. After processing, each ion comprised an exact mass-retention time (EMRT) that contained the retention time, intensity-weighted average charge, inferred molecular weight based on charge and *m/z*, and the deconvoluted intensity. Then, the processed spectra were searched against *P. brasiliensis* (*Pb18*) protein sequences (<http://www.uniprot.proteomes/>), including reverse sequences. The mass error tolerance for peptide identification was under 50 ppm. The protein identification criteria also included the detection of at least 2 fragment ions per peptide, 5 fragments per protein and the determination of at least 1 peptide per protein. The identification of the protein was allowed with a maximum 4% false positive discovery rate in at least three technical replicate injections. The searches were performed with fixed modification of carbamidomethyl-C, and variable modifications were phosphorylation of serine, threonine and tyrosine. One missed cleavage site was allowed. A protein that showed a variance coefficient of 0,057 and that was detected in all replicates was used to normalize the protein expression levels in the samples (PADG_04570). Expression^E informatics v.3.0.2 was used for quantitative comparisons. The identified proteins were organized by the Expression^E algorithm, into a statistically significant list, corresponding to induced and reduced regulation ratios between the test and control groups. The mathematical model used to calculate the ratios was a part of the Expression^E algorithm inside the PLGS software from the Waters Corporation ⁶⁰. The minimum repeat rate for each protein in all

replicates was 2. Protein tables generated by ProteinLynx Global Server were merged, and the dynamic range of the experiment was calculated using the software program MassPivot v1.0.1. Microsoft Excel (Microsoft, USA) was used for table manipulations. The data obtained by NanoUPLC-MS^E were subjected to *in silico* analysis in databases to identify the functional classification. For this analysis we used Funcat2 database (<http://pedant.gsf.de/genomes.jsp?prefix=P&category=fungal>).

Ethics statement

Animal manipulation was carried out in accordance with the ethical principles of animal research adopted by the Brazilian Society of Laboratory Animal Science and a Brazilian Federal Law 11.749 (October, 2008). Male BALB/c mice aged between 6 to 8 weeks were purchased from the Animal house of the Instituto de Patologia Tropical e Saúde Pública – UFG, and were maintained in the Animal Facilities at the Laboratório de Biologia Molecular, Universidade Federal de Goiás. Animal experimentation was approved by institutional Ethics Commission on Animal Use of the Universidade Federal de Goiás – UFG (reference number 089/17).

Results and discussion

Expression of genes involved in biosynthesis and transport of siderophores

We have previously demonstrated that *Paracoccidioides* spp. is able to use the heterologous siderophore ferrioxamine B (FOB) as an iron source ³⁹. Based on this result, we evaluated the expression of genes related to the siderophore transporters (*sit1*, *mirB* and *mirC*) in yeast cultured in the presence of FOB for 6 h and 24 h. Cells grown in the presence of the iron chelator BPS were used as the experimental control. The genes of siderophores carriers were up-regulated when the fungus was cultured in the presence of FOB (Figure 1A and 1B). After 6 h of incubation we observed an increase in the expression of *mirB* and *mirC*, while *sit1* was induced after 24 h. Expression of *mirB* and *mirC* decreased in yeast upon treatment with FOB at 24h (Figure 1B). The increased expression of these transporters at 6 h may be due to the presence of FOB or because the fungus is producing siderophores. To verify if yeast cells are producing siderophores in presence of FOB, we evaluated the expression of genes related to siderophore biosynthesis (*sidA* and *sidH*). The results demonstrated that *sidA* was down-regulated

along 24 h of incubation with FOB (Figures 1C and 1D), whilst *sidH* expression decreased at 24 h (Figures 1C and 1D). In contrast to *sidA*, *sidH* presented increased expression upon 6 h of FOB treatment. This enzyme belongs to the enoyl-CoA hydratase protein family, which members are related to the β-oxidation³⁰. So, this increase in expression may be explained by the other function performed by members of this family. Activation of siderophore biosynthesis pathway is not necessary along incubation with FOB given that the fungus can use the iron attached to this xenosiderophore. Thus, we may speculate that the increased expression of the siderophores transporters was due to the capture of extracellular FOB.

Several works have shown the importance of siderophores transporters in fungal survival. *Cryptococcus neoformans* Sit1 is essential for the use of ferrioxamine B as source of iron and also for fungus growth in environments where iron availability is low⁶¹. In *Candida albicans*, besides participating in the transport of hydroxamate-type siderophore, Sit1 is required for epithelial invasion⁶². The deletion of some specific regions of the amino acid sequence of *A. fumigatus* MirB transporter impaired fungal growth when cultured in the presence of the siderophore TAFC⁶³.

SidA/SidH recombinant proteins and polyclonal antibodies production

P. brasiliensis SidA and SidH proteins were expressed in *E. coli* Rosetta (DE3). The heterologous expression of SidA rendered a protein with molecular mass of 79.5 kDa, corresponding to 53.5 kDa of SidA fused to 26 kDa of GST (Figure 2A). Regarding to SidH the heterologous expression provided a 57.3 kDa protein, corresponding to 31.3 kDa of SidH and 26 kDa of GST (Figure 2C). Following induction with IPTG (Figures 2A and 2C), the recombinant proteins were cut from the polyacrylamide gel and subjected to in-gel protein digestion for identification by LC-MS/MS. Analysis of the MS/MS spectra confirmed the identities of SidA and SidH recombinant proteins (Supplementary Figures 1A and 1B, respectively; Supplementary Table 2). Polyclonal antibodies, produced after injection of the recombinant proteins cut from the polyacrylamide gel, were used in Western blotting experiments performed with cytoplasmic protein extracts from yeast cells upon 24 hours of incubation in BPS or FOB. The immunoblotting results revealed the presence of the proteins SidA and SidH (53.5 kDa and 31.3 kDa, respectively) in both culture conditions. The expression of SidA in FOB was, however, lower when compared to the BPS condition (Figure 2B). Similar to what was observed

during analysis of gene expression. Regarding SidH, no difference was observed between the two conditions (Figure 2D).

SidA and SidH localization in yeast cells

A study carried out in *Aspergillus* spp. showed that enzymes (SidI, SidH and SidF) of the TAFC biosynthesis pathway are located in peroxisome and that biosynthesis of this siderophore works as long as the three enzymes are located in the same compartment⁶⁴. To date, the subcellular localization of SidA is unknown in fungi. To determine the localization of SidA and SidH in *P. brasiliensis* yeast cells grow in the presence of FOB, we performed immunocytochemical analysis using SidA and SidH polyclonal antibodies. SidA (Figure 3A) and SidH (Figure 3B) were detected in *P. brasiliensis* yeast cells cytoplasm and cell wall, respectively. In Figure 3B some gold particles were also observed in the cytoplasm. The control samples for SidA and SidH were free of label when incubated with the mouse and rabbit preimmune sera (Figures 3C and 3D, respectively). Besides that, the cellular location of SidA and SidH, determined by Wolf PSORT program, is cytoplasmic. The cellular localization (membrane or cytoplasm) of lysine hydroxylase from *E. coli*, which is related to production of the aerobactin siderophore and is functionally related to the ornithine hydroxylase of *Pseudomonas aeruginosa*, was discussed. It was suggested that lysine hydroxylase would be located on the membrane after identification of hydrophobic stretches in amino acids sequence⁶⁵. Later it was suggested that these hydrophobic regions would be involved in coenzyme binding (FAD and NADPH)⁶⁶. *P. brasiliensis* SidA presented cellular localization similar to lysine hydroxylase, as shown in the Figure 3A.

L-ornithine-N⁵-oxygenase enzymatic activity

The enzymatic activity of SidA was performed. As expected, enzyme activity was lower when the fungus was grown in the presence of FOB (Figure 4). We can suggest, with these results, that the presence of an exogenous siderophore in the culture medium can repress synthesis of endogenous siderophore because the fungus can be using the siderophore present in the medium.

Molecular modeling of SidA and SidH

Molecular modeling was performed with the objective of characterizing the three-dimensional structure of *P. brasiliensis* SidA and SidH. The enzyme SidA has a conserved domain of the superfamily of oxygenases (Pfam 13434); to perform the catalytic activity, it requires NADPH and FAD as cofactors. The crystallized protein with the more similar three-dimensional structure corresponds to the SidA of *A. fumigatus*, with 47% identity (PDBID: 4B63). The three-dimensional modeling of *P. brasiliensis* SidA was performed by the iTASSER server, and was based on the *A. fumigatus* protein as the main template in the model generation. This model presented a C-score of -0.25 and TM-score of 0.68 and, according to the prediction of gene ontology of iTASSER, this enzyme binds to FAD and NAD, is involved in oxireduction process.

The structural similarity between *A. fumigatus* and *P. brasiliensis* SidA presented only 0.3 Å of RMSD when aligning the two structures in the Pymol viewer. This fact was essential for analysis of the active site, since the *A. fumigatus* protein was crystallized with the substrate and the cofactors. Figure 5A shows the alignment of SidA of *A. fumigatus* (gray) and *P. brasiliensis* (blue) evidencing the interacting molecules ornithine, FAD and NADPH. The alignment made it possible to identify the amino acid residues of *P. brasiliensis* SidA that bind to FAD, NADPH and L-ornithine. The amino acid residues described in the literature that interact with L-ornithine in *A. fumigatus* are LYS107, ASN323 and SER469, that in the *P. brasiliensis* SidA model correspond to LYS88, ASN306 and SER448, respectively. The amino acids of *P. brasiliensis* that interact with ornithine are shown in Figure 5B. According to previous studies, the interaction between the NADPH and FAD cofactors and SidA protein occurs by a triad of amino acids GLN102, VAL168 and ARG279 in the crystal of *A. fumigatus*, corresponding to GLN83, VAL149 and LYS262 in *P. brasiliensis* (Figure 5C).

In order to obtain a higher quality model of *P. brasiliensis* SidA, the protein was submitted to molecular dynamic simulation. The simulation was performed by the GROMACS package for 100 nanoseconds. The histidine protonation states were predicted by the PDB2PQR server at pH 7.0. Analyzes of the RMSD and Cluster graphs demonstrated that the equilibration was started at 20 ns and completely stabilized at 60 ns approximately (Supplementary Figures 2A and 2B). The most relevant cluster was the first one, which appeared at 20 ns and remained until the end of the simulation, demonstrating that there were no significant differences between the conformational

models during this simulation period. Therefore, the conformational model chosen for the later analysis is that representing cluster number 1.

The quality analysis of the model was carried out in the Molprobity server, used to evaluate the model from the iTASSER and after the molecular dynamics. Parameters generated by the Molprobity server, such as clashscore and MolProbity, were taken into account during the quality review. Clashscore refers to the score of steric shocks between the atoms that makes up the molecule and MolProbity score is a general score of the model, which considers clashscore and other physicochemical parameters of quality. Thus, the lower the values obtained for clashscore and MolProbity score the better the protein model. We observed that the clashscore and MolProbity scores of the model before the molecular dynamics presented high values (12.28 and 3.18, respectively). However, after the molecular dynamics, the values were 0 for the clashscore and 1.28 for the MolProbity score, showing a significant improvement in the quality of the structure, especially considering the decrease of shocks between the atoms (Supplementary Table 3).

In the ramachandran diagrams (Supplementary Figures 2C and 2D) it was also possible to observe a decrease of amino acid residues in forbidden regions, confirming once again the importance of the use of molecular dynamics in the protein energy minimization process, searching for a model that is as close as possible to the native structure. Supplementary Figures 2E and 2F show the RMSF graph and three-dimensional structure of SidA with the pockets and most flexible regions (red), respectively. Such structure can be used for further studies of virtual screening of drugs anti-PCM or protein-protein interactions, since it presents good quality.

The crystallized protein with three-dimensional structure more similar to *P. brasiliensis* SidH is enoyl-CoA hydratase/isomerase from *Mycobacterium abscessus*, with 37% identity (PDBID: 3trr). For three-dimensional modeling of *P. brasiliensis* SidH using the iTASSER server we based on the *M. abscessus* protein as the main template in the generation of our model. The structural similarity between *M. abscessus* and *P. brasiliensis* SidH (Figure 6A), after aligning the two structures in the Pymol viewer, presented 2.2 Å of RMSD. In an attempt to confirm the probable region of enzymatic activity of this protein we looked for another protein with higher similarity. We identified the protein crotonase (PDBID: 3q0j) of *Mycobacterium tuberculosis* that presented a more complementary alignment to SidH, with about 1.9 Å of difference (Figure 6B). Despite these similarities, it was not possible to confirm the exact location of the active

site, since these *Mycobacterium* enzymes are not yet fully described and do not have this region already defined.

In order to obtain a higher quality model of *P. brasiliensis* SidH, the protein was submitted to molecular dynamics simulation. The simulation was performed by the GROMACS package for 100 nanoseconds. The histidine protonation states were predicted by the PDB2PQR server at pH 7.2. The figure 6C presents the structure of *P. brasiliensis* SidH before and after molecular dynamics. The RMSD graph (Figure 6D) shows that the protein varied throughout the simulation, but this variation did not exceed 0.45 nm. For this reason, in Cluster graph, we had only one cluster (grouping of conformations for the cutoff of 0.35 nm) for all simulation (Supplementary Figure 3A). As the RMSD graph showed some peaks and valleys by the end of the simulation (demonstrating certain instability) we performed the residue fluctuation analysis to verify which regions of highest variation may be contributing mostly to the instability observed in the RMSD. As seen in the Figure 6E, two regions showed higher fluctuations (exceeding 0.6 nm) and these regions represent a terminal and a loop region where higher flexibility is expected (Figure 6F). During analysis of protein pockets we observe two larger pockets (higher volume), which are more likely to be active site regions (Figure 6F). It is noted that more flexible regions are not contained in any of these pockets, confirming several studies that consider the active site as a more conserved region and the external loops often as controllers of what comes into and out of these pockets.

The Molprobity server was used in the quality analysis of the model. We evaluated the model from the iTASSER and after the molecular dynamics. It was observed reduction of clashscore and molprobity score. Before the molecular dynamics the values for clashscore and molprobity score were 15.83 and 3.34, respectively, and after the molecular dynamics these values reduced to 0 and 1.23, respectively. These results show a significant progress in the quality of the structure, mainly regarding shocks between the atoms, represented by the values of clashscore. These data, presented in Supplementary Table 3, confirm the importance of using molecular dynamics simulation to improve a protein model. The decrease of amino acid residues in forbidden regions, after molecular dynamics, was observed in the Ramachandran diagrams (Supplementary Figures 3B and 3C). The results obtained with analysis of quality confirm the importance of using molecular dynamics simulation in the protein energy minimization process, in search for a model as close as possible to the native structure. As for SidA, this structure can be used for further studies of virtual screening or protein-protein interactions.

Proteomic analysis of *P. brasiliensis* grown in the presence of FOB

FOB is an effective iron source and, as such, promotes the repression of siderophore biosynthesis in *P. brasiliensis*. In order to have an overview of proteome dynamics, we performed proteomic analysis of *P. brasiliensis* yeast cells in presence of FOB. Equimolar amounts of proteins extracts obtained from three independent experiments were used. The protein extracts were run in three technical replicates and only proteins found in two of the three replicates were considered for further analysis. After merged data, we identified a total of 431 and 475 proteins in samples of Pb18 cultivated in BPS or FOB for 6 h and 24 h, respectively (data not shown). The resulting nanoUPLC-MS^E protein and peptide data generated by PLGS process are in agreement the acceptable standard of quality (data not shown).

The results were used to search for proteins related to the biosynthesis of siderophores. The table 1 features the identified proteins which includes proteins regulated and unregulated. Proteins such as Arginase (PADG_00637), Ornithine aminotransferase (PADG_01328), Glutamate-5-semialdehyde dehydrogenase (PADG_05337), NADP-specific glutamate dehydrogenase (PADG_04516), Argininosuccinate synthase (PADG_00888), Hydroxymethylglutaryl-CoA lyase (PADG_07031) and Acetyl-CoA acetyltransferase (PADG_2751), which are related to the synthesis of ornithine, arginine and acetyl-CoA were identified in the proteome (Figure 7). The enzyme L-ornithine 5-monooxygenase (PADG_00097), which is directly related to the siderophores biosynthesis pathway, was detected only after treatment with BPS. In this way, it was the only protein related to siderophores biosynthesis negatively regulated when Pb18 was cultivated in FOB. SidA is the first enzyme of the siderophore biosynthesis pathway that catalyzes N⁵-hydroxylation of ornithine^{28,67}. This proteomic result reinforces the results previously obtained by our group in which showed that in the presence of FOB, *P. brasiliensis* represses siderophore synthesis.

Conclusions

During the infectious process the host tries to prevent the proliferation of invading microrganism and one of the mechanisms is the deprivation of nutrients. The iron limitation induces *Paracoccidaides* spp. to establish strategies for survival. In this work we evaluated the fungus behavior in the presence of the xenosiderophore ferrioxamine B. Expression analysis revealed that in the presence of an extracellular siderophore,

activation of the siderophore biosynthesis pathway is not required and that the increase of gene encoding for transporter probably occurred for FOB uptake. The enzymes of the siderophore biosynthesis pathway SidA and SidH are located in the cytoplasm and in the cell wall, respectively. Proteomic data once again showed that siderophore biosynthesis is not activated in presence of FOB. Based on these results, we conclude that the presence of FOB allows *P. brasiliensis* to grow and leads to repression of siderophore synthesis.

References

1. Sánchez, M., Sabio, L., Gálvez, N., Capdevila, M. & Dominguez-Vera, J. M. Iron chemistry at the service of life. *IUBMB Life* **69**, 382–388 (2017).
2. Kosman, D. J. Molecular mechanisms of iron uptake in fungi. *Mol. Microbiol.* **47**, 1185–1197 (2003).
3. Halliwell, B. & Gutteridge, J. M. C. Oxygen toxicity, oxygen radicals, transition metals and disease. *Biochem. J* **219**, 1–14 (1984).
4. Haber, F. & Weiss, J. The catalytic decomposition of hydrogen peroxide by iron salts. *Proc R Soc L.* 332–351 (1934).
5. Gunshin, H. *et al.* Cloning and characterization of a mammalian proton-coupled metal-ion transporter. *Nature* **388**, 482–488 (1997).
6. Hentze, M. W., Muckenthaler, M. U., Galy, B. & Camaschella, C. Two to Tango: Regulation of Mammalian Iron Metabolism. *Cell* **142**, 24–38 (2010).
7. Ganz, T. Iron in Innate immunity: Starve the Invaders. *Curr Opin Immunol* 63–67 (2009). doi:doi:10.1016/j.coi.2009.01.011
8. Nemeth, E. *et al.* IL-6 mediates hypoferremia of inflammation by inducing the synthesis of the iron regulatory hormone hepcidin. *J. Clin. Invest.* **113**, 1271–1276 (2004).
9. Appelberg, R. Macrophage nutriprive antimicrobial mechanisms. *J. Leukoc. Biol.* **79**, 1117–1128 (2006).
10. Gruenheid, S., Pinner, E., Desjardins, M. & Gros, P. Natural resistance to infection with intracellular pathogens: the Nramp1 protein is recruited to the membrane of the phagosome. *J. Exp. Med.* **185**, 717–30 (1997).
11. Raymond, K. N., Dertz, E. A. & Kim, S. S. Enterobactin: An archetype for microbial iron transport. *Proc. Natl. Acad. Sci.* **100**, 3584–3588 (2003).
12. Bailão, E. F. L. C. *et al.* Metal acquisition and homeostasis in fungi. *Curr. Fungal Infect. Rep.* **6**, 257–266 (2012).
13. Canessa, P. & Larrondo, L. F. Environmental responses and the control of iron homeostasis in fungal systems. *Appl. Microbiol. Biotechnol.* **97**, 939–955 (2013).

14. Kornitzer, D. Fungal mechanisms for host iron acquisition. *Curr. Opin. Microbiol.* **12**, 377–383 (2009).
15. Dancis, A., Klausner, R. D., Hinnebusch, A. G. & Barriocanal, J. G. Genetic evidence that ferric reductase is required for iron uptake in *Saccharomyces cerevisiae*. *Mol. Cell. Biol.* **10**, 2294–2301 (1990).
16. Georgatsou, E. & Alexandraki, D. Two distinctly regulated genes are required for ferric reduction, the first step of iron uptake in *Saccharomyces cerevisiae*. *Mol. Cell. Biol.* **14**, 3065–3073 (1994).
17. Luca, N. G. & Wood, P. M. Iron uptake by Fungi: contrasted mechanisms with internal or external reduction. *Adv. Microb. Physiol.* **43**, 39–74 (2000).
18. Weissman, Z. & Kornitzer, D. A family of Candida cell surface haem-binding proteins involved in haemin and haemoglobin-iron utilization. *Mol. Microbiol.* **53**, 1209–1220 (2004).
19. Kuznets, G. *et al.* A Relay Network of Extracellular Heme-Binding Proteins Drives *C. albicans* Iron Acquisition from Hemoglobin. *PLoS Pathog.* **10**, 1–15 (2014).
20. Okamoto-shibayama, K., Kikuchi, Y., Kokubu, E. & Sato, Y. Csa2, a member of the Rbt5 protein family, is involved in the utilization of iron from human hemoglobin during *Candida albicans* hyphal growth. *FEMS Yeast Res.* **14**, (2014).
21. Nasser, L. *et al.* Structural basis of haem-iron acquisition by fungal pathogens. *Nat. Microbiol.* 1–10 (2016). doi:10.1038/nmicrobiol.2016.156
22. Pendrak, M. L., Chao, M. P., Yan, S. S. & Roberts, D. D. Heme Oxygenase in *Candida albicans* Is Regulated by Hemoglobin and Is Necessary for Metabolism of Exogenous Heme and Hemoglobin to α-Biliverdin. *J. Biol. Chem.* **279**, 3426–3433 (2004).
23. Weissman, Z., Shemer, R., Conibear, E. & Kornitzer, D. An endocytic mechanism for haemoglobin-iron acquisition in *Candida albicans*. *Mol. Microbiol.* **69**, 201–217 (2008).
24. França, E. J. G., Furlaneto-Maia, L. & Furlaneto, M. C. Hemolytic capability and expression of a putative haem oxygenase-encoding gene by blood isolates of *Candida tropicalis* are influenced by iron deprivation and the presence of hemoglobin and erythrocytes. *Microb. Pathog.* **105**, 235–239 (2017).
25. Neilands, J. B. Siderophores. *Arch. Biochem. Biophys.* **302**, 1–3 (1993).
26. Hissen, A. H. T., Chow, J. M. T., Pinto, L. J. & Moore, M. M. Survival of

- Aspergillus fumigatus* in Serum involves removal of iron from transferrin: the role of siderophores. *Infect. Immun.* **72**, 1402–1408 (2004).
27. Blatzer, M. *et al.* SidL, an *Aspergillus fumigatus* transacetylase involved in biosynthesis of the siderophores ferricrocin and hydroxyferricrocin. *Appl. Environ. Microbiol.* **77**, 4959–4966 (2011).
28. Schrettl, M. *et al.* Siderophore Biosynthesis But Not Reductive Iron Assimilation Is Essential for *Aspergillus fumigatus* Virulence. *J. Exp. Med.* **200**, 1213–1219 (2004).
29. Schrettl, M. *et al.* Distinct roles for intra- and extracellular siderophores during *Aspergillus fumigatus* infection. *PLoS Pathog.* **3**, 1195–1207 (2007).
30. Yasmin, S. *et al.* Mevalonate governs interdependency of ergosterol and siderophore biosyntheses in the fungal pathogen *Aspergillus fumigatus*. *Proc. Natl. Acad. Sci.* **109**, E497–E504 (2011).
31. Nevitt, T. & Thiele, D. J. Host iron withholding demands siderophore utilization for *Candida glabrata* to survive macrophage killing. *PLoS Pathog.* **7**, (2011).
32. Haas, H. *et al.* Characterization of the *Aspergillus nidulans* transporters for the siderophores enterobactin and triacetylfusarinine C. *C.* **513**, 505–513 (2003).
33. Haas, H. Molecular genetics of fungal siderophore biosynthesis and uptake: the role of siderophores in iron uptake and storage. *Appl Microbiol Biotechnol* 316–330 (2003). doi:10.1007/s00253-003-1335-2
34. Hwang, L. H., Mayfield, J. A., Rine, J. & Sil, A. *Histoplasma* requires *SID1*, a member of an iron-regulated siderophore gene cluster, for host colonization. *PLoS Pathog.* **4**, (2008).
35. Restrepo M, A. The ecology of *Paracoccidioides brasiliensis*: A puzzle still unsolved. *Med. Vet. Mycol.* **23**, 323–334 (1985).
36. San-Blas, G., Nino-Vega, G. & Iturriaga, T. *Paracoccidioides brasiliensis* and paracoccidioidomycosis: Molecular approaches to morphogenesis, diagnosis, epidemiology, taxonomy and genetics. *Med. Mycol.* 225–242 (2002).
37. Restrepo, A., McEwen, J. G. & Castañeda, E. The habitat of *Paracoccidioides brasiliensis*: how far from solving the riddle? *Med. Mycol.* **39**, 233–241 (2001).
38. McEwen, J. G., Bedoya, V., Patino, M. M., Salazar, M. E. & Restrepo, A. Experimental murine paracoccidioidomycosis induced by the inhalation of conidia. *J Med Vet Mycol* **25**, 165–175 (1987).
39. Silva-Bailão, M. G. *et al.* Hydroxamate production as a high affinity iron acquisition mechanism in *Paracoccidioides* Spp. *PLoS One* **9**, (2014).

40. Bailão, E. F. L. C. *et al.* *Paracoccidioides* spp. ferrous and ferric iron assimilation pathways. *Front. Microbiol.* **6**, 1–12 (2015).
41. Silva, M. G. *et al.* The homeostasis of iron, copper, and zinc in *Paracoccidioides brasiliensis*, *Cryptococcus neoformans* var. *Grubii*, and *Cryptococcus gattii*: A comparative analysis. *Front. Microbiol.* **2**, 1–19 (2011).
42. Parente, A. F. A. *et al.* Proteomic analysis reveals that iron availability alters the metabolic status of the pathogenic fungus *Paracoccidioides brasiliensis*. *PLoS One* **6**, (2011).
43. Restrepo, A. & Jimenez, B. E. Growth of *Paracoccidioides brasiliensis* yeast phase in a chemically defined culture medium. *J. Clin. Microbiol.* **12**, 279–281 (1980).
44. Cox, C. Deferration of laboratory media and assays for ferric and ferrous ions. *Methods Enzymol.* 315–329 (1994).
45. Bookout, A. L., Cummins, C. L., Mangelsdorf, D. J., Pesola, J. M. & Kramer, M. F. High-throughput real-time quantitative reverse transcription PCR. *Curr. Protoc. Mol. Biol. Chapter 15*, Unit 15.8 (2006).
46. Bradford, M. A rapid and sensitive method for the quantification of microgram quantities of protein utilizing the principle of protein-dye binding. *Anal. Biochem.* **72**, 248–254 (1976).
47. Rezende, T. C. V *et al.* A quantitative view of the morphological phases of *Paracoccidioides brasiliensis* using proteomics. *J. Proteomics* **75**, 572–587 (2011).
48. Lima, P. de S., Chung, D., Bailão, A. M., Cramer, R. A. & Soares, C. M. de A. Characterization of the *Paracoccidioides* Hypoxia Response Reveals New Insights into Pathogenesis Mechanisms of This Important Human Pathogenic Fungus. *PLoS Negl. Trop. Dis.* **9**, 1–25 (2015).
49. de Curcio, J. S. *et al.* Identification of membrane proteome of *Paracoccidioides lutzii* and its regulation by zinc. *Futur. Sci. OA* **3**, FSO232 (2017).
50. Zhou, L. W., Haas, H. & Marzluf, G. A. Isolation and characterization of a new gene, sre, which encodes a GATA-type regulatory protein that controls iron transport in *Neurospora crassa*. *Mol. Gen. Genet.* **259**, 532–540 (1998).
51. Yang, J. & Zhang, Y. Protein Structure and Function Prediction Using I-TASSER. *Curr. Protoc. Bioinforma.* **52**, 5.8.1-5.8.15 (2015).
52. Zhang, C., Freddolino, P. L. & Zhang, Y. COFACTOR: Improved protein function prediction by combining structure, sequence and protein-protein

- interaction information. *Nucleic Acids Res.* **45**, W291–W299 (2017).
53. Yang, J., Roy, A. & Zhang, Y. Protein-ligand binding site recognition using complementary binding-specific substructure comparison and sequence profile alignment. *Bioinformatics* **29**, 2588–2595 (2013).
54. Schrödinger, L. The PyMOL Molecular Graphics System, Version 1.8. *Schrodinger LLC Wwpymolorg.* (2015).
55. Pronk, S. *et al.* GROMACS 4.5: A high-throughput and highly parallel open source molecular simulation toolkit. *Bioinformatics* **29**, 845–854 (2013).
56. Costa, F. G. *et al.* Alkaloids as inhibitors of malate synthase from paracoccidioides spp.: Receptor-ligand interaction-based virtual screening and molecular docking studies, antifungal activity, and the adhesion process. *Antimicrob. Agents Chemother.* **59**, 5581–5594 (2015).
57. Chen, V. B. *et al.* MolProbity: All-atom structure validation for macromolecular crystallography. *Acta Crystallogr. Sect. D Biol. Crystallogr.* **66**, 12–21 (2010).
58. Murad, A. M., Souza, G. H. M. F., Garcia, J. S. & Rech, E. L. Detection and expression analysis of recombinant proteins in plant-derived complex mixtures using nanoUPLC-MSE. *J. Sep. Sci.* **34**, 2618–2630 (2011).
59. Lima, P. de S. *et al.* Transcriptional and proteomic responses to carbon starvation in *Paracoccidioides*. *PLoS Negl. Trop. Dis.* **8**, (2014).
60. Geromanos, S. J. *et al.* The detection, correlation, and comparison of peptide precursor and product ions from data independent LC-MS with data dependant LC-MS/MS. *Proteomics* **9**, 1683–1695 (2009).
61. Tangen, K. L., Jung, W. H., Sham, A. P., Lian, T. & Kronstad, J. W. The iron- and cAMP-regulated gene SIT1 influences ferrioxamine B utilization, melanization and cell wall structure in *Cryptococcus neoformans*. *Microbiology* **153**, 29–41 (2007).
62. Heymann, P. *et al.* The siderophore iron transporter of *Candida albicans* (Sit1p/Arn1p) mediates uptake of ferrichrome-type siderophores and is required for epithelial invasion. *Infect. Immun.* **70**, 5246–5255 (2002).
63. Raymond-Bouchard, I. *et al.* Structural requirements for the activity of the MirB ferrisiderophore transporter of *Aspergillus fumigatus*. *Eukaryot. Cell* **11**, 1333–1344 (2012).
64. Gründlinger, M. *et al.* Fungal siderophore biosynthesis is partially localized in peroxisomes. *Mol. Microbiol.* **88**, 862–875 (2013).
65. Herrero, M., Lorenzo, V. D. E. & Neilands, J. B. Nucleotide Sequence of the

- iucD Gene of the pColV-K30 Aerobactin Operon and Topology of Its Product Studied with phoA and lacZ Gene Fusions. *J. Bacteriol.* **170**, 56–64 (1988).
66. Stehr, M. *et al.* A hydrophobic sequence motif common to N-hydroxylating enzymes. *Trends Biochem Sci* **1**, 97–98 (1998).
67. Eisendle, M., Oberegger, H., Zadra, I. & Haas, H. The siderophore system is essential for viability of *Aspergillus nidulans*: Functional analysis of two genes encoding L-ornithine N5-monooxygenase (sidA) and a non-ribosomal peptide synthetase (sidC). *Mol. Microbiol.* **49**, 359–375 (2003).

FIGURES

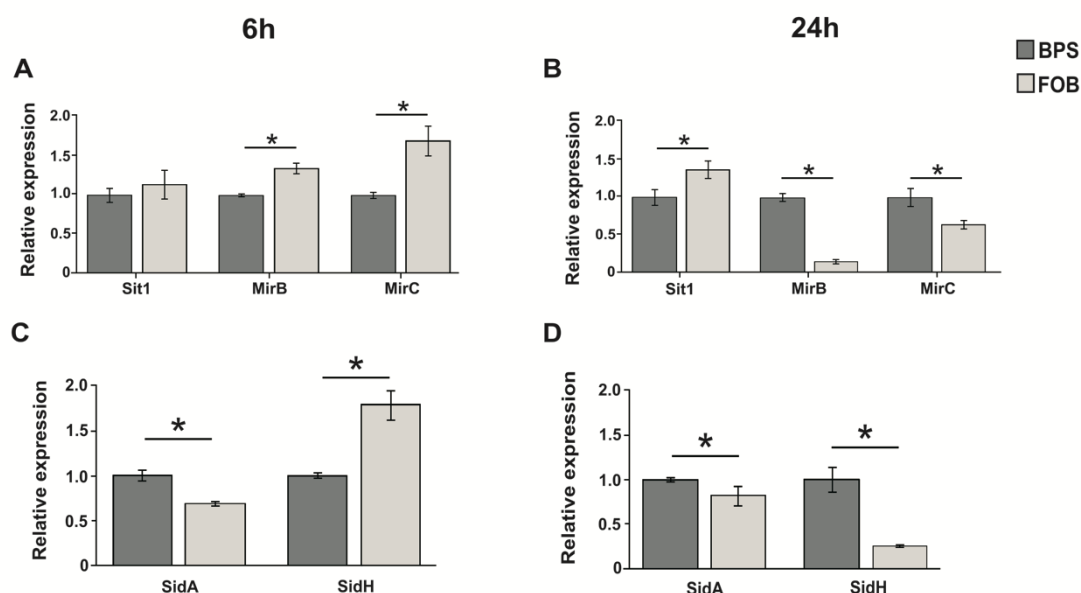


Figure 1. Expression of the siderophore transporters and siderophore biosynthesis genes. Relative expression of siderophore transporters (A) and siderophore biosynthesis (C) genes at 6 hours upon yeast cells incubation with FOB (10 µM) or BPS (50 µM). Relative expression of siderophore transporters (B) and siderophore biosynthesis (D) genes at 24 hours. Data were normalized to the 28 kDa ribonucleoprotein (GenBank XP_015701336). Student's t test was used for statistical comparisons. Error bars represent standard deviation from three biological replicates while * represents $p \leq 0.05$.

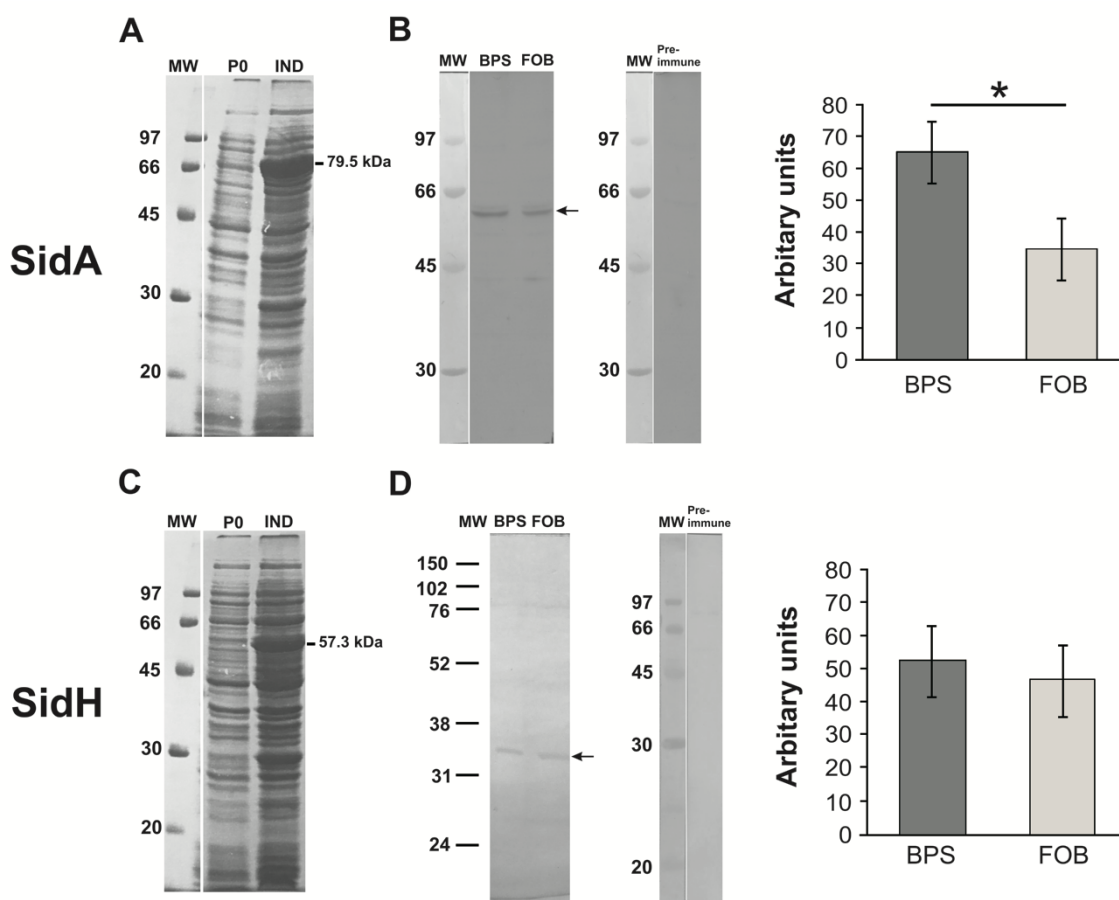


Figure 2. Expression of the recombinant proteins SidA and SidH and immunoblotting analysis. SDS-PAGE results of expression of the recombinant proteins SidA (A) and SidH (C) by *E. coli* Rosetta (DE3). Membranes containing total proteins extract of *P. brasiliensis* cultivated in BPS or FOB for 24 hours were incubated with anti-SidA (B) and anti-SidH (D) polyclonal sera. The native SidA and SidH proteins show a molecular mass of 53.5 kDa and 31.3 kDa, respectively. The pixel intensity of the bands of immunoblotting was analyzed using the ImageJ 1.51 software. The pixel intensity was generated and expressed as arbitrary units. **MW:** molecular weight marker. **P0:** *E. coli* before induction. **IND:** *E. coli* after induction (1 mM IPTG for 2 hours). * indicates statistically significant differences.

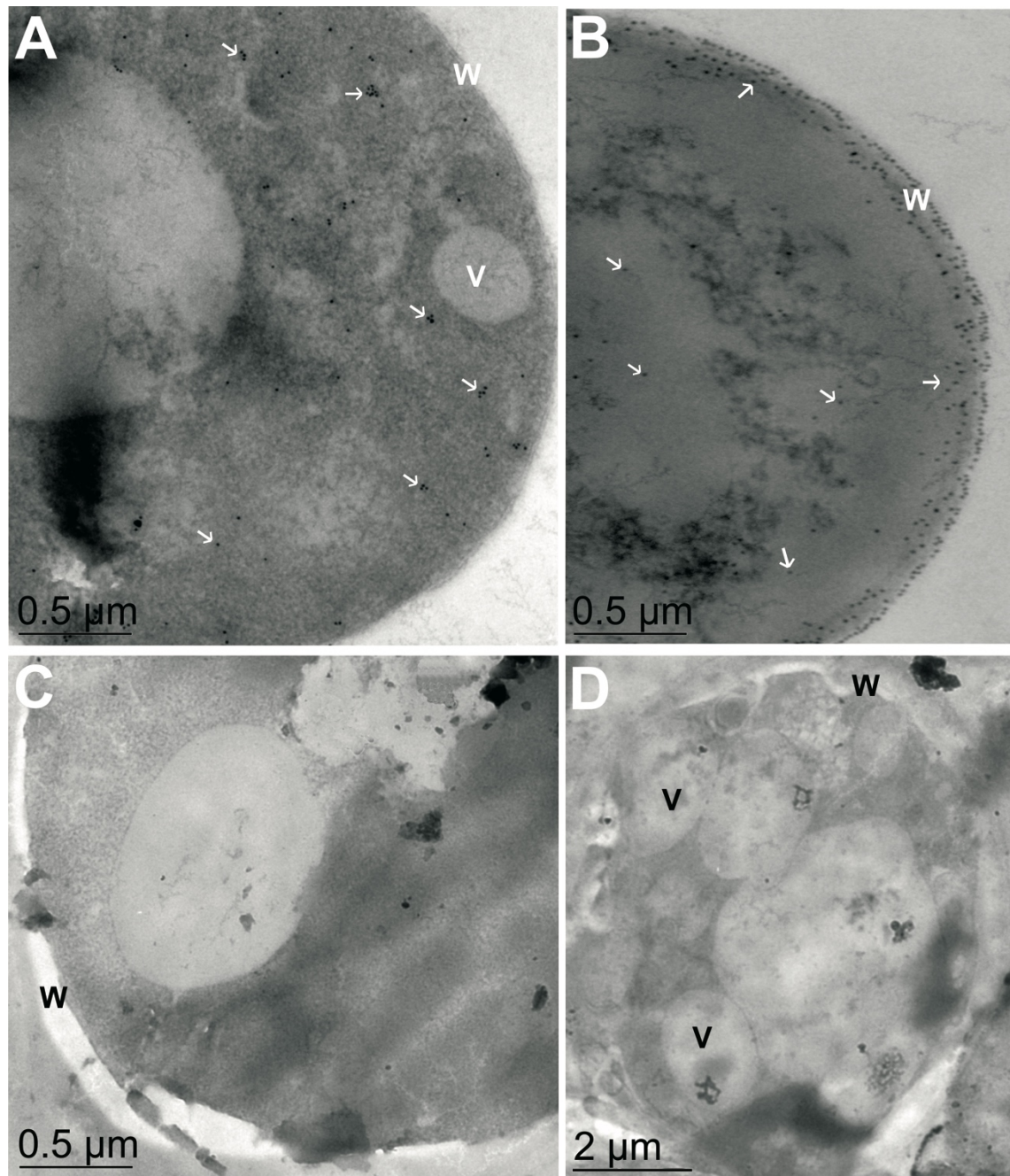


Figure 3. Immunocytochemical analysis of *P. brasiliensis* yeast cells by TEM. SidA (A) and SidH (B) proteins are represented by the black dots as indicated by the white arrows. Samples incubated with the mouse (C) and rabbit (D) preimmune serum. (W) cell wall; (V) vesicle

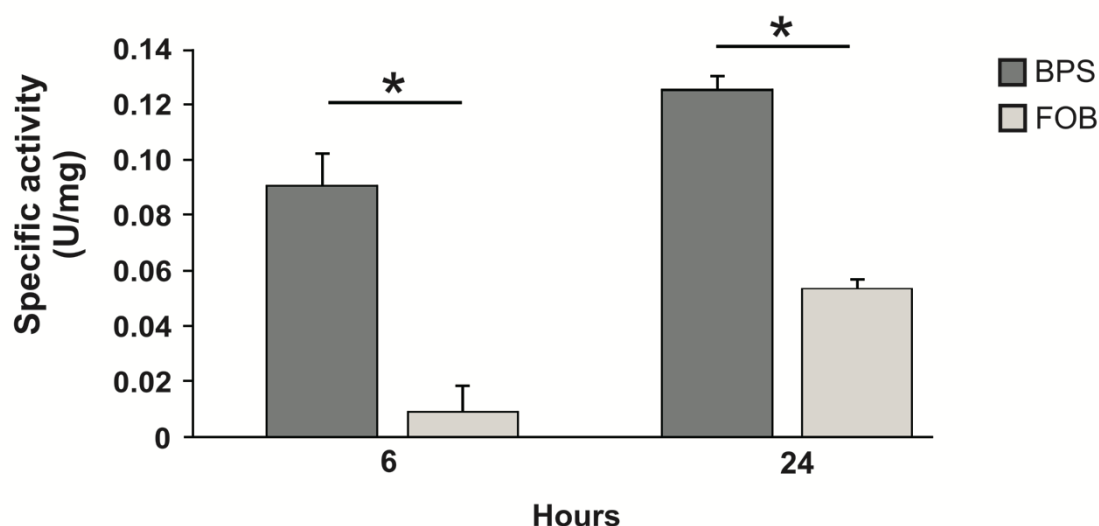


Figure 4. SidA enzymatic activity in *P. brasiliensis* yeast cells upon FOB treatment.
* $p \leq 0.05$

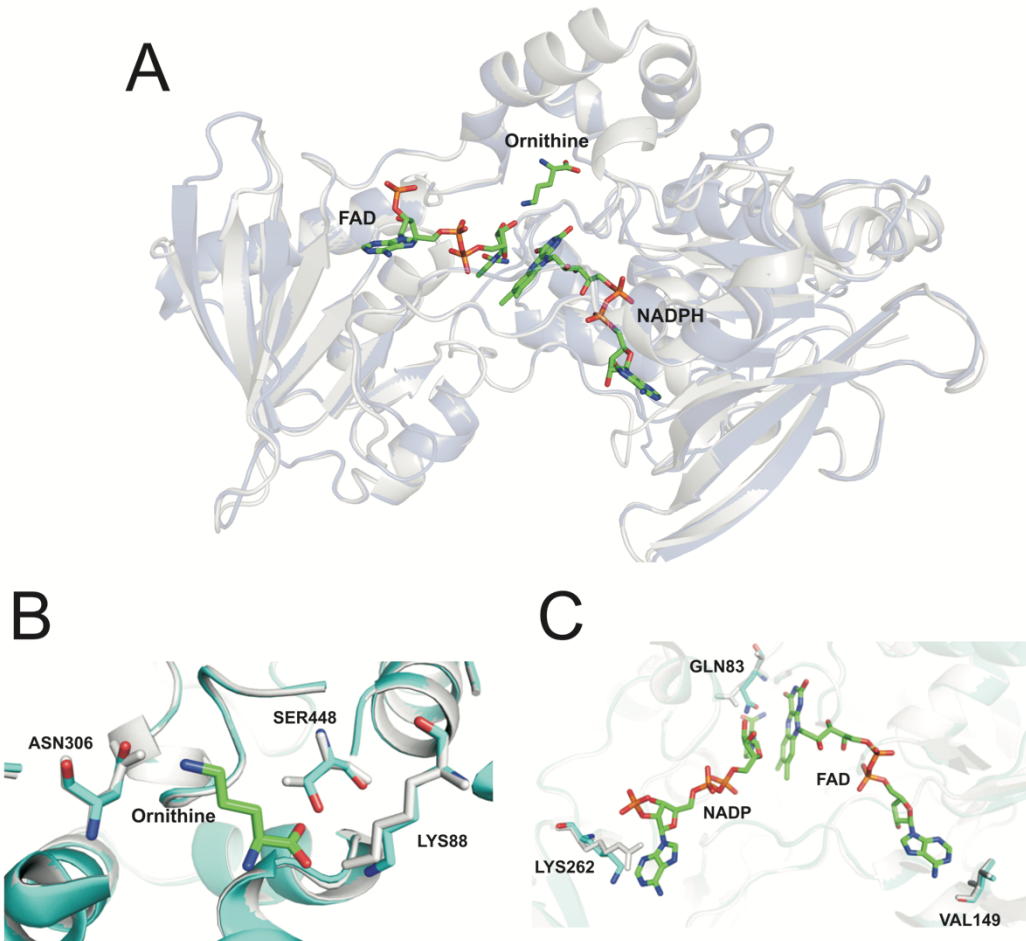


Figure 5. Molecular structure of L-ornithine-N⁵-monooxygenase. **A.** AfSidA (gray) and *Pb*SidA (blue) aligned using the Pymol program, evidencing the interacting molecules ornithine, FAD and NADPH are evidenced. It is noted that the 3D structure is highly conserved in these two fungi, and therefore the active site of binding of these molecules is also conserved. **B.** Amino acid residues of *P. brasiliensis* described as mainly involved in the interaction with Ornithine; **C:** Amino acid residues of *P. brasiliensis* SidA that interact with cofactors and are essential for the maintenance of cofactors in the active site.

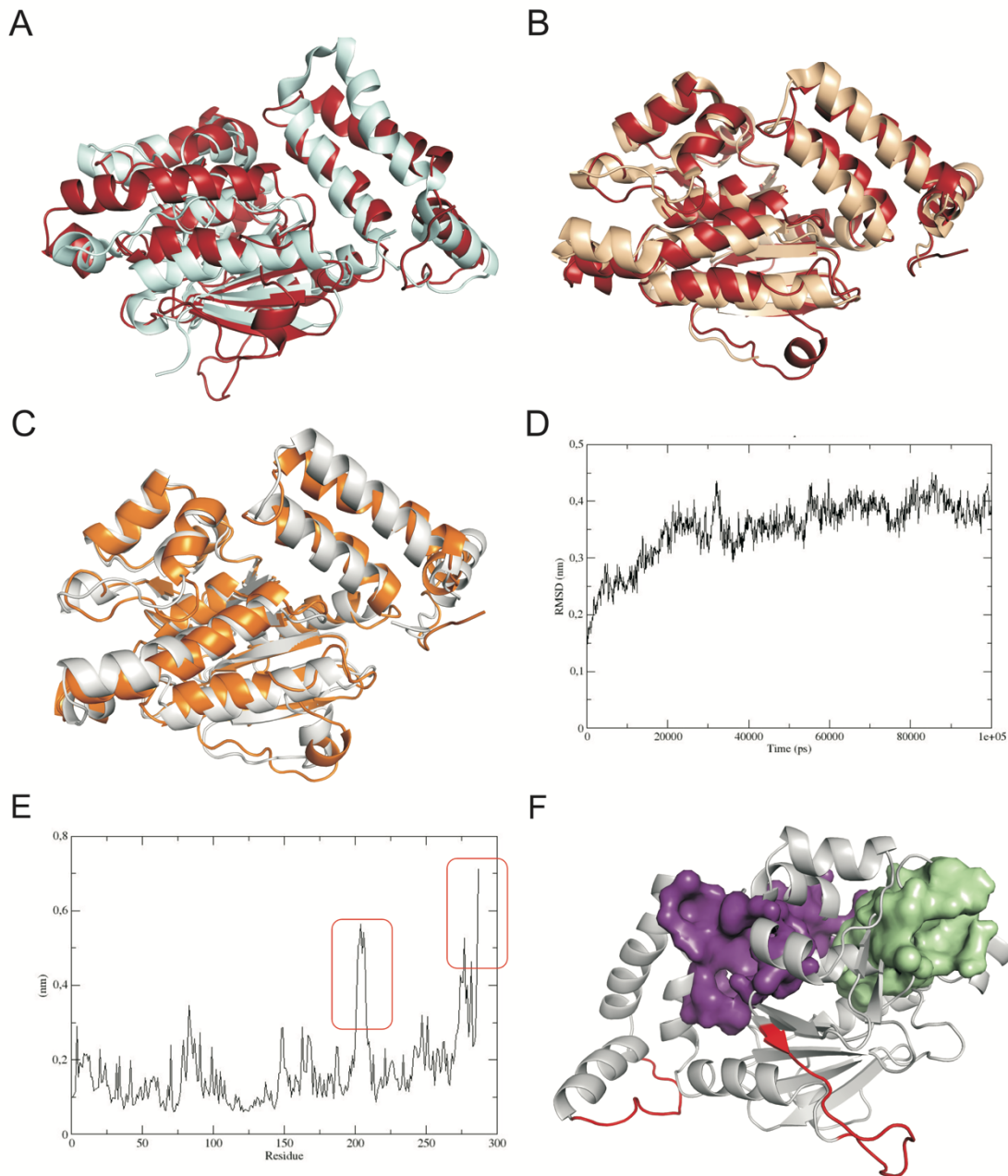


Figure 6. Molecular structure of enoyl-CoA hydratase (SidH) and quality graphs of molecular dynamics. **A.** Structural similarity between SidH of *P. brasiliensis* (red) and enoyl-CoA hydratase of *M. abscessus* (blue). **B.** Structural similarity between *P. brasiliensis* SidH (red) and crotonase of *M. tuberculosis* (salmon). **C.** Structure of *P. brasiliensis* SidH before (gray) and after (orange) molecular dynamics. **D.** RMSD graph showing the mean deviation of the initial time structure until the final time of the simulation. **E.** RMSF graph showing the residues more flexible along the molecular dynamics. Red squares demonstrate regions of higher fluctuations (exceeding 0,6 nm). **F.** Protein pockets and location of more flexible residues (red).

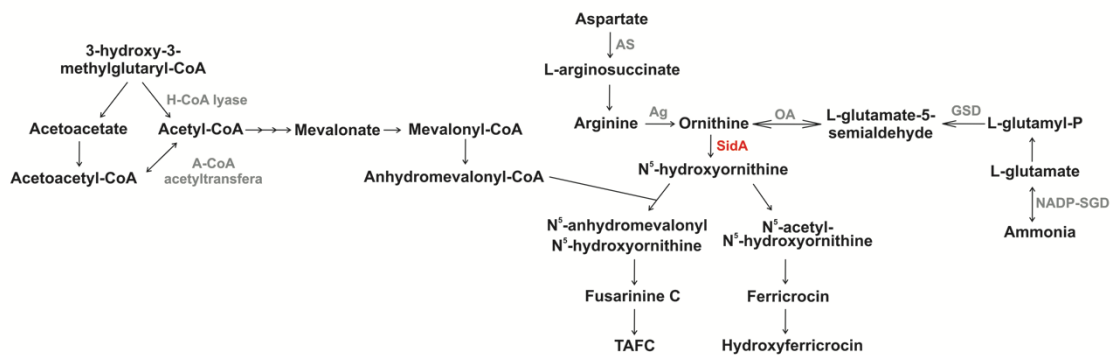
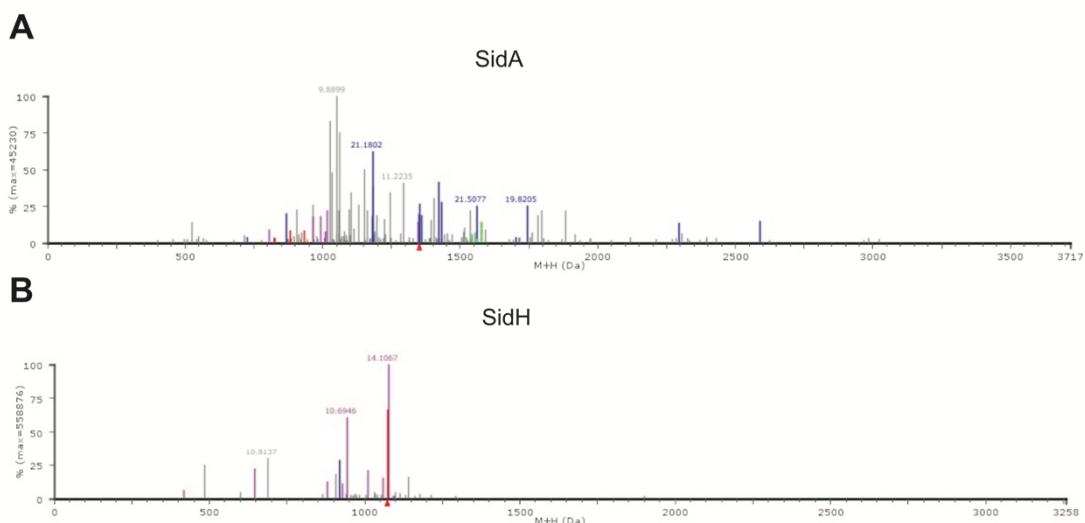
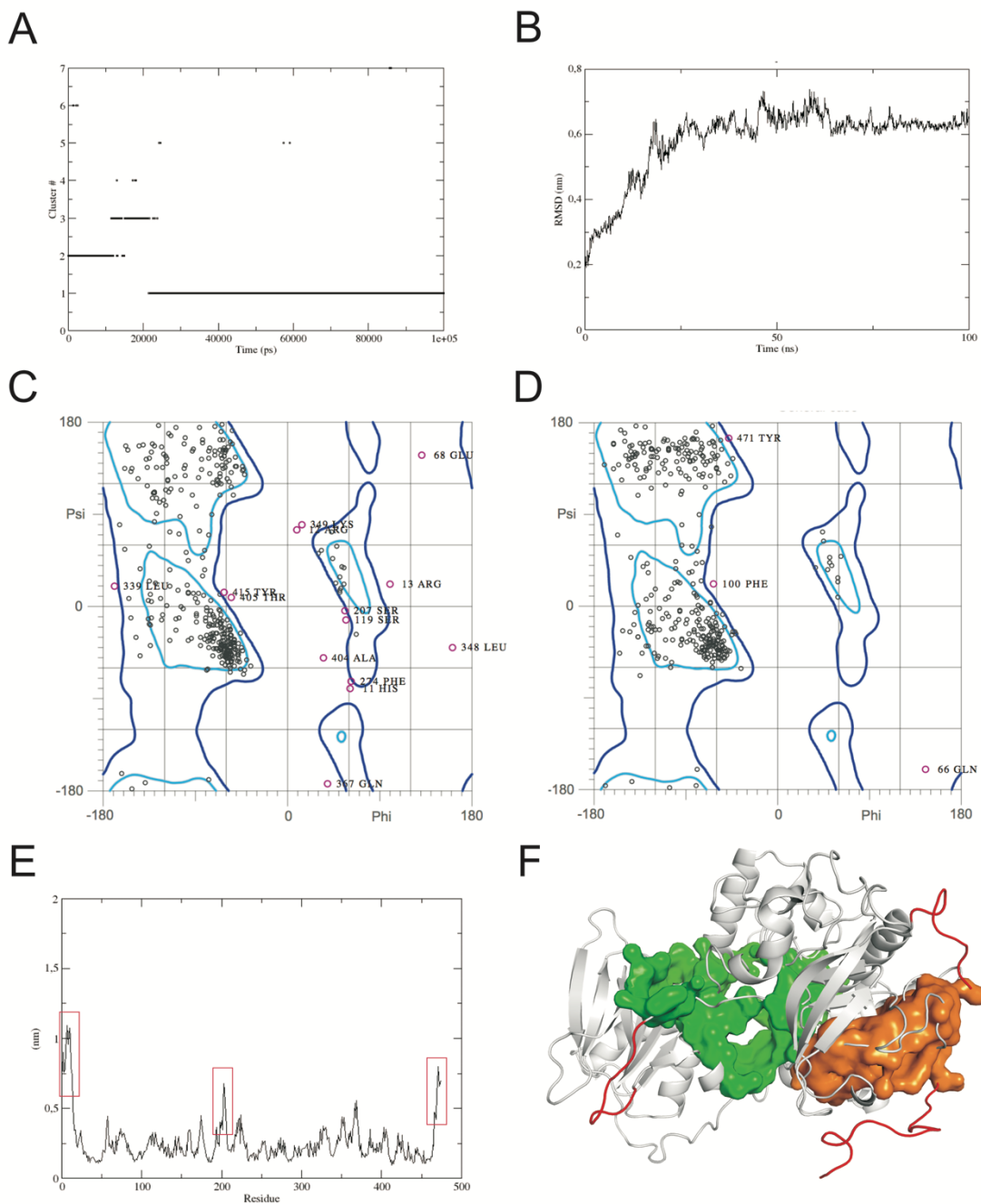


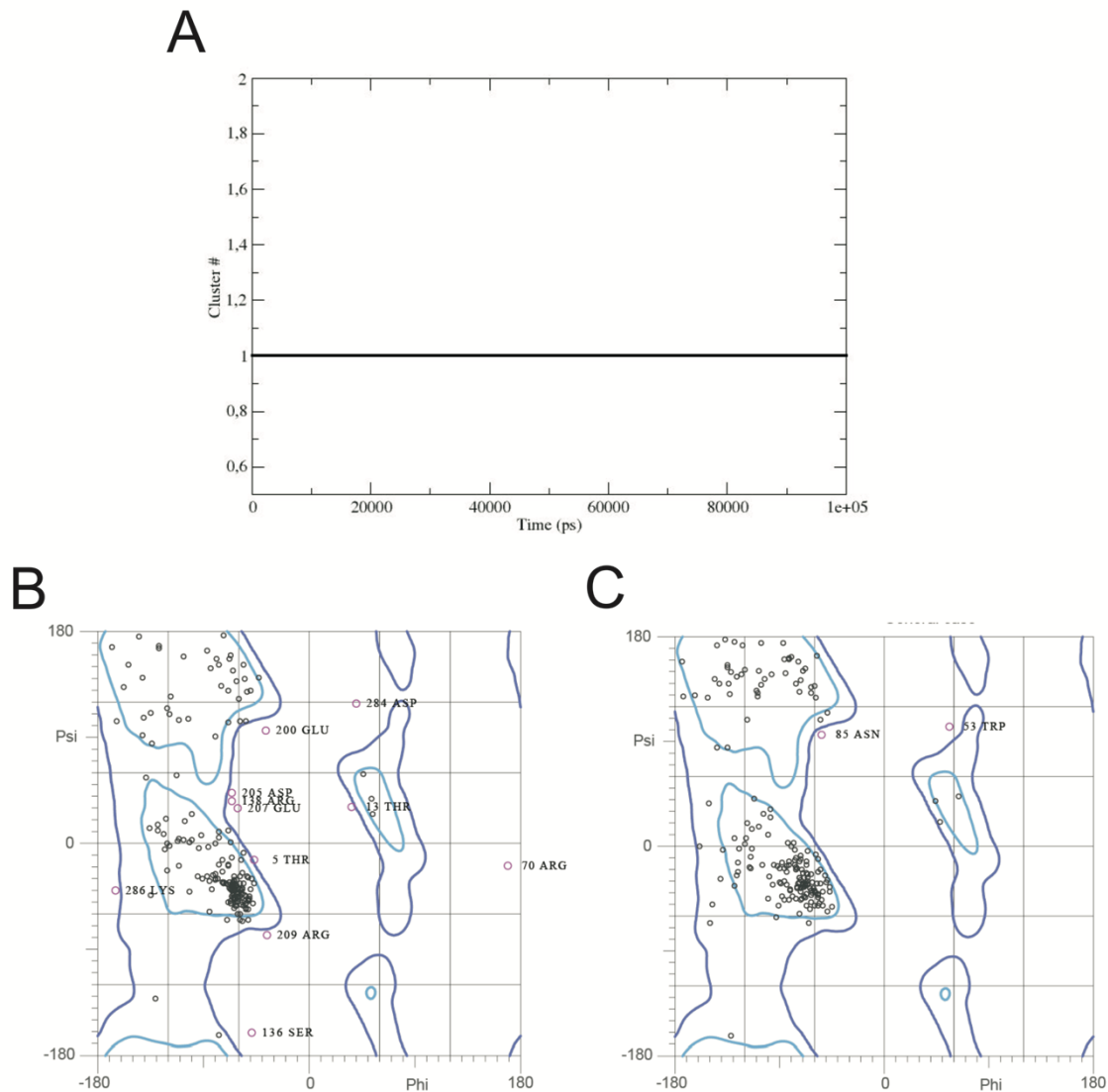
Figure 7. Proteins related to siderophore synthesis identified in the proteome. AS: Argininosuccinate synthase. Ag: Arginase. OA: Ornithine aminotransferase. GSD: Glutamate-5-semialdehyde dehydrogenase. NADP-SGD: NADP-specific glutamate dehydrogenase. H-CoA lyase: Hydroxymethylglutaryl-CoA lyase. A-CoA acetyltransferase: Acetyl-CoA acetyltransferase. SidA: L-ornithine-N⁵-monooxygenase. Red: repressed enzyme.



Supplementary Figure 1. Characterization of the recombinant proteins. A and B. MS/MS spectrum of the recombinant proteins SidA and SidH, respectively, identified by mass spectrometry.



Supplementary Figure 2. Quality graphs of molecular dynamics of *P. brasiliensis* SidA. Cluster (A) and RMSD (B) graphs. It is observed that the stability starts at approximately 20 ns, and that the most representative conformational mode of the trajectory is cluster 1. Ramachandran diagrams of the three-dimensional model of SidA before (C) and after (D) molecular dynamics. E. RMSF graph showing the more flexible residues in red along the molecular dynamics. F. Three-dimensional structure of SidA showing the most flexible regions (red) and pockets (green and orange).



Supplementary Figure 3. Quality graphs of molecular dynamics of *P. brasiliensis* SidH. A. Cluster graphs. Ramachandran diagrams of the three-dimensional model of SidH before (**B**) and after (**C**) molecular dynamics.

TABLES

Table 1. Proteins related to the biosynthesis of siderophores identified in proteomic analysis

Accession number ^a	Description ^b	Time ^c	Score ^d
PADG_00637	Arginase (325 aa)	6h	1131.29
PADG_00637	Arginase (325 aa)	24h	1171.88
PADG_01328	Ornithine aminotransferase (461 aa)	6h	2299.86
PADG_01328	Ornithine aminotransferase (461 aa)	24h	1175.4
PADG_00888	Argininosuccinate synthase (416 aa)	6h	3507.13
PADG_00888	Argininosuccinate synthase (416 aa)	24h	4840.6
PADG_07031	Hydroxymethylglutaryl-CoA lyase (357 aa)	6h	2406.52
PADG_07031	Hydroxymethylglutaryl-CoA lyase (357 aa)	24h	2627.2
PADG_05337	Glutamate-5-semialdehyde dehydrogenase (457 aa)	6h	1209.7
PADG_05337	Glutamate-5-semialdehyde dehydrogenase (457 aa)	24h	771.05
PADG_04516	NADP-specific glutamate dehydrogenase (460 aa)	24h	501.85
PADG_02751	Acetyl-CoA acetyltransferase (400 aa)	6h	4328.06
PADG_02751	Acetyl-CoA acetyltransferase (400 aa)	24h	3019.16
PADG_00097	L-ornithine 5-monooxygenase (475 aa)*	24h	360.99

a, b Accession number and description of protein according to database of *Paracoccidioides* spp.

c Time of treatment

d Protein score obtained from MS data using the PLGS.

* Regulated Protein

Supplementary Table 1. Sequences of forward and reverse oligonucleotides

Accession number	Sequence
<i>sidA</i> (PADG_00097)	F: GCGACGATAGCCCATTGTC R: ATTAGCAGGATTAGGATCAAGG
<i>sidH</i> (PADG_01370)	F: CTGGGGCAGATTGAAAGAATG R: TGGCAATGACGATATCGGCG
<i>sit1</i> (PADG_00462)	F: GGCAATCATTTCCCTGTGTG R: CGCGAAGACTGCAATCAAAG
<i>mirB</i> (PADG_00095)	F: GTCTTCTACTGGGTCGGGTAT R: GACCATTCAAGGAAGGCTGTC
<i>mirC</i> (PADG_05373)	F: CAGAATGTGGTGAACGCCGT R: AGAATTGCAGTCCTGTTAAC

Supplementary Table 2. Identification of SidA and SidH recombinant proteins identification data by mass spectrometry.

Accession number ^a	PADG_00097	PADG_01370
Description ^b	Hypothetical protein (475aa)	Hypothetical protein (288aa)
mW (Da) ^c	53505	31241
pI ^d	7.0854	6.2563
Protein Score ^e	1805.296	322.455
Peptides ^f	18	6
Peptide sequence ^g	RSSELLDSILASSKR RYDVVVLATGYTRN KFLDPNPANWSLRL RLSLLESVYEKL KELPNNQVELHVKD KRAENYARL REFGWHTGMLLPGSKM KMQISFIKD RELSNEPLPSTVIHSSVYLESEQKF RELSAKH RRVLFLERQ KWCASHFDDWVQYKQ RAENYARL KDTQSGQIESSGERY RERGGSYRF KQEVLVAAAEARPGWPAEHFKV AENYARL REFGWHTGMLLPGSKM	KRLNEGENLKE RLNEGENLKE NEGENLKE GENLKE GENLKE KRLNEG
Coverage (%) ^h	44.3038	3.1359

^a Available at NCBI database (<https://www.ncbi.nlm.nih.gov>)

^b Protein annotation of the *Paracoccidioides* genome database.

^c Molecular Weight.

^d Isoelectric point.

^e Protein score obtained from MS data using the PLGS.

^f Number of peptides identified.

^g Sequence of identified peptides.

^h Average coverage.

Supplementary Table 3. Analysis of the quality of the SidA and SidH models through the Molprobity server.

	SidA model before DM	SidA model after DM	SidH model before DM	SidH model after DM
Clashscore	12.28	0	15.83	0
Molprobity score	3.18	1.28	3.34	1.23
Ramachandran outliers	26 aa	3 aa	20 aa	5 aa



Capítulo 3

CONSIDERAÇÕES FINAIS

A privação de ferro é uma condição que os fungos do complexo *Paracoccidioides* enfrentam durante a infecção. Para conseguir sobreviver à essa condição, estes patógenos desenvolveram mecanismos que auxiliam na absorção deste micronutriente. A capacidade de produção e captação de sideróforos é um exemplo destes mecanismos. Neste trabalho analisamos a biossíntese de sideróforos em *Paracoccidioides brasiliensis* quando cultivado na presença de ferrioxamina B. Análises de expressão revelaram que, na presença de um sideróforo extracelular, a ativação da via de biossíntese de sideróforos nativos, naquele momento, não é necessária. O aumento da expressão dos genes que codificam os transportadores provavelmente ocorreu para captação de FOB. As enzimas da via de biossíntese de sideróforo, SidA e SidH, estão localizadas no citoplasma e na parede celular, respectivamente. Adicionalmente, os dados proteômicos confirmaram que a biossíntese de sideróforo é reprimida na presença de FOB. Com base nestes resultados concluímos que a presença de FOB permite *P. brasiliensis* crescer e leva à repressão da síntese de sideróforo.

PERSPECTIVAS

A partir dos dados obtidos no presente trabalho podemos seguir com as seguintes perspectivas:

- Identificar os fatores responsáveis pela inibição da biossíntese de sideróforos na presença de ferrioxamina B;
- Buscar possíveis inibidores (compostos e/ou peptídeos) de SidA e SidH, visto que ortólogos de genes codificantes para essas proteínas não estão presentes em humanos.

Referências

- ABE, F. et al. Effects of iron and desferrioxamine on *Rhizopus* infection. **Mycopathologia**, p. 87–91, 1990.
- APPELBERG, R. Macrophage nutriprive antimicrobial mechanisms. **Journal of Leukocyte Biology**, v. 79, n. 6, p. 1117–1128, 2006.
- ARANTES, T. D. et al. Detection of *Paracoccidioides* spp . in environmental aerosol samples. **Medical Mycology**, n. January, p. 83–92, 2013.
- ARDON, O. et al. Identification of a *Candida albicans* Ferrichrome Transporter and Its Characterization by Expression in *Saccharomyces cerevisiae*. v. 276, n. 46, p. 43049–43055, 2001.
- ARISTIZABAL, B. H.; CLEMONS, K. V; STEVENS, D. A. Morphological Transition of *Paracoccidioides brasiliensis* Conidia to Yeast Cells : In Vivo Inhibition in Females. **Infection and Immunity**, v. 66, n. 11, p. 5587–5591, 1998.
- BAGAGLI, E. et al. High frequency of *Paracoccidioides brasiliensis* infection in armadillos (*Dasypus novemcinctus*): an ecological study. **Medical Mycology**, v. 41, n. 3, p. 217–223, jan. 2003.
- BAGAGLI, E. et al. Phylogenetic and evolutionary aspects of *Paracoccidioides brasiliensis* reveal a long coexistence with animal hosts that explain several biological features of the pathogen. **Infection, Genetics and Evolution**, v. 6, p. 344–351, 2006.
- BAGAGLI, E. et al. *Paracoccidioides brasiliensis*: phylogenetic and ecological aspects. **Mycopathologia**, p. 197–207, 2008.
- BAILÃO, E. F. L. C. et al. *Paracoccidioides* spp. ferrous and ferric iron assimilation pathways. **Frontiers in Microbiology**, v. 6, n. JUL, p. 1–12, 2015.
- BENARD, G. An overview of the immunopathology of human paracoccidioidomycosis. **Mycopathologia**, p. 209–221, 2008.
- BITTENCOURT, J. I.; OLIVEIRA, R.; COUTINHO, Z. F. Paracoccidioidomycosis mortality in the State of Paraná , Brazil , 1980 / 1998. **Cad Saúde Pública**, v. 21, n. 6, p. 1856–1864, 2005.
- BLATZER, M. et al. SidL, an *Aspergillus fumigatus* transacetylase involved in biosynthesis of the siderophores ferricrocin and hydroxyferricrocin. **Applied and Environmental Microbiology**, v. 77, n. 14, p. 4959–4966, 2011.
- BOCCA, A. L. et al. Paracoccidioidomycosis: eco-epidemiology, taxonomy and clinical and therapeutic issues. **Future Microbiology**, v. 8, n. 9, p. 1177–1191, 2013.

BOELAERT, J. R. et al. Mucormycosis during Deferoxamine Therapy Is a Siderophore-mediated Infection In Vitro and In Vivo Animal Studies. **J. Clin Invest**, v. 91, p. 1979–1986, 1993.

BOELAERT, J. R. et al. Deferoxamine augments growth and pathogenicity of *Rhizopus*, while hydroxypyridinone chelators have no effect. **Kidney International**, v. 45, n. 3, p. 667–671, 1994.

BORBA, C. D. M.; SCHAFFER, G. M. V. *Paracoccidioides brasiliensis* : virulence and an attempt to induce the dimorphic process with fetal calf serum. **Mycoses**, v. 179, p. 174–179, 2002.

BRUMMER, E. et al. Paracoccidioidomycosis : an Update. **Clinical Microbiology Reviews**, v. 6, n. 2, p. 89–117, 1993.

BUSTAMANTE-SIMON, B. et al. Characteristics of the conidia produced by the mycelial form of *Paracoccidioides brasiliensis*. **Journal of Medical and Veterinary Mycology**, p. 407–414, 1985.

CANO, L. U. Z. E. et al. Inhibitory Effect of Deferoxamine or Macrophage Activation on Transformation of *Paracoccidioides brasiliensis* Conidia Ingested by Macrophages : Reversal by Holotransferrin. **Infection and Immunity**, v. 62, 1994.

CAPON, R. J. et al. Citromycetins and bilains A-C: New aromatic polyketides and diketopiperazines from Australian marine-derived and terrestrial *Penicillium* spp. **Journal of Natural Products**, v. 70, n. 11, p. 1746–1752, 2007.

CARRERO, L. L. et al. New *Paracoccidioides brasiliensis* isolate reveals unexpected genomic variability in this human pathogen. **Fungal Genetics and Biology**, v. 45, n. 5, p. 605–612, 2008.

CASSAT, J. E.; SKAAR, E. P. Iron in Infection and Immunity. **Cell Host Microbe**, p. 509–519, 2013.

CHI, Z. et al. The unique role of siderophore in marine-derived *Aureobasidium pullulans* HN6.2. n. 5, p. 219–230, 2012.

CONTI-DIAZ, I. A. On the unknown ecological niche of *Paracoccidioides brasiliensis*. our hypothesis of 1989: present status and perspectives. **Rev Inst Med Trop São Paulo**, v. 49, n. 2, p. 131–134, 2007.

CORREDOR, G. G. et al. The naked-tailed armadillo *Cabassous centralis* (Miller 1899): a new host to *Paracoccidioides brasiliensis*. Molecular identification of the isolate. **Medical mycology**, v. 43, n. 3, p. 275–80, maio 2005.

DIAS-MELICIO, L. A. et al. Inhibitory effect of deferoxamine on *Paracoccidioides brasiliensis* survival in human monocytes: Reversal by holotransferrin not by apotransferrin. **Revista do Instituto de Medicina Tropical de São Paulo**, v. 47, n. 5, p. 263–266, 2005.

DOMENICO, I. et al. The molecular Mechanism of Hepcidin-mediated Ferroportin down-regulation. **Molecular biology of the Cell**, v. 79, n. 3, p. 297–316, 2017.

DUKIK, K. et al. HHS Public Access. **Mycoses**, v. 60, n. 5, p. 296–309, 2017.

EISENDLE, M. et al. The siderophore system is essential for viability of *Aspergillus nidulans*: Functional analysis of two genes encoding L-ornithine N5-monooxygenase (sidA) and a non-ribosomal peptide synthetase (sidC). **Molecular Microbiology**, v. 49, n. 2, p. 359–375, 2003.

FORTES, M. R. et al. Immunology of paracoccidioidomycosis. **An. Bras. Dermatol.**, p. 516–524, 2010.

FOSTER, L. A. Utilization and cell-surface binding of hemin by *Histoplasma capsulatum*. **Can J Microbiol**, p. 437–442, 2002.

FRANÇA, E. J. G.; FURLANETO-MAIA, L.; FURLANETO, M. C. Hemolytic capability and expression of a putative haem oxygenase-encoding gene by blood isolates of *Candida tropicalis* are influenced by iron deprivation and the presence of hemoglobin and erythrocytes. **Microbial Pathogenesis**, v. 105, p. 235–239, 2017.

FROISSARD, M. et al. Trafficking of Siderophore Transporters in *Saccharomyces cerevisiae* and Intracellular Fate of Ferrioxamine B Conjugates. **Traffic**, p. 1601–1616, 2007.

GANZ, T. Iron and infection. **International Journal of Hematology**, v. 107, n. 1, p. 7–15, 2018.

GANZ, T.; NEMETH, E. Iron Sequestration and Anemia of Inflammation. **Seminars in Hematology**, v. 46, n. 4, p. 387–393, 2009.

GARCIA, N. M. et al. Paracoccidioides brasiliensis, a new strain isolated from a fecal matter of a penguin (*Pygoscelis adeliae*). **Rev. Inst. Med. Trop. São Paulo**, n. June 1993, 1993.

GARDENGHI, S. et al. Distinct roles for hepcidin and interleukin-6 in the recovery from anemia in mice injected with heat-killed *Brucella abortus*. **Blood**, v. 123, n. 8, p. 1137–1145, 2014.

GRUENHEID, S. et al. Natural resistance to infection with intracellular pathogens: the Nramp1 protein is recruited to the membrane of the phagosome. **The Journal of experimental medicine**, v. 185, n. 4, p. 717–30, 1997.

GRUNDLINGER, M. et al. *Aspergillus fumigatus* SidJ mediates intracellular siderophore hydrolysis. **Applied and Environmental Microbiology**, v. 79, n. 23, p. 7534–7536, 2013.

GUNSHIN, H. et al. Cloning and characterization of a mammalian proton-coupled metal-ion transporter. **Nature**, v. 388, n. 6641, p. 482–488, 1997.

HAAS, H. et al. Characterization of the *Aspergillus nidulans* transporters for the siderophores enterobactin and triacetylfusarinine C. v. 513, p. 505–513, 2003.

HAAS, H. Fungal siderophore metabolism with a focus on *Aspergillus fumigatus*. **Natural Product Reports**, v. 31, n. 10, p. 1266–1276, 2014.

HAAS, H.; EISENDLE, M.; TURGEON, B. G. Siderophores in Fungal Physiology and Virulence. **Annual Review of Phytopathology**, v. 46, n. 1, p. 149–187, 2008.

HALLIWELL, B.; GUTTERIDGE, J. M. C. Oxygen toxicity, oxygen radicals, transition metals and disease. **Biochem. J.**, v. 219, p. 1–14, 1984.

HENNIGAR, S. R.; MCCLUN, J. P. Nutritional Immunity: starving pathogens of trace minerals. **American Journal of Lifestyle Medicine**, 2016.

HENTZE, M. W. et al. Two to Tango: Regulation of Mammalian Iron Metabolism. **Cell**, v. 142, n. 1, p. 24–38, 2010.

HERRERO, M.; LORENZO, V. D. E.; NEILANDS, J. B. Nucleotide Sequence of the iucD Gene of the pColV-K30 Aerobactin Operon and Topology of Its Product Studied with phoA and lacZ Gene Fusions. **Journal of Bacteriology**, v. 170, n. 1, p. 56–64, 1988.

HISSEN, A. H. T. et al. Survival of *Aspergillus fumigatus* in Serum involves removal of iron from transferrin: the role of siderophores. **Infection and Immunity**, v. 72, n. 3, p. 1402–1408, 2004.

HISSEN, A. H. T. et al. The *Aspergillus fumigatus* Siderophore Biosynthetic Gene sidA , Encoding L -Ornithine N 5 -Oxygenase , Is Required for Virulence. **Infection and Immunity**, v. 73, n. 9, p. 5493–5503, 2005.

HOF, C. et al. Siderophore synthesis in *Magnaporthe grisea* is essential for vegetative growth , conidiation and resistance to oxidative stress. **Fungal Genetics and Biology**, v. 46, n. 4, p. 321–332, 2009.

HWANG, L. H. et al. *Histoplasma* requires *SID1*, a member of an iron-regulated siderophore gene cluster, for host colonization. **PLoS Pathogens**, v. 4, n. 4, 2008.

JUNG, H. W. et al. Iron source preference and regulation of iron uptake in *Cryptococcus neoformans*. **PLoS Pathogens**, v. 4, n. 2, 2008.

JUNG, W. H. et al. Role of ferroxidases in iron uptake and virulence of *Cryptococcus neoformans*. **Eukaryotic Cell**, v. 8, n. 10, p. 1511–1520, 2009.

KEHL-FIE, T. E.; SKAAR, E. P. **Nutritional immunity beyond iron: a role for manganese and zinc** *Current Opinion in Chemical Biology*, 2010.

KHAN, A.; SINGH, P.; SRIVASTAVA, A. Synthesis, nature and utility of universal iron chelator – Siderophore : A review. **Microbiological Research**, n. October, p. 0–1, 2017.
KNIGHT, S. A. B. et al. Iron Acquisition from Transferrin by *Candida albicans* depends on the reductive pathway. **Society**, v. 73, n. 9, p. 5482–5492, 2005.

KOSMAN, D. J. Molecular mechanisms of iron uptake in fungi. **Molecular Microbiology**, v. 47, n. 5, p. 1185–1197, 2003.

KRAGL, C. et al. EstB-Mediated Hydrolysis of the Siderophore Triacetyl fusarinine C Optimizes Iron Uptake of *Aspergillus fumigatus*. **Eukaryotic Cell**, v. 6, n. 8, p. 1278–1285, 2007.

KWOK, E. Y.; SEVERANCE, S.; KOSMAN, D. J. Evidence for iron channeling in the Fet3p-Ftr1p high-affinity iron uptake complex in the yeast plasma membrane. **Biochemistry**, v. 45, n. 20, p. 6317–6327, 2006.

LACAZ, C. et al. **Tratado de Micologia Médica**. 9th. ed. São Paulo: Sarvier, 2002.

LOCHT, M.; BOELAERT, J.; SCHNEIDER, Y.-J. Iron uptake from ferrioxamine and from ferrirhizoferrin by germinating spores of *Rhizopus microsporus*. **Biochemical Pharmacology**, v. 47, n. 10, p. 1843–1850, 1994.

MARQUES, S. A. Paracoccidioidomycosis. **Clinics in Dermatology**, p. 610–615, 2012.
MARTINEZ, R. New Trends in Paracoccidioidomycosis Epidemiology. **Journal of Fungi**, p. 1–13, 2017.

MATUTE, D. R. et al. Cryptic Speciation and Recombination in the Fungus *Paracoccidioides brasiliensis* as Revealed by Gene Genealogies. **Mol Biol Evol**, 2006.

MATZANKE, B. et al. Role of Siderophores in Iron Storage in Spores of *Neurospora crassa* and *Aspergillus ochraceus*. v. 169, n. 12, p. 5873–5876, 1987.

MCEWEN, J. G. et al. Experimental murine paracoccidioidomycosis induced by the

inhalation of conidia. **J Med Vet Mycol**, v. 25, n. 3, p. 165–175, 1987.

MEI, B.; BUDET, A. D.; LEONG, S. A. sid1 , a gene initiating siderophore biosynthesis in *Ustilago maydis*: Molecular characterization, regulation by iron, and role in phytopathogenicity. **Proc. Natl. Acad. Sci.**, v. 90, n. February, p. 903–907, 1993.

MENDES, R. P. et al. Paracoccidioidomycosis : Current Perspectives from Brazil. **Open Microbiology Journal**, p. 224–282, 2017.

MIETHKE, M.; MARAHIEL, M. A. Siderophore-Based Iron Acquisition and Pathogen Control. **Microbiology and Molecular Biology Reviews**, v. 71, n. 3, p. 413–451, 2007.

MOORE, R. E.; KIM, Y.; PHILPOTT, C. C. The mechanism of ferrichrome transport through Arn1p and its metabolism in *Saccharomyces cerevisiae*. **Pnas**, 2003.

NEILANDS, J. B. Siderophores. **Archives of biochemistry and biophysics**, v. 302, n. 1, p. 1–3, 1993.

NEMETH, E. et al. Hepcidin , a putative mediator of anemia of inflammation , is a type II acute-phase protein. v. 101, n. 7, p. 2461–2463, 2003.

NEMETH, E. et al. IL-6 mediates hypoferremia of inflammation by inducing the synthesis of the iron regulatory hormone hepcidin. v. 113, n. 9, p. 1271–1276, 2004.

NEVITT, T.; THIELE, D. J. Host iron withholding demands siderophore utilization for *Candida glabrata* to survive macrophage killing. **PLoS Pathogens**, v. 7, n. 3, 2011.

NICOLAS, G. et al. Lack of hepcidin gene expression and severe tissue iron overload in upstream stimulatory factor 2 (USF2) knockout mice. **Proceedings of the National Academy of Sciences of the United States of America**, v. 98, p. 8780–8785, 2001.

NICOLAS, G. et al. The gene encoding the iron regulatroy peptide hepcidin is regulated by anemica, hypoxia and inflammation. **The journal of Clinical Investigation**, v. 110, 2002.

OBEREGGER, H. et al. Identification of members of the *Aspergillus nidulans* SREA regulon : genes involved in siderophore biosynthesis and utilization. **Biometals**, p. 6–8, 2002.

OBEREGGER, H.; SCHÖESER, M.; ZADRA, I. SREA is involved in regulation of siderophore biosynthesis , utilization and uptake in *Aspergillus nidulans*. **Molecular Microbiology**, v. 41, p. 1077–1089, 2001.

PAO, S. S.; PAULSEN, I. A. N. T.; SAIER, M. H. Major Facilitator Superfamily. **Microbiology and Molecular Biology Reviews**, v. 62, n. 1, p. 1–34, 1998.

PARENTE, A. F. A. et al. Proteomic analysis reveals that iron availability alters the metabolic status of the pathogenic fungus *Paracoccidioides brasiliensis*. **PLoS ONE**, v. 6, n. 7, 2011.

PARK, C. H. et al. Hepcidin, a Urinary Antimicrobial Peptide Synthesized in the Liver. **Journal of Biological Chemistry**, v. 276, n. 11, p. 7806–7810, 2001.

PENDRAK, M. L. et al. Heme Oxygenase in *Candida albicans* Is Regulated by Hemoglobin and Is Necessary for Metabolism of Exogenous Heme and Hemoglobin to α -Biliverdin. **Journal of Biological Chemistry**, v. 279, n. 5, p. 3426–3433, 2004.

PHILPOTT, C. C.; PROTCHENKO, O. Response to Iron Deprivation in *Saccharomyces cerevisiae*. **Eukaryotic Cell**, v. 7, n. 1, p. 20–27, 2008.

PRADO, M. et al. Mortality due to systemic mycoses as a primary cause of death or in association with AIDS in Brazil : a review from 1996 to 2006. **Mem Inst Oswaldo Cruz**, v. 104, n. May, p. 513–521, 2009.

QIU, A. et al. Identification of an Intestinal Folate Transporter and the Molecular Basis for Hereditary Folate Malabsorption. **Cell**, v. 127, n. 5, p. 917–928, 2006.

RESTREPO, A.; MCEWEN, J. G.; CASTAÑEDA, E. The habitat of *Paracoccidioides brasiliensis*: how far from solving the riddle? **Medical Mycology**, v. 39, n. 3, p. 233–241, 2001.

RESTREPO M, A. The ecology of *Paracoccidioides brasiliensis*: A puzzle still unsolved. **Medical and Veterinary Mycology**, v. 23, n. 5, p. 323–334, 1985.

RICCI, G. et al. Canine paracoccidioidomycosis. **Med Mycol**, n. May 2014, 2004.
RODRIGUES DE FARIAS, M. et al. Paracoccidioidomycosis in a Dog : Case Report of Generalized Lymphadenomegaly. **Mycopathologia**, n. March, 2011.

RODRIGUEZ, R. et al. Hepcidin induction by pathogens and pathogen-derived molecules is strongly dependent on interleukin-6. **Infection and Immunity**, v. 82, n. 2, p. 745–752, 2014.

ROONEY, P. J.; KLEIN, B. S. Linking fungal morphogenesis with virulence. **Cellular Microbiology**, v. 4, p. 127–137, 2002.

SALAZAR, M. E.; RESTREPO, A.; STEVENS, D. A. Inhibition by estrogens of Conidium-to-Yeast Conversion in the Fungus *Paracoccidioides brasiliensis*. **Infection and Immunity**, v. 56, n. 3, p. 711–713, 1988.

SALGADO-SALAZAR, C.; JONES, L. R.; MCEWEN, J. G. Cladistics The human fungal pathogen *Paracoccidioides brasiliensis* (Onygenales : Ajellomycetaceae) is a complex of two species : phylogenetic evidence from five mitochondrial markers.

Cladistics, v. 26, p. 613–624, 2010.

SAN-BLAS, G.; NINO-VEGA, G.; ITURRIAGA, T. *Paracoccidioides brasiliensis* and paracoccidioidomycosis: Molecular approaches to morphogenesis, diagnosis, epidemiology, taxonomy and genetics. **Medical Mycology**, n. June 2001, p. 225–242, 2002.

SANO, A. et al. Pathogenicities and GP43kDa gene of three *Paracoccidioides brasiliensis* isolates originated from a nine-banded armadillo (*Dasypus novemcinctus*). **Mycopathologia**, v. 1, p. 61–65, 1999.

SCHADE, A. L.; CAROLINE, L. Raw hen egg white and the role of iron in growth inhibition of *Shigella dysenteriae*, *Staphylococcus aureus*, *Escherichia coli* and *Saccharomyces cerevisiae*. **Science**, 1944.

SCHRETTL, M. et al. Distinct roles for intra- and extracellular siderophores during *Aspergillus fumigatus* infection. **PLoS Pathogens**, v. 3, n. 9, p. 1195–1207, 2007.

SHANKAR, J. et al. Hormones and the Resistance of Women to Paracoccidioidomycosis. **Clinical Microbiology Reviews**, v. 24, n. 2, p. 296–313, 2011.

SHIKANAI-YASUDA, M. A. et al. Consenso em paracoccidioidomicose. **Rev Soc Bras Med Trop**, v. 39, n. 3, p. 297–310, 2006.

SHIKANAI-YASUDA, M. A. et al. Consensus Brazilian guidelines for the clinical management of paracoccidioidomycosis. **Rev Soc Bras Med Trop**, v. 50, n. June, p. 715–740, 2017.

SHIKE, H. et al. Bass hepcidin is a novel antimicrobial peptide induced by bacterial challenge. **European Journal of Biochemistry**, v. 269, n. 8, p. 2232–2237, 2002.

SILVA-BAILÃO, M. G. et al. Hydroxamate production as a high affinity iron acquisition mechanism in *Paracoccidioides* Spp. **PLoS ONE**, v. 9, n. 8, 2014.

SILVA, C. et al. Argentilactone Molecular Targets in *Paracoccidioides brasiliensis* Identified by chemoproteomics. **Antimicrobial Agents and Chemotherapy**, n. August, p. 55–62, 2018a.

SILVA, L. C. et al. Computer-aided identification of novel anti-paracoccidioidomycosis compounds. **Future microbiology**, 2018b.

SILVA, M. G. et al. The homeostasis of iron, copper, and zinc in *Paracoccidioides brasiliensis*, *Cryptococcus neoformans* var. *Grubii*, and *Cryptococcus gattii*: A comparative analysis. **Frontiers in Microbiology**, v. 2, n. MAR, p. 1–19, 2011.

SYLVESTRE, T. F. et al. Serological proteomic biomarkers to identify *Paracoccidioides* species and risk of relapse. **PLoS ONE**, p. 1–14, 2018a.

SYLVESTRE, T. F. et al. Ceruloplasmin , transferrin and apolipoprotein A-II play important role in treatment ' s follow- up of paracoccidioidomycosis patients. **PLoS ONE**, p. 1–18, 2018b.

TEIXEIRA, M. M. et al. Phylogenetic analysis reveals a high level of speciation in the *Paracoccidioides* genus. **Molecular Phylogenetics and Evolution**, v. 52, n. 2, p. 273–283, 2009.

TEIXEIRA, M. M. et al. Paracoccidioides Species Complex: Ecology, Phylogeny, Sexual Reproduction, and Virulence. **PLoS Pathogens**, v. 10, n. 10, p. 4–7, 2014.

TERÇARIOLI, G. R. et al. Ecological study of *Paracoccidioides brasiliensis* in soil : growth ability , conidia production and molecular detection. **BMC microbiology**, v. 8, p. 1–8, 2007.

THEODORO, R. C. et al. Genus *Paracoccidioides*: Species recognition and biogeographic aspects. **PLoS ONE**, v. 7, n. 5, 2012.

THEURL, I. et al. Regulation of iron homeostasis in anemia of chronic disease and iron deficiency anemia: diagnostic and therapeutic implications. **Blood**, v. 113, n. 21, p. 5277–5287, 2009.

THIEKEN, A.; WINKELMANN, G. Rhizoferrin: A complexone type siderophore of the Mucorales and Entomophthorales (Zygomycetes). **FEMS Microbiology Letters**, v. 94, n. 1–2, p. 37–41, 1992.

TRAVASSOS, L. R.; TABORDA, C. P. Paracoccidioidomycosis vaccine. **Human Vaccines & Immunotherapeutics**, v. 8, n. 10, p. 1450–1453, 2012.

TREJO-CHÁVEZ, A. et al. Disseminated Paracoccidioidomycosis in a Southern Two-Toed Sloth (*Choloepus didactylus*). **J. Comp. Pathol**, v. 144, p. 231–234, 2011.

TURISSINI, D. A. et al. Species boundaries in the human pathogen *Paracoccidioides*. **Fungal Genetics and Biology**, v. 106, n. June, p. 9–25, 2017a.

TURISSINI, D. A. et al. Species boundaries in the human pathogen *Paracoccidioides*. **Fungal Genetics and Biology**, v. 106, n. June, p. 9–25, 2017b.

UNTEREINER, W. A.; SCOTT, J. A.; SIGLER, L. The Ajellomycetaceae , a New Family of Vertebrate-Associated Onygenales The Ajellomycetaceae , a new family of vertebrate-associated Onygenales. **Mycologia**, n. October, 2016.

VALDEZ, Y. et al. Nramp1 drives an accelerated inflammatory response during *Salmonella*-induced colitis in mice. **Cellular Microbiology**, v. 11, n. 2, p. 351–362, 2009.

VALLE, A. C. F. et al. Paracoccidioidomycosis after Highway Construction, Rio de Janeiro, Brazil. **Emerging Infectious Diseases**, v. 23, n. 11, p. 1917–1919, 2017.

VIEIRA, G. D. D. et al. Paracoccidioidomycosis in a western Brazilian Amazon State: Clinical-epidemiologic profile and spatial distribution of the disease. **Revista Da Sociedade Brasileira De Medicina Tropical**, v. 47, n. January, p. 63–68, 2014.

VISCA, P.; CIERVO, A.; ORST, N. Cloning and Nucleotide Sequence of the *pvdA* Gene Encoding the Pyoverdin Biosynthetic Enzyme L-Ornithine N5-Oxygenase in *Pseudomonas aeruginosa*. **Journal of Bacteriology**, v. 176, n. 4, p. 1128–1140, 1994.

WEINBERG, E. D. Nutritional Immunity: Host's Attempt to Withhold Iron From Microbial Invaders. **JAMA: The Journal of the American Medical Association**, v. 231, n. 1, p. 39–41, 1975.

WEISSMAN, Z. et al. An endocytic mechanism for haemoglobin-iron acquisition in *Candida albicans*. **Molecular Microbiology**, v. 69, n. 1, p. 201–217, 2008.

WEISSMAN, Z.; KORNITZER, D. A family of *Candida* cell surface haem-binding proteins involved in haemin and haemoglobin-iron utilization. **Molecular Microbiology**, v. 53, n. 4, p. 1209–1220, 2004.

WHO. Iron Deficiency Anaemia: Assessment, prevention and control. 2001.

WINKELMANN, G. Microbial siderophore-mediated transport. **Biometals**, 2002.

YASMIN, S. et al. Mevalonate governs interdependency of ergosterol and siderophore biosyntheses in the fungal pathogen *Aspergillus fumigatus*. **Proceedings of the National Academy of Sciences**, v. 109, n. 8, p. E497–E504, 2011.

ZIEGLER, L. et al. Functional characterization of the ferroxidase, permease high affinity iron transport complex from *Candida albicans*. v. 1, n. 3, p. 233–245, 2011.



Anexo

Identification of membrane proteome of *Paracoccidioides lutzii* and its regulation by zinc

Aim: During infection development in the host, *Paracoccidioides* spp. faces the deprivation of micronutrients, a mechanism called nutritional immunity. This condition induces the remodeling of proteins present in different metabolic pathways. Therefore, we attempted to identify membrane proteins and their regulation by zinc in *Paracoccidioides lutzii*. **Materials & methods:** Membranes enriched fraction of yeast cells of *P. lutzii* were isolated, purified and identified by 2D LC–MS/MS detection and database search. **Results & conclusion:** Zinc deprivation suppressed the expression of membrane proteins such as glycoproteins, those involved in cell wall synthesis and those related to oxidative phosphorylation. This is the first study describing membrane proteins and the effect of zinc deficiency in their regulation in one member of the genus *Paracoccidioides*.

Lay abstract: The methodology of protein identification allows the characterization of biological processes performed by those molecules. Therefore, we performed a membrane proteomic analysis of *Paracoccidioides lutzii* and further evaluated the responses of the fungus to zinc deprivation. The results obtained in the work allowed the characterization of membrane proteins present in organelles that are related to different cellular functions. Zinc deprivation changes processes related to cellular physiology and metabolism. These results help us to understand the process of pathogen–host interaction, since zinc deprivation is a condition present during infection.

First draft submitted: 6 April 2017; Accepted for publication: 21 June 2017; Published online: 25 July 2017

Keywords: membranes • nanoUPLC-MS^E • *Paracoccidioides lutzii* • proteome
• zinc deprivation

The genus *Paracoccidioides* comprises the etiologic agents of paracoccidioidomycosis, the most widespread systemic mycosis in Latin America. As other thermodimorphic fungi, members of the genus *Paracoccidioides* grow as mycelia in the environment and as yeast cells at 36°C and in host tissues [1]. The infection occurs through the host respiratory route [2], in which inhalation of conidia or mycelial propagules allows these structures to reach the host pulmonary alveoli, in which they perform the dimorphic transition and

differentiate into yeast cells [3]. This mycosis represents an important public health problem due the quantity of premature deaths, particularly in certain segments of society, such as rural workers [4].

Zinc is a metal of importance for the development of microorganisms. It serves as a structural or catalytic cofactor for many proteins, participating in several processes, such as cell division and differentiation [5]. Zinc homeostasis, a critical process to cells, is maintained at both transcriptional and post-

Juliana Santana de Curcio^{‡,1},
Marielle Garcia Silva^{‡,1},
Mirelle Garcia Silva Bailão¹,
Sônia Nair Báo³, Luciana
Casaletti¹, Alexandre Mello
Bailão¹ & Célia Maria de
Almeida Soares^{*,1}

¹Laboratório de Biologia Molecular,
Instituto de Ciências Biológicas,
Universidade Federal de Goiás, Goiânia,
Goiás, Brazil

²Unidade Acadêmica Especial Ciências da
Saúde, Universidade Federal de Goiás,
Jataí, Goiás, Brazil

³Laboratório de Microscopia,
Universidade de Brasília, Brasília, Brazil

⁴Escola de Engenharia, Pontifícia
Universidade Católica de Goiás, Goiás,
Brazil

*Author for correspondence:
Tel.: +55 62 35211736
cmasoares@gmail.com

[‡]Authors contributed equally

translational levels occurring in response to changes in intracellular zinc levels [6]. The uptake of zinc in *Saccharomyces cerevisiae* is mediated by two systems: the high-affinity uptake system, which is active in zinc-limited conditions [7]; and the low-affinity uptake system, which is active in the presence of sufficient zinc concentrations [8]. The expression and activity of the high-affinity zinc transporter (*Zrt1*) and low-affinity zinc transporter (*Zrt2*) are regulated by the transcription factor, *Zap1* [9,10]. During zinc limitation, *Zap1* induces the expression of *Zrt1* and *Zrt2* [11]. The regulation at post-translational level occurs when the cell, under low zinc concentration, is exposed to high extracellular levels of zinc. This exposure causes the internalization of *Zrt1p* protein via endocytosis and subsequent degradation in the vacuole [10]. Another mechanism of zinc uptake, at the intracellular level, includes the *Msc2p* and *Zrg17p* transporters, which are localized at the endoplasmic reticulum and induced under zinc deficiency [12,13]. The vacuole is the main site of zinc sequestration and detoxification in the yeast *S. cerevisiae* [14]. Two transporters of the cation diffusion facilitator family named *Zrc1p* and *Cot1p* are responsible for vacuole zinc accumulation [15]. *Zrt3p* is another transporter localized at vacuolar membrane, which is responsible for the release of zinc into the cytoplasm upon metal deficiency in *S. cerevisiae* [15,16].

In *Paracoccidioides* spp., *in silico* analyses identified zinc transporters homologs to those described in *S. cerevisiae* such as *Zrt1p*, *Zrt2p*, *Zrc1p*, *Cot1p* and *Msc2p*. Moreover, a homolog to the transcriptional factor *Zap1* is also present in the genome of *Paracoccidioides* spp. [17]. Studies demonstrated the induction of *Zrt1* and *Zrt2* expression in yeast cells upon zinc deprivation [18,19] and induction of *Zrt2* in neutral to alkaline pH during zinc deficiency, as described to *ZrfC* in *Aspergillus fumigatus* [18]. Moreover, studies on *Paracoccidioides* sp., after contact with human plasma and liver of mice revealed the induction of high-affinity zinc transporter under these conditions [20,21].

Plasma membrane plays an important role in cells, acting as a physical barrier, regulating the exchange of information, ions and metabolites between the cell and the environment [22]. Moreover, membranes are responsible for the intracellular compartmentalization of organelles [23]. Membrane proteins perform a variety of functions such as transport, cell adhesion, signal receptors and nutrient uptake. Zinc transporters (*Zrt1p* and *Zrt2p*) are located at the plasma membrane [9] on dependence of the concentration of zinc in the medium [10,23]. Around 30% of the open-reading frames in eukaryote genomes encode for integral membrane proteins [24]. However, analysis of membrane proteins is underrepresented in proteomic

analyses, owing to the heterogeneous nature of those molecules [23]. Insolubility in aqueous buffers, hindering the extraction steps of the lipid bilayer [25] and inhibition of the tryptic activity in the segments of the integral membrane proteins [26] make those molecules underrepresented in proteomic analysis. Therefore, the establishment of a methodology able to encompass all these characteristics is a challenge in proteomic sciences [27].

Although membrane proteins perform cellular processes essential to cell survival, the knowledge about this class of proteins is still limited in *Paracoccidioides* spp. To our knowledge, *Paracoccidioides* spp. membrane proteome has not been analyzed yet. Therefore, the current study is intended to investigate, using nanoUPLC-MS^E and label-free approach, proteins in membranes of *Paracoccidioides lutzii* and their responses to zinc deprivation. This study allowed the identification of proteins belonging to the whole membrane system, comprising plasma membrane and membranes of cytoplasmic organelles, such as mitochondria, peroxisome, vacuole and endoplasmic reticulum. The biological processes performed by zinc-regulated proteins include composition of cell wall, vesicles traffic, oxidative phosphorylation, zinc uptake in the vacuole and glycosylation in the endoplasmic reticulum. Besides depicting the first large-scale depository of membrane proteins in the genus *Paracoccidioides*, this article highlights protein candidates potentially involved in the response to zinc limitation, a condition found in the host.

Materials & methods

Fungal strain, growth conditions & zinc deprivation experiments

The experiments were performed with *P. lutzii*, *Pb01* (ATCC MYA-826). The yeast phase was maintained at 36°C in Fava Netto's medium (1% [w/v] peptone, 0.5% [w/v] yeast extract, 0.3% [w/v] proteose peptone, 0.5% [w/v] beef extract, 0.5% [w/v] NaCl, 4% [w/v] glucose, 1.2% [w/v] agar, pH 7.2) [28] supplemented with 4% (w/v) glucose. Yeast cells were inoculated in Fava Netto's liquid medium for 72 h at 36°C, 150 rpm, in order to obtain cells at the exponential growth phase. Afterward, the cells were centrifuged at 1200 × g for 10 min at 4°C and washed in phosphate-buffered saline (PBS 1X). The supernatant was discarded, the cells were resuspended in PBS 1× and inoculated at the concentration of 10⁶ cells/ml in McVeigh/Morton' liquid medium (MMcM) containing: 4% (w/v) glucose, 0.15% (w/v) KH₂PO₄, 0.05% (w/v) MgSO₄·7H₂O, 0.015% (w/v) CaCl₂·2H₂O, 0.2% (w/v) (NH₄)₂SO₄, 0.2% (w/v) L-asparagine, 0.02% (w/v) L-cystine, 1% (v/v) of vitamin supplement (0.006% [w/v] thiamine, 0.006% [w/v] niacin

B3, 0.006% [w/v] Ca²⁺ pantothenate, 0.001% [w/v] inositol B7, 0.0001% [w/v] biotin B8, 0.001% [w/v] riboflavin, 0.01% [w/v] folic acid B9, 0.01% [w/v] choline chloride, 0.01% [w/v] pyridoxine) and 0.1% (v/v) of trace elements supplement (0.0057% [w/v] H₃BO₃, 0.0081% [w/v] MnSO₄.14H₂O, 0.0036% [w/v] (NH₄)₆MO₇O₂₄.4H₂O, 0.0157% [w/v] CuSO₄.H₂O, 0.1404% [w/v] Fe(NH₄)₂(SO₄)₂.6H₂O) [29], pH 7.0, for 24 h.

Following 24 h of cultivation in MMCM medium, 10⁶ cells/ml were transferred to the same medium containing 30 μM ZnSO₄.7H₂O, or depleted of zinc. The depleted medium was prepared with no addition of ZnSO₄ and was supplemented with the zinc chelator N,N,N,N-tetrakis(2-pyridyl-methyl) ethylenediamine (Sigma-Aldrich, MO, USA) at a concentration of 0.05 mM. The cultures were incubated with gentle shaking at 36°C for 24 h, 150 rpm, as previously described [19].

Extraction of membrane proteins

The protocol described by Vidakovics *et al.* [30] was used with some modifications. Experiments were performed in biological triplicates as three independent experiments. Yeast cells cultured in MMCM medium were centrifuged at 1200×g for 10 min at 4°C, frozen in liquid nitrogen and disrupted by maceration using a gral and pestle until a fine powder was obtained [31]. After this step, the sample was transferred to a conical tube and resuspended in 50 mM Tris-HCl, pH 7.5. Glass beads were added to the conical tube and after agitation for 20 min at 4°C, the sample was subjected to centrifugation at 8000 × g for 10 min at 4°C. The supernatant was diluted in 10 ml of 0.1 M sodium carbonate (Na₂CO₃) pH 11 for 1 h. The carbonate treated sample was submitted to ultracentrifugation in a Beckman Coulter Optima L-90K centrifuge at 115,000 × g for 1 h, at 4°C. The supernatant was discarded and the pellet containing the membranes fraction was resuspended in 50 mM Tris-HCl pH 7.5 using a glass homogenizer (grinder) on ice, to solubilize the membranes fraction. The sample was submitted to another step of ultracentrifugation at 115,000 × g for 1 h at 4°C. An aliquot of the pellet was used for the transmission electron microscopy (TEM) analysis while the remainder was resuspended in 50 mM ammonium bicarbonate pH 8.0 and stored at -80°C.

Transmission electron microscopy

TEM was performed to evaluate the quality of the sample. TEM of the membranes fraction was performed according to standard protocols [32]. The samples of the membrane fraction and intact cells of *P. lutzii* were fixed in 2% (w/v) paraformaldehyde and 2% (v/v) glutaraldehyde in 0.1 M sodium caco-

dylate buffer, pH 7.2, for 2 h, at room temperature. After washing in 0.1 M sodium cacodylate buffer pH 7.2, the samples were postfixed in 2% (w/v) osmium tetroxide, 1.6% (w/v) potassium fericyanide (1:1) and 5 mM CaCl₂ in sodium cacodylate buffer, pH 7.2, for 1 h, at room temperature, followed by washing in 0.1 M sodium cacodylate buffer, pH 7.2. The samples were maintained for 12 h in an aqueous solution of 0.5% (v/v) uranyl acetate at 4°C, washed in distilled water and dehydrated in an ascending series of acetone (v/v) (30, 50, 70, 90 and 100%). The material was embedded in a mixture of (3:1) acetone/Spurr resin (Eletron Microscopy Sciences, Co.) for 6 h, (2:1) acetone/Spurr resin overnight, (1:1) acetone/Spurr resin for 6 h, (1:2) acetone/Spurr resin overnight and finally in pure resin for 6 h. The samples were imbibed in Spurr resin for 3 days in an incubator, at 60°C. The ultrathin sections were contrasted with 3% (v/v) aqueous uranyl acetate and 10% (v/v) lead citrate. The samples were analyzed in a TEM, JEM 1011 (Electron Microscopy Sciences, Co, Jeol, Tokyo, Japan.)

Preparation of membrane proteins for nanoUPLC-MS^E analysis

The amount of protein in the membrane extract was determined using the Bradford reagent (Sigma-Aldrich) [33]. The samples were analyzed using nanoscale LC-MS/MS. Sample aliquots (100 μg) were prepared for nanoUPLC-MS^E as previously described [34]. Briefly, ammonium bicarbonate pH 8.5 at 50 mM and 75 μl of 0.2% (v/v) RapiGEST (Waters Corp, MA, USA) were sequentially added to the samples. After, the solution was vortexed and incubated in dry bath for 15 min at 80°C. After incubation, the samples were centrifuged and the proteins reduced by adding 2.5 μl of a 100 mM DTT solution, followed by incubation for 30 min at 60°C. The alkylation of proteins was performed by addition of 2.5 μl of 300 mM iodoacetamide and incubation in a dark room for 30 min. An aliquot of 40 μl of trypsin (Promega, WI, USA) 50 ng/μl in 50 mM ammonium bicarbonate was added. The sample was vortexed slightly and digested at 37°C for 16 h. Following digestion, the hydrolysis of RapiGEST was performed by addition of 10 μl of 5% (v/v) trifluoroacetic acid and incubation at 37°C for 90 min. The sample was centrifuged at 20,000 × g at 6°C for 30 min, and the supernatant was transferred to microfuge tubes and dried in a speed vacuum. Peptides were solubilized in 30 μl of ultrapure water, submitted to purification and concentration using a pipette tip with a bed of chromatographic media (ZipTips® C18 Pipette Tips, MA, USA) and dried in a speed vacuum. The peptides were resuspended in a solution of 1 pmol/μl MassPREP Digestion Standard (rabbit phos-

phorilase B; Waters Corp) to prepare the final concentration of 200 fmol/μl of the rabbit phosphorilase B. The buffer solution of 20 mM ammonium formate was used to increase the pH. After solubilization, peptides were transferred to a Waters Total Recovery vial (Waters Corp).

NanoUPLC-MS^E analysis

The proteomic analysis was performed using a label-free nanoUPLC-MS^E technology. Briefly, tryptic peptides were separated by RP-RP-HPLC using a nano-ACQUITY™ system (Waters Corp), as described before [35]. The first column was loaded with 5 μg digests and sequentially, separated in ten fractions in the mobile phase at pH 10. Each fraction was subjected to the second dimension of RP chromatography with a mobile phase at pH 2.5. Label-free data-independent scanning (MS^E) experiments were performed with a Synapt HDMS mass spectrometer (Waters, Manchester, UK), which switched between low collision energy (3 eV) and elevated collision energy (12–40 eV) applied to the trap ‘T-wave’ CID cell with argon gas, as described [36].

The protein identifications and quantitative packaging were generated using specific algorithms [37,38] and search was performed against an in-house *P. lutzii*-specific database. The ProteinLynx Global server v.2.5.2 (PLGS) was used to perform the spectral processing, database searching conditions and quantitative comparisons. The specific database was randomized in order to access the false-positive rate of identification (4%). The intensity measurements were typically adjusted for these components, in other words, the deisotoped and charge state-reduced exact mass-retention times that were replicated throughout the entire experiment for the analysis at the exact mass retention-time cluster level. Components were typically clustered with a 10 ppm mass precision and a 0.25 min time tolerance against the database-generated theoretical peptide ion masses with a minimum of one matched peptide. The alignment of elevated energy ions with low-energy precursor peptide ions was performed with an approximate precision of 0.05 min. The precursor and fragmentation tolerances were determined automatically. The search parameters used were: trypsin as digest reagent, 1 missed cleavage, carbamidomethyl as fixed modification and phosphorylation STY and oxidation M were used as variable modifications. The minimum fragment ion matches per peptide, the minimum fragment ion matches per protein and the minimum peptide matches per protein were, respectively, set as 2, 5 and 1. The mass variation tolerance was set to 50 ppm. A protein detected in all replicates, presenting a variance coefficient less than 10%

(PAAG_08059), was used to normalize the expression data to compare the protein levels between control and zinc-limiting conditions. Protein and peptides tables generated by PLGS were merged and the dynamic range of the experiments, peptides detection type and mass accuracy were determined for each condition [39]. Software FBAT [40], MassPivot (kindly provided by AM Murad), Spotfire® (© TIBCO Software Inc.) and Microsoft Office Excel (Microsoft©) were used.

In silico analysis

The data obtained after analysis by nanoUPLC-MS^E and identification in ProteinLynx were submitted to *in silico* search in database in order to determine proteins subcellular location and association with cell membranes. The subcellular location was determined by using WoLF PSORT (www.genscript.com/psort/wolf_psorth.html) [41] and Gene Ontology (GO; <http://pedant.gsf.de/>) databases [42]. The protein association with membranes evaluated the presence of transmembrane domains and prenylation, myristylation, palmitoylation and GPI anchor. The TMHMM program, version 2.0 (www.cbs.dtu.dk/services/TMHMM) [43] was used to predict transmembrane regions. The big-PI Fungal Predictor program (http://mendel.imp.ac.at/gpi/fungi_server.html) [44] was used to predict glycosylphosphatidylinositol anchors. The search for myristoylated proteins was performed using the programs, Myristoylator (<http://web.expasy.org/myristoylator/>) [45] and TerminiNator (www.isv.cnrs-gif.fr/terminator3/index.html) [26]. The last was also utilized for the prediction of palmitoylated proteins, while the prediction of prenylation was achieved with the PrePS-Prenylation Prediction Suite (<http://mendel.imp.ac.at/sat/PrePS/index.html>) software [46]. The search for signal peptide was performed using the SignalP program, version 4.1 (www.cbs.dtu.dk/services/SignalP/) [47]. Loctree program (<https://rostlab.org/services/loc-tree2/>) [48] was employed in order to determine in which organelle membrane proteins were localized. The functional classification of proteins present in membranes fraction was accomplished using Funcat2 database (http://pedant.gsf.de/pedant3htmlview/pedant3view?Method=analysis&Db=p3_r48325_Par_brasil_Pb01).

Analysis of chitin amount in the cell wall of *P. lutzii*

Calcoflour white (CFW, Sigma Biochemical) was utilized to stain *P. lutzii* (Pb01) yeast cells in order to evaluate the effect of zinc deprivation at the cell wall. *P. lutzii* yeast cells were grown under zinc deprivation or in presence of this metal for 24 h. For analysis of chitin amount, the cells were fixed in 100% methanol at -80°C for 20 min, at -20°C for additional 20 min

and subsequently washed by centrifugation. The cells were collected, stained with CFW (100 µg/ml in PBS 1×) for 30 min and washed with PBS 1×. The specimens were analyzed under a fluorescence microscope (Zeiss AxioCam MRc – Scope A1) [49]. CFW fluorescence intensity was measured using the AxioVision Software (Carl Zeiss AG, Germany). The minimum of 100 cells for each microscope slides, in triplicates, were used to evaluate fluorescence intensity of the cells upon zinc presence or deprivation, for 24 h. The software provided the fluorescence intensity (in pixels) and the standard error of each analysis. Statistical comparisons were performed using the Student's t test and p-values ≤0.05 were considered statistically significant.

Schiff periodic acid staining of proteins

The staining with Schiff periodic acid was performed in order to evaluate the profile of glycosylated proteins during zinc deficiency. After separation of membrane proteins by electrophoresis, the proteins were fixed in 10% (v/v) acetic acid and 25% (v/v) isopropanol by 18 h at 4°C. After this step, the polyacrylamide gel was washed twice during 15 min with 7.5% (v/v) acetic acid and immersed in a solution of 0.4% (v/v) periodic acid for 1 h at 4°C. Afterward, the gel was immersed in Schiff reagent for 1 h at 4°C in the dark, and subsequently washed three times, 10 min each, in 0.5% (v/v) potassium metabisulfite in the dark. The gel was washed with 7.5% (v/v) acetic acid for 5 min and stored in the same solution at 4°C [50].

Analysis of glycosylated proteins & glucans by fluorescence microscopy

The profile of glycosylated proteins during zinc deprivation was evaluated by staining with Concanavalin A (ConA) TYPE VI conjugated to FITC (Sigma, catalog n.C7642). The yeast cells cultured in the presence or absence of zinc were stained with ConA+FITC at a final concentration of 100 µg/ml [51]. ConA+FITC in a volume of 200 µl was incubated with yeast cells of *P. lutzii* at 37°C, for 30 min, under stirring. After, the cells were washed with PBS 1×, twice. The cells were incubated with aniline blue solution 100% (v/v) (Sigma, catalog n.B8563) for 5 min under stirring and subsequently washed twice with PBS 1× [52]. Both samples stained with ConA+FITC or aniline blue were visualized under a fluorescence microscope (Zeiss AxioCam MRc-Scope A1). Fluorescence intensity was calculated as described above, for both dyes.

Results

TEM of *Pb01* membranes fraction

The membrane proteins of *Pb01* were obtained according to the steps shown in the workflow chart

(Supplementary Figure 1). TEM was performed in order to confirm the enrichment of samples with cell membranes of *P. lutzii*. As shown in Figure 1, the membrane fragments detected in the electron micrograph corroborate the enrichment of the extract.

Proteomic data

NanoUPLC-MS^E is a method that improves protein and proteome coverage compared with the conventional LC–MS/MS approach [34]. The results presented here are from merged data of three replicates, leading to the identification of 746 proteins from the total membranes preparation of *P. lutzii*. Of the 746 proteins, 717 were identified with two or more peptides (data not shown). The resulting nanoUPLC-MS^E protein and peptide data generated by PLGS process are shown in Supplementary Figures 2 & 3. The experiments resulted in 2938 and 2237 identified peptides; 55 and 59% were obtained from peptide match-type data in the first pass to control and zinc deprivation conditions, respectively, and 16% were obtained in the second pass in both conditions (Supplementary Figure 2). A total of 14% of the peptides were identified by a missed trypsin cleavage in both experimental conditions, whereas in source fragmentation rates of 4 and 1% were obtained to control and zinc deprivation, respectively (Supplementary Figure 2). The results obtained from dynamic range detection are presented in Supplementary Figure 3. This graphic represents the concentration of proteins identified in their detection range.

Subcellular localization of *P. lutzii* membrane proteins

The identified proteins in the whole membrane system in number of 746 were evaluated regarding to the subcellular localization using the cellular component information of GO and WoLF PSORT softwares (Supplementary Table 1). The proteins were present in at least two replicates, to be included in the analysis (data not shown). *In silico* analysis revealed that 27.61% (206 proteins) of the identified proteins are presumably not present in membranes, but located in the cytoplasmic region; 25.2% (188 proteins) of the identified proteins were present in membranes, including plasma membrane, mitochondria, endoplasmic reticulum, Golgi complex, peroxisome and vacuole; 24.66% (184 proteins) were presumably inside mitochondria (Supplementary Figure 4).

Proteins in the whole membrane system of *P. lutzii*

The criteria for considering proteins as associated with membranes were the presence of transmem-

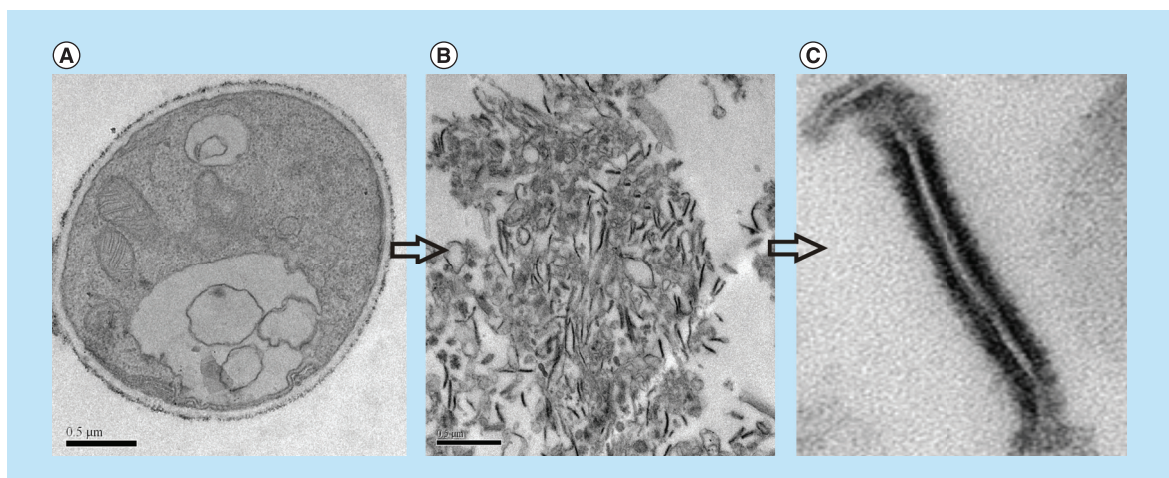


Figure 1. Transmission electron microscopy of *Paracoccidioides lutzii*, whole membranes system fraction. (A) Intact cells of *P. lutzii*. (B) Membranes extract. (C) Fragment of membrane, evidencing the lipid bilayer (increase of 40,000 times).

brane domains and post-transcriptional modifications (prenylation, myristoylation, palmitoylation and GPI anchor). In addition, proteins described in GO terms as belonging to cell membranes with score higher than 50 were classified as membrane proteins. From the total of 746 identified proteins (*Supplementary Table 1*), 25.2% (188 proteins) were classified as belonging to the membranes of *P. lutzii* (*Supplementary Table 2*).

Regarding to the 188 proteins identified as members of the membranes in yeast cells of *P. lutzii*, we analyzed the type of cellular membrane that they belong to. According to Loctree software annotations, the identified membrane proteins originated from various organelles, and this finding confirms the ability of the used method to access all cellular membranes. According to our data depicted in *Supplementary Figure 5*, from the whole membrane system, 38% (71 proteins) represent mitochondrial membrane proteins, 24% (46 proteins) and 16% (30 proteins) represent endoplasmic reticulum and plasma membrane proteins, respectively. Besides, Golgi complex membrane proteins represent 5% (10 proteins), vacuole membrane proteins comprise 3% (6 proteins) and nucleus membrane proteins represent 2% (4 proteins). Some proteins exhibited transmembrane domains or post-translational modifications such as prenylation and myristoylation, although they were not classified by the Loctree software. *Table 1* depicts the ten most abundant membrane proteins in this study. Those proteins are present in membranes of different organelles such as mitochondria, peroxisome, endoplasmic reticulum and plasma membrane.

Supplementary Table 3 shows the cell membranes in which proteins are localized. Proteins present at the plasma membrane of yeast cells were represented by

those with known functions, such as plasma membrane ATPase (PAAG_08082), chitin synthase B (PAAG_03391), osmosensor protein (PAAG_04025), a zinc transporter (PAAG_00105) of the Zip family, as well as by proteins with unknown functions. The proteins associated with the endoplasmic reticulum comprise in high number enzymes of the protein glycosylation pathway. Nevertheless, proteins with known mitochondrial localization and functions were detected, such as those involved in import of proteins, enzymes of the electron transport chain and of ATP synthesis. Proteins involved in vesicles transport present in Golgi apparatus were identified, such as ADP ribosylation factor (PAAG_07702), SNARE Ykt6 (PAAG_01588). Furthermore, proteins involved in transport in vacuole and peroxisomes were also identified.

As summarized in *Supplementary Table 3*, eight proteins present in the endoplasmic reticulum and one Golgi membrane protein were involved in protein glycosylation. Oligosaccharyltransferase (PAAG_04719/PAAG_01037) represented with two subunits in the proteome of the endoplasmic reticulum membrane, catalyzes the initial step of N-glycosylation, with the transfer of N-glycan precursor to nascent polypeptide [53]. In addition, calnexin (PAAG_07037), a protein involved in the correct folding of glycoproteins in mammalian cells [54] and fungus [55], was identified as well. The addition of the outer chain to the N-linked core oligosaccharide at Golgi is performed by mannosyltransferases; two α -1,2-mannosyltransferases (PAAG_02462/PAAG_07238) were found in membranes of the endoplasmic reticulum and Golgi, as depicted in *Supplementary Table 3*. In addition, dolichol phosphate mannosyltransferases (PAAG_01874), which perform protein N-glycosylation/O-glyco-

Table 1. The most abundant membrane proteins.

Accession number [†]	Protein identification [‡]	Score protein [§]	f mol [¶]	TMH [#]	PTM	SignalP score ≥ 0.5
PAAG_08620	ADP ATP carrier protein 310 aa	28,165	1955.942	3	–	–
PAAG_08082	Plasma membrane ATPase 930 aa	27,274.75	1292.34	9	–	–
PAAG_07564	Outer mitochondrial membrane protein porin 285 aa [§]	17,746.9	601.808	–	–	–
PAAG_00850	Glucosamine fructose 6 phosphate aminotransferase 489 aa [§]	16,121.64	527.8133	–	–	–
PAAG_00481	Membrane biogenesis protein Yop1 171 aa	11,930.6	449.3233	3	–	–
PAAG_04838	ATP synthase subunit 4 245 aa [§]	13,824.06	372.026	–	–	–
PAAG_04570	ATP synthase D chain mitochondrial 175 aa [§]	3393.7	388.8589	–	–	–
PAAG_05350	Mitochondrial phosphate carrier protein 422 aa [§]	5905.8	335.2175	–	–	–
PAAG_08028	GTP-binding protein ypt1 202 aa	25,168.0	448.6622	–	C:20	–
PAAG_02265	Mitochondrial F1FO ATP synthase subunit 102 aa	14,358.8	295.1655	1	–	–

^{†,‡}Accession number and description of protein according to database of *Paracoccidioides* spp. (www.broadinstitute.org/annotation/genome/paracoccidioides_brasiensis/MultiHome.html).[§]Protein score obtained from MS data using the PLGS.[¶]Quantification of membrane proteins according to internal standard.[#]Represents the amount of transmembrane domains identified in proteins using the program TMHMM version 2.0 (www.cbs.dtu.dk/services/TMHMM/).^{||}Indicates the presence of post-translational modification. The program TerminusNator (www.isv.cnrs-gif.fr/terminator3/test.php) and Myristoylator (<http://web.expasy.org/myristoylator/>) were employed in search for myristoylated proteins. To search for palmitoylated proteins was performed with the program TerminusNator (www.isv.cnrs-gif.fr/terminator3/test.php). For identification of prenylated proteins, the program PrePS (<http://mendel.imp.ac.at/sat/prePS/index.html>). The prediction for GPI anchor was performed with the program big-PI fungi predictor (http://mendel.imp.ac.at/gpi/fungi_server.html). C:14 and C:16 indicate the presence of a myristoyl or palmitoyl group in the protein, respectively. C:15 indicates the presence of a farnesylation site to the addition of a farnesyl group by the enzyme FT and C:20 indicates the presence of a recognition site to addition of a geranyl group by the enzyme GGT2. GPI represents the presence of a GPI anchor in protein.^{|||}The program SignalP version 4.0 (www.cbs.dtu.dk/services/SignalP/) was employed in the search for signal peptide. The values demonstrate the score protein with signal peptide. The D-Score must be higher or equal to the value of (0.05).^{|||}In all cases, the symbol represents absence in the analyzed category.The functional classification was performed using the database of FunCat2 (http://pedant.gsf.de/pedant3view/pedant3view?Method=analysis&Db=p3_r48325_Par_brasili_Pb01).The database GO using the information relative to cellular component was employed to evaluate the possible localization of proteins in cell membranes of *Paracoccidioides* sp.^{|||}Some proteins did not show any form of classical association with the lipid bilayer, but they presented the subcellular localization in GO as belonging to the membrane with score ≥ 50. FT: Farnesylyltransferase; GGT1: Geranylgeranylyltransferase; GG12: Rab Geranylgeranylyltransferase; GC: Gene ontology; GPI: Lipid anchor modified; GTP: Guanosine triphosphate; Pt: Big-PI fungi database; PLGS: ProteinLynx Global Server; PrePS: Prenylation Prediction Suite; PTM: Post-translational modification; TMH: Transmembrane helices.

sylation [56], and members of this family were also detected in this study. Proteins related to the glycosylation pathway, such as α -1,2-mannosyltransferase (kre5p, ktr4), mannosyltransferases (PMTs), Stt3p and calnexin [57], were also identified in the membrane proteome of *A. fumigatus*.

Regulation of *P. lutzii* membrane proteins by zinc

Proteomic membrane analyses revealed that whole membrane system proteins alter their abundance in response to different stress conditions [30,58]. Therefore, we investigated zinc regulation of membrane proteins in yeast cells grown upon zinc deficiency. Previous studies demonstrated a remodeling of *P. lutzii* metabolism in response to oxidative stress induced during zinc deprivation [19]. A 1.5-fold change was used as a threshold to determine the up- and downregulated membrane proteins under zinc deprivation. A total of 115 proteins, corresponding to 60.85% of the classified membrane proteins, depicted in Supplementary Table 2, were downregulated upon zinc deprivation (Supplementary Table 4). Eighty one of those proteins were not detectable in the membranes of yeast cells deprived of zinc, only in the control. The functional classification of downregulated membrane proteins revealed that most of them in a percentage of 31% (36 proteins) were involved in transport events (Figure 2). Of special note, proteins of mitochondrial membrane functionally related to electron transport and oxidative phosphorylation were downregulated, suggesting that energy production by the respiratory chain was inhibited during zinc deprivation. Additionally, the glycosylation of proteins seems to be affected by zinc deprivation, as demonstrated by the downregulation of several enzymes/proteins involved in the process (Supplementary Table 4).

Eighteen proteins corresponding to 9.52% of those classified as belonging to membranes were upregulated upon zinc deprivation (Supplementary Table 5). Sixteen of those proteins were only identified upon zinc deprivation. A total of 56% (10 proteins) of the 18 proteins were involved in transport events and 6% (1 protein) was involved in protein fate (Figure 2).

The classification of regulated proteins, according to the predicted membranes they belong to, is presented in Supplementary Figure 6. It was observed that 43% (49 proteins) of the downregulated membrane proteins are predicted to be mitochondrial, followed by endoplasmic reticulum 30% (34 proteins) and plasma membrane 15% (17 proteins). Among the upregulated proteins, 28% (5 proteins) were predicted as belonging mainly to mitochondrial membrane and 22% (4 proteins) to plasma membrane.

Modification of *P. lutzii* yeast cell wall upon zinc deprivation

Chitin, glucans, lipids and proteins are the main constituents of the cell walls of mycelium and yeast forms of *Paracoccidioides* spp. [59,60]. Proteomic analysis revealed that proteins involved in the deposit of chitin in the cell wall, such as chitin synthase B (PAAG_03391) [61] and phosphoinositide phosphatase Sac1 (PAAG_03162) [62], were downregulated under zinc deprivation. Moreover, the enzyme 1-acyl-sn-glycerol-3-phosphate acyltransferase- β (1-AGPAT; PAAG_07503), involved in production of phospholipids, cell wall constituents of *Paracoccidioides* spp. [63], was also downregulated at zinc-limited conditions. Therefore, fluorescence microscopy was performed in order to investigate changes in the cell wall using the fluorophore CFW that binds specifically the chitin present in the cell wall. As shown in Figure 3A, fluorescence of cell wall in zinc-deprived cells decreased when compared with the control. Quantitative analyzes of the fluorescence intensity (in pixels) of cells growing in the presence and absence of zinc, demonstrated a significant decrease of the fluorescence in cells under zinc deprivation ($p < 0.05$; Figure 3B).

Zinc availability modulates glycosylation events

Several proteins of endoplasmic reticulum involved in events of glycosylation were downregulated during zinc deprivation. It includes dolichyl-phosphate-mannose-protein mannosyltransferase (PAAG_05910/PAAG_04725), α -1,2-mannosyltransferase KTR1 (PAAG_07238) and dolichyl-di-phosphooligosaccharide-protein glycotransferase (PAAG_04110). Staining with Schiff periodic acid allows the detection of glycoproteins, through the oxidation reaction between the periodic acid and the glycoproteins. Thus, the intensity of color depends on the number and the nature of sugar moieties bound to the glycoprotein [64]. Under zinc deficiency, the intensity of Schiff staining was lower when compared with the control, as depicted in Figure 4A. The use of ConA conjugated to FITC revealed a significant decrease in the fluorescence of *P. lutzii* cells after zinc deprivation, as depicted in Figure 4B & C. ConA is a lectin that specifically binds glucan and mannan moieties [65]. Additionally, the use of aniline blue which selectively stains cell β -(1,3) glucan [52], did not show any difference on fluorescence in cells cultured in the presence or absence of zinc (Figure 5). In this way, the reduction of protein glycosylation is probably a result of the stress caused by zinc deprivation and not a consequence of a reduced amount of glucans.

Discussion

In the whole membrane proteome of *P. lutzii*, obtained with the use of sodium carbonate pH 11

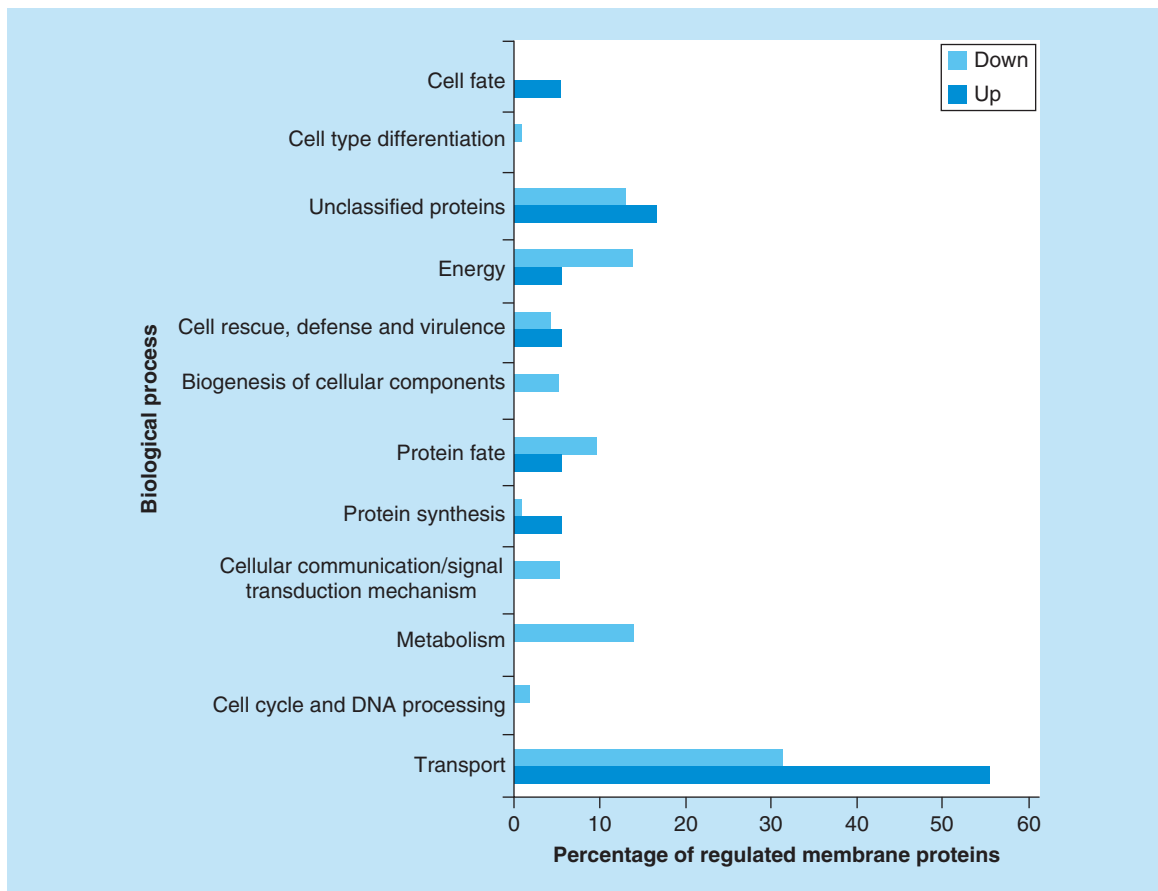


Figure 2. Functional classification of membrane proteins regulated by zinc availability. The database FunCat2 was used to perform this classification. Light gray bars represent downregulated proteins and dark gray bars represent upregulated proteins. Proteins upregulated: Transport – 56% (10 proteins), Cell cycle and DNA processing – 0% (0 protein), Metabolism – 0% (0 protein), Cellular communication – 0% (0 protein), Protein synthesis – 6% (1 protein), Protein fate – 6% (1 protein), Biogenesis of cellular components – 0% (0 protein), Cell rescue – 6% (1 protein), Energy – 6% (1 protein), Unclassified – 17% (3 proteins), Cell-type differentiation – 0% (0 protein), Cell fate – 6% (1 protein). Proteins downregulated: Transport – 31% (36 proteins), Cell cycle and DNA processing – 2% (2 proteins), Metabolism – 14% (16 proteins), Cellular communication – 5% (6 proteins), Protein synthesis – 1% (1 protein), Protein fate – 10% (11 proteins), Biogenesis of cellular components – 5% (6 proteins), Cell rescue – 4% (5 proteins), Energy – 14% (16 proteins), Unclassified – 13% (15 proteins), Cell-type differentiation – 1% (1 protein), Cell fate – 0% (0 protein).

and ultracentrifugation, 188 proteins were described (*Supplementary Table 2*). Literature search and *in silico* analyses revealed proteins associated with different cell membranes. When cells are lysed in an aqueous environment, the cell-limiting membrane and membranes of organelles may fragment and form vesicles that can be separated from the cytosol by partitioning or sedimentation. However, cytoplasmic proteins may be entrapped in vesicles formed after cell lysis. Thus, in order to get a true membrane protein extract, steps employing solutions, such as sodium carbonate, are used to remove proteins that do not show a strong association with membranes [25,30,66]. The use of sodium carbonate pH 11 has been described in the literature as a tool to obtain membrane proteins. Analysis of whole membrane system proteome of pathogenic and

nonpathogenic microorganisms, such as *Escherichia coli* [67], *Bordetella pertussis* [30] and *S. cerevisiae* [58], employing sodium carbonate pH 11 and steps of ultracentrifugation, allowed the identification of several membrane proteins. The success of the technique utilized for obtaining *P. lutzii* membrane proteins can be evaluated by comparing our data to those in the literature. In analyses of plasma membrane proteome of *S. cerevisiae* during salt stress, 24% of the identified proteins belong to the plasma membrane while 25 and 33% were represented by ribosomal proteins and proteins from the early secretory pathway belonging to endoplasmic reticulum and Golgi apparatus, respectively [58]. At this work, 25.2% (188 proteins) of the total of identified proteins were predicted as belonging to membranes (*Supplementary Figure 4*).

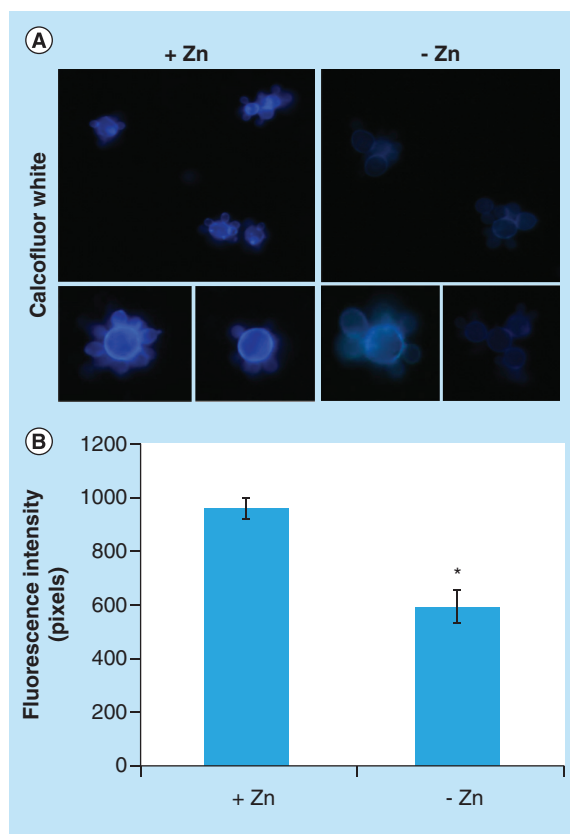


Figure 3. Effect of zinc deprivation in *Paracoccidioides lutzii* yeast cells wall. Yeast cells were cultivated in MMCM medium depleted or supplemented with zinc for 24 h. (A) The cells were fixed and stained with CFW (increase of 40 times). (B) Fluorescence intensity (in pixels) of the cells under zinc deprivation. The AxioVision Software (Carl Zeiss) was used to obtain the values of fluorescence intensity and the standard error of each analysis were used to plot the graph. Data are expressed as mean \pm standard error (represented using error bars). * $p \leq 0.05$. CFW: Calcofluor white; MMCM: McVeigh/Morton' liquid medium.

In this study we identified 188 proteins of membranes, and from those, 63.3% (119 proteins) presented at least one transmembrane domain, 9.04% (17 proteins) presented post-translational modifications such as prenylation, myristylation, palmitoylation, GPI anchor and 9.57% (18 proteins) presented signal peptide (Supplementary Table 2). In *C. albicans*, from 214 identified proteins in a preparation of plasma membrane, 47.66% (102 proteins) showed at least one transmembrane domain and 13.55% (29 proteins) presented signal peptide [68]. Comparing the data, it is possible to see that the forms of association with cell membranes approximate to the number found in this work.

In this work, membrane proteins involved in synthesis or maintenance of cell wall, in glycosylation path-

ways and in the electron transport chain were identified (Supplementary Table 2), similarly to data described in *C. albicans* [68]. Also, the whole membrane proteome of *P. lutzii* includes proteins related to vesicle traffic, such as ADP ribosylation factor (PAAG_07702), SNARE (PAAG_01588). In addition, some proteins were described only in this work compared with *C. albicans* [68] and *A. fumigatus* [57], such as zinc transporter (PAAG_00105), sideroflexin-1 (PAAG_09064) and peroxin (PAAG_08209; Supplementary Table 2). Bioinformatics analyses allowed the identification and classification of membrane proteins, not yet described in some proteomic works.

Some studies with *Paracoccidioides* spp. under metals deprivation allowed the characterization of metabolic and adaptive responses to iron [69] and zinc [19]. Due to the importance of zinc in pathogens survival and in the development of diseases, we evaluated membrane proteins in yeast cells of *P. lutzii* upon deprivation of this metal. Analysis of whole membrane system proteome during zinc deprivation allowed identification of a probable alteration on glycerophospholipid metabolism, as predicted by the regulation of enzymes located in endoplasmic reticulum membrane, such as the 1-AGPAT (PAAG_07503). This enzyme catalyzes the formation of phosphatidic acid (PA) from lysophosphatidic acid by incorporating an acyl moiety at sn-2 position. The PA produced by the 1-AGPAT activity is a substrate of the pathway for production of phospholipids, such as phosphatidylserine (PS), phosphatidylinositol (PI), phosphatidylethanolamine (PE) and phosphatidylcholine (PC), which are present at the cell wall of *S. cerevisiae* [70] and *Paracoccidioides* spp. [63]. Similarly, in *S. cerevisiae*, the activities of the enzymes involved in PS, PE and PC pathways were decreased under zinc deficiency [71]. As PA is the upstream substrate in the synthesis of all those phospholipids, we may suggest that the decreased production of PA by repression of the 1-AGPAT can lead to the reduction in PS, PE and PC levels and possible alterations in cell wall composition. Additionally to the descriptions above, another protein of the endoplasmic reticulum membrane, named Sac1, is involved in structure of cell wall and was downregulated in *P. lutzii* upon zinc deprivation, strongly suggesting modifications in the cell wall structure. Studies in *C. albicans* demonstrated that Sac1-p is related to the cell wall integrity. The deletion of *Sac1* increases the sensitivity to stress of the cell wall and alters the content and distribution of chitin in the mutant [72]. Moreover, chitin synthase B (PAAG_03391), a plasma membrane protein, was also downregulated in this study in the absence of zinc. The reduced level of those proteins possibly alters the quantity of chitin at the cell wall, as depicted in Figure 3.

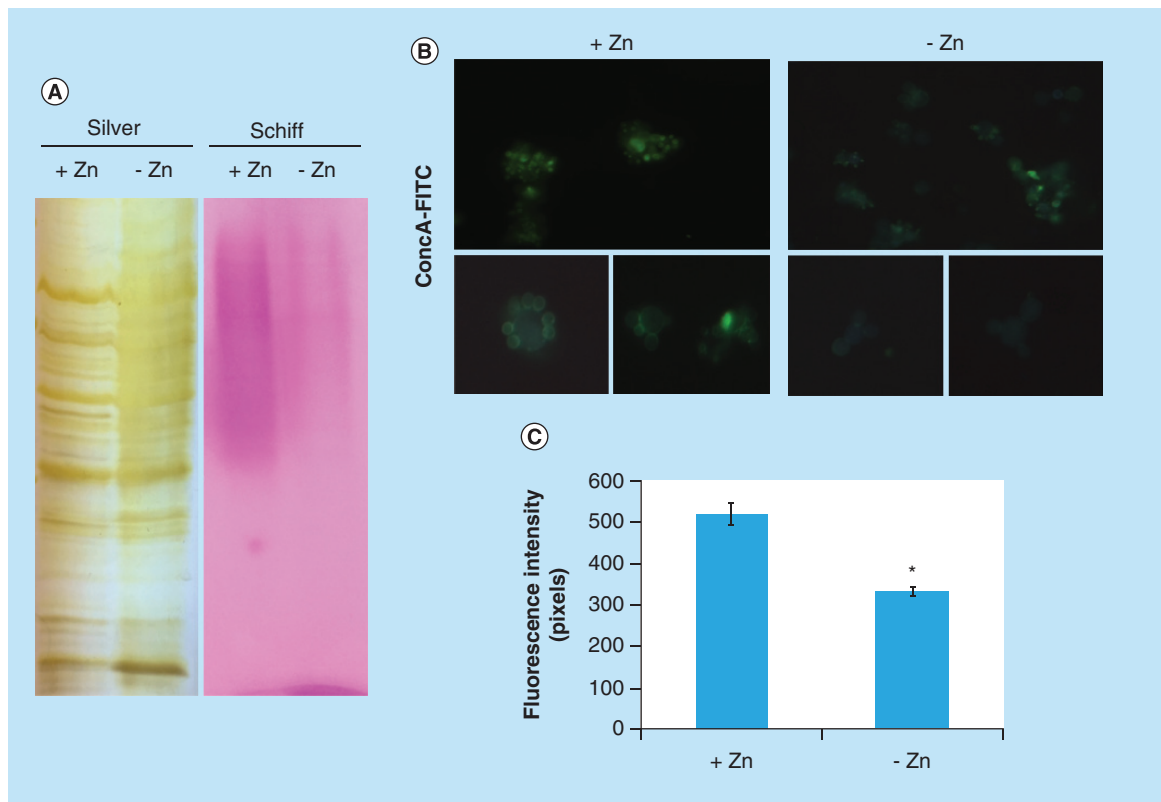


Figure 4. Zinc deprivation alters proteins glycosylation. **(A)** Protein extracts of membranes were fractionated by electrophoresis and stained with periodic acid Schiff. The same extracts were stained with silver. **(B)** Fluorescence microscopy of *P. lutzii* cells that were cultured in the presence or absence of zinc for 24 h and subsequently incubated with ConA conjugated to FITC (increase of 40 times). **(C)** Fluorescence intensity graph. The data for fluorescence intensity evaluation were obtained through the AxioVision Software (Carl Zeiss). The values of fluorescence intensity (in pixels) and the standard error of each analysis were used to plot the graph. Data are expressed as mean \pm standard error (represented using error bars), (*) represents $p \leq 0.05$. ConA: Concanavalin A; FITC: Fluorescein isothiocyanate.

Zinc deprivation repressed proteins present in membranes of organelles such as mitochondria and vacuole, as depicted in [Supplementary Table 4](#). Studies performed with *S. cerevisiae* revealed that the transport of zinc into the vacuole has an ATP-dependent mechanism, requiring an H⁺ gradient generated by the V-ATPase. Thus, changes in the proton gradient generated by V-ATPase inhibit zinc uptake by the vacuole [73]. In this work, a vacuolar ATP synthase of 98 kDa (PAAG_02679) was repressed during zinc deprivation. As the vacuole is the main organelle responsible for zinc storage [14], the cells possibly inhibit the storage of this micronutrient in order to try to overcome zinc deprivation, allowing this metal available in the cytoplasm.

Protein glycosylation is the most common post-translational modification in eukaryotic cells. This process occurs by connecting a saccharide unit to a protein and is involved in the maintenance of protein conformation and activity, in protein protection from proteolytic degradation, and in protein intracellular

trafficking and secretion [74]. In studies performed with *Candida albicans*, it was observed that the process of glycosylation is important for cell wall integrity and for host–fungus interactions [75,76]. Also, in *C. albicans*, Hall *et al.* [77] observed that the Mnn2 mannosyltransferase family is related in immune recognition, virulence and cell wall integrity. Based on these facts, the reduction in the level of glycosylated proteins may interfere in the success of infection. In this work, we described downregulated membrane proteins present at the endoplasmic reticulum and Golgi apparatus involved in the process of N-O-glycosylation [57], such as α -1,2 mannosyltransferase KTR1 (PAAG_07238), dolichol-di-phosphooligosaccharide-protein glycotransferase (PAAG_04110), calnexin (PAAG_07037), oligosaccharyl transferases (PAAG_04719/PAAG_01037). The dolichol-phosphate mannose Dpm1p protein, localized at the endoplasmic reticulum membrane, was downregulated under zinc-limited conditions. Dpm1p synthesizes Dol-P-Man, a compound that serves as mannose donor for glycosylation reactions

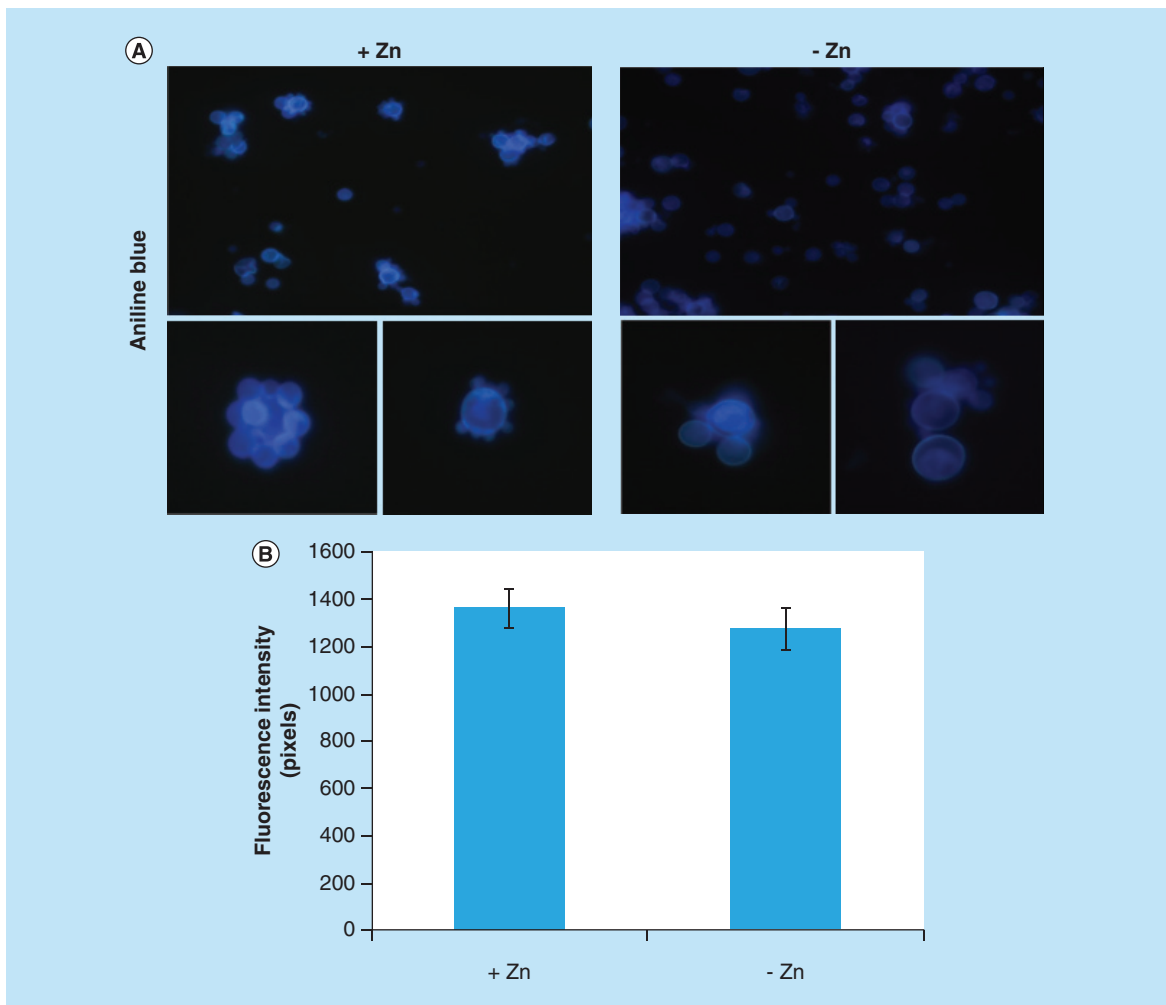


Figure 5. Evaluation of β -1,3 glucan quantities in the cell wall of *Paracoccidioides lutzii*. (A) Aniline blue was used to evaluate, by fluorescence microscopy, the presence of β -1,3 glucan in the cell wall of *P. lutzii* after growth in the presence and absence of zinc (increase of 40 times). (B) Fluorescence intensity graph. The values of fluorescence intensity (in pixels) and the standard error of each analysis were used to plot the graph. Data are expressed as mean \pm standard error (represented using error bars).

in the endoplasmic reticulum lumen [78]. We suggest that repression of those proteins upon zinc deprivation affects the glycosylation process in the endoplasmic reticulum in *P. lutzii* and, consequently, the profile of glycosylated proteins is less evident under zinc deprivation (Figure 4). Furthermore, the aniline blue staining confirmed that the reduction of protein glycosylation is not a consequence of a reduced amount of glucans (Figure 5), but probably a result of the stress caused by zinc deprivation. Furthermore, the deletion of genes encoding proteins of the N-glycosylation pathway, such as α -glucosidase-I and O-Mannosyltransferases, in *A. fumigatus* and *S. pombe* resulted in abnormalities in the cell wall [79–81]. We hypothesized that the repression of proteins involved in the glycosylation pathway in *P. lutzii* during zinc deprivation contributes to changes in the cell wall organization in this fungus.

Another response to zinc deprivation identified in this work was at the mitochondrial membrane level. Part of the energy used by cells is obtained during the process of oxidative phosphorylation that occurs in the inner mitochondrial membrane. Electrons generated in glycolysis and tricarboxylic acid cycle are used during energy achievement. A study with *S. cerevisiae* revealed that zinc deficiency leads to increased oxidative stress [82]. *Aspergillus niger* submitted to long-term oxidative stress reduces glucose uptake [83] and induces enzymes involved in the gluconeogenesis pathway. Parente *et al.* [19] observed that *P. lutzii* yeast cells cultivated for 24 h under zinc deprivation also induce gluconeogenesis. Furthermore, Gupta *et al.* [84] found that the tricarboxylic acid cycle had decreased activity when *Aspergillus parasiticus* is cultured in medium with zinc deficiency. In the present study, we observed that

proteins of oxidative phosphorylation were downregulated upon zinc deficiency (**Supplementary Table 4**). Additionally, the mitochondrial inner membrane Sco1 protein (PAAG_06668) [85], which is essential for cytochrome oxidase assembly [86], was also repressed during zinc deficiency in *P. lutzii*, corroborating previous data that pointed to a metabolism shift in *P. lutzii* upon zinc deficiency.

Proteins associated with traffic of vesicles were regulated by zinc, as well. GTP-binding proteins play a role in vesicle traffic through a cycle of GTP-binding and hydrolysis. GTP-binding proteins present at the surface of carrier vesicles are responsible for the delivery of these structures to the appropriate acceptor compartment. The presence of Rab-GTPases GTP-bound (active) and GDP-bound (inactive) form is mediated by interaction with regulatory proteins. The active form of Rab proteins interacts with Rab effectors and GTPase-activating proteins and in inactive form, these proteins are recognized by guanine nucleotide exchange factors [87]. The Rab GDP-dissociation inhibitor protein (PAAG_06344) of *P. lutzii* was upregulated upon zinc deprivation (**Supplementary Table 5**). Its homolog Gdi1p, from *S. cerevisiae* induces the inhibition of GDP dissociation from Sec4p. A reversible modification of either Sec4p or Gdip would cause a dissociation of this complex, allowing attachment of Sec4p to a new vesicle [88]. The upregulation of Rab GDP-dissociation inhibitor in membrane proteome during zinc deprivation, here described, may induce the formation of a soluble inactive complex between Rabp and Sec4p proteins and, consequently, the presence of this complex could decrease the binding of Sec4 to new vesicles during zinc deprivation. The protein homolog to Sec4p, the GTP-binding protein SAS1 (PAAG_01500) was downregulated. The repression of those proteins may be associated with induction of Rab GDP-dissociation inhibitor protein and formation of complex Rabp/Sec4p, and consequently suppression on the traffic of vesicles under zinc limitation.

Upon microbial infection, the host sequesters zinc from either extra- and intracellular compartments [89,90] in order to limit microorganisms growth and proliferation. Considering this perspective, the use of zinc chelators during infection treatment may be suggested. Laskaris *et al.* [91] showed that mice infected with *A. fumigatus* had survival improved with administration of zinc-chelating agents in monotherapy and in combination with the antifungal caspofungin. Also, the use of metal chelators has been well documented in respect of iron [92–94]. As demonstrated here and also by Parente *et al.* [19], zinc plays a role in essential processes that contribute to the maintenance of *P. lutzii*

physiology. Taking this fact into account, the use of agents able to sequester this metal, alone or together with antifungals, may be an alternative in paracoccidioidomycosis treatment.

Conclusion & future perspective

The development and advance of strategies of treatment in the field of infectious diseases are based on the knowledge of a microorganism's physiology and metabolism. Information of pathogen behavior in situations that mimic conditions found in the host are valuable, since they can be used as guides in the definition of targets for treatment. To our knowledge, this is the first report that describes whole membrane system proteome and the response of *P. lutzii* to micro-nutrient starvation at the membrane proteome level. Identification of total membrane proteome of a member of the genus *Paracoccidioides* provides a starting point for future studies on functional analysis. Protein glycosylation and chitin content at the cell wall, both processes important in host–fungus interaction, were decreased under zinc deprivation, a condition found in the host. These and other metabolic changes described in this study may contribute to the arsenal of targets used in the development of new drugs in the future. Additionally, the establishment of a protocol for *Paracoccidioides* spp. membrane protein extraction opens new possibilities for the understanding of fungus biology.

Financial & competing interests disclosure

This work was supported by grants from Conselho Nacional de Desenvolvimento Científico e Tecnológico (CNPq) and Fundação de Amparo à Pesquisa do Estado de Goiás (FAPEG) – Instituto Nacional de Ciência e Tecnologia (INCT) de Estratégias de Interação Patógeno Hospedeiro (IPH) and Fundo Newton. JS de Curcio and MG Silva are fellows from Coordenação de Aperfeiçoamento de Pessoal de Nível Superior (CAPES) and CNPq, respectively. The authors have no other relevant affiliations or financial involvement with any organization or entity with a financial interest in or financial conflict with the subject matter or materials discussed in the manuscript apart from those disclosed.

No writing assistance was utilized in the production of this manuscript.

Author contributions

CMA Soares, JS de Curcio and MG Silva conceived and designed the experiments. JS de Curcio, MG Silva and L Casaletti performed the experiments. JS de Curcio, MG Silva, MGS Bailão, AM Bailão and CMA Soares analyzed and/or interpreted the data. SN Bão and CMA Soares contributed to reagents and materials. JS de Curcio, MG Silva and CMA Soares wrote the manuscript.

Open access

This work is licensed under the Creative Commons Attribution

4.0 License. To view a copy of this license, visit <http://creativecommons.org/licenses/by/4.0/>

Summary points

- This was the first work describing the whole membrane proteins of the pathogenic fungus *Paracoccidioides lutzii* and its regulation in a condition that mimics that found in the host.
- In this study, employing a methodology for extracting membrane proteins and nanoUPLC-MS^E, 188 proteins from the membrane system were identified.
- Under conditions of zinc deprivation, membrane proteins are regulated. In general, this stress alters several cellular processes carried out by proteins such as glycosylation, energy production, storage of zinc in vacuoles and vesicle traffic.
- Proteomic data revealed that membrane proteins involved in cell wall synthesis were repressed by zinc deprivation. This finding was confirmed by fluorescence microscopy. The cell wall is essential for the contact of the pathogen with the host.
- The data of this article allowed the characterization of the membrane proteins of *P. lutzii* in response to stress mediated by zinc deprivation.

References

Papers of special note have been highlighted as: • of interest;
•• of considerable interest

- 1 Restrepo AM. The ecology of *Paracoccidioides brasiliensis*: a puzzle still unsolved. *Sabouraudia J. Med. Vet. Mycol.* 23(5), 323–334 (1985).
- 2 San-Blas G, Niño-Vega G, Iturriaga T. *Paracoccidioides brasiliensis* and paracoccidioidomycosis: molecular approaches to morphogenesis, diagnosis, epidemiology, taxonomy and genetics. *Med. Mycol.* 40(3), 225–242 (2002).
- 3 McEwen JG, Bedoya V, Patino MM, Salazar ME, Restrepo A. Experimental murine paracoccidioidomycosis induced by the inhalation of conidia. *J. Med. Vet. Mycol.* 25(3), 165–175 (1987).
- 4 Shikanai-Yasuda MA, Telles FD, Mendes RP, Colombo AL, Moretti ML, Paracoccidioidomycose G. Guideliness in paracoccidioidomycosis. *Rev. Soc. Bras. Med. Trop.* 39(3), 297–310 (2006).
- 5 Van Ho A, Ward DM, Kaplan J. Transition metal transport in yeast. *Annu. Rev. Microbiol.* 56, 237–261 (2002).
- 6 Eide DJ. Multiple regulatory mechanisms maintain zinc homeostasis in *Saccharomyces cerevisiae*. *J. Nutr.* 133(5 Suppl. 1), S1532–S1535 (2003).
- Reports the mechanisms of zinc uptake in different organelles and the importance of this metal in cell homeostasis.
- 7 Zhao H, Eide D. The yeast *ZRT1* gene encodes the zinc transporter protein of a high-affinity uptake system induced by zinc limitation. *Proc. Natl Acad. Sci. USA* 93(6), 2454–2458 (1996).
- Reports the high-affinity transporter induced during zinc deprivation.
- 8 Zhao H, Eide D. The *ZRT2* gene encodes the low affinity zinc transporter in *Saccharomyces cerevisiae*. *J. Biol. Chem.* 271(38), 23203–23210 (1996).
- 9 Zhao H, Eide DJ. Zap1p, a metalloregulatory protein involved in zinc-responsive transcriptional regulation in *Saccharomyces cerevisiae*. *Mol. Cell. Biol.* 17(9), 5044–5052 (1997).
- 10 Gitan RS, Luo H, Rodgers J, Broderius M, Eide D. Zinc-induced inactivation of the yeast ZRT1 zinc transporter occurs through endocytosis and vacuolar degradation. *J. Biol. Chem.* 273(44), 28617–28624 (1998).
- 11 Rutherford JC, Bird AJ. Metal-responsive transcription factors that regulate iron, zinc, and copper homeostasis in eukaryotic cells. *Eukaryot. Cell* 3(1), 1–13 (2004).
- 12 Wu YH, Frey AG, Eide DJ. Regulation of the Zrg17 zinc transporter in the yeast secretory pathway. *Biochem. J.* 435(1), 259–266 (2011).
- 13 Ellis CD, Wang F, MacDiarmid CW, Clark S, Lyons T, Eide DJ. Zinc and the Msc2 zinc transporter protein are required for endoplasmic reticulum function. *J. Cell Biol.* 166(3), 325–335 (2004).
- 14 Ramsay LM, Gadd GM. Mutants of *Saccharomyces cerevisiae* defective in vacuolar function confirm a role for the vacuole in toxic metal ion detoxification. *FEMS Microbiol. Lett.* 152, 293–298 (1997).
- 15 MacDiarmid CW, Gaither LA, Eide D. Zinc transporters that regulate vacuolar zinc storage in *Saccharomyces cerevisiae*. *EMBO J.* 19(12), 2845–2855 (2000).
- 16 Eide DJ. Zinc transporters and the cellular trafficking of zinc. *Biochim. Biophys. Acta* 1763(7), 711–722 (2006).
- Reports the trafficking of zinc and transporters involved in this process.
- 17 Silva MG, Schrank A, Bailão EFLC et al. The homeostasis of iron, copper, and zinc in *Paracoccidioides brasiliensis*, *Cryptococcus neoformans* var. *Grubii*, and *Cryptococcus gattii*: a comparative analysis. *Front. Microbiol.* 2, 1–19 (2011).
- Describes the genes involved in homeostasis of micronutrients in the fungi: *Paracoccidioides* spp. and *Cryptococcus* spp.
- 18 Bailão EFLC, Parente AFA, Parente JA et al. Metal acquisition and homeostasis in fungi. *Curr. Fungal Infect. Rep.* 6(4), 257–266 (2012).
- Describes the mechanisms of micronutrients acquisition in fungi and the iron sources in the host.

- 19 Parente AFA, de Rezende TCV, de Castro KP *et al.* A proteomic view of the response of *Paracoccidioides* yeast cells to zinc deprivation. *Fungal Biol.* 117(6), 399–410 (2013).
- Reports the regulation of expression of cytoplasmatic proteins during zinc deprivation in *Paracoccidioides*.
- 20 Bailão AM, Schrank A, Luiz C *et al.* Differential gene expression by *Paracoccidioides brasiliensis* in host interaction conditions: representational difference analysis identifies candidate genes associated with fungal pathogenesis. *Microbes Infect.* 8(12–13), 2686–2697 (2006).
- 21 Bailão AM, Shrank A, Borges CL *et al.* The transcriptional profile of *Paracoccidioides brasiliensis* yeast cells is influenced by human plasma. *FEMS Immunol. Med. Microbiol.* 51(1), 43–57 (2007).
- Reports the induction of high-affinity zinc transporter after incubation with human plasma.
- 22 Ephritikhine G, Ferro M, Rolland N. Plant membrane proteomics. *Plant Physiol. Biochem.* 42(12), 943–962 (2004).
- 23 Tan S, Hwee TT, Chung MCM. Membrane proteins and membrane proteomics. *Proteomics* 8(19), 3924–3932 (2008).
- 24 Wallin E, von Heijne G. Genome-wide analysis of integral membrane proteins from eubacterial, archaean, and eukaryotic organisms. *Protein Sci.* 7(4), 1029–1038 (1998).
- 25 Santoni V, Molloy M, Rabilloud T. Membrane proteins and proteomics: un amour impossible? *Electrophoresis* 21(6), 1054–1070 (2000).
- 26 Hopff D, Wienkoop S, Lüthje S. The plasma membrane proteome of maize roots grown under low and high iron conditions. *J. Proteomics* 91, 605–618 (2013).
- 27 Ručević M, Hixson D, Josic D. Mammalian plasma membrane proteins as potential biomarkers and drug targets. *Electrophoresis* 32(13), 1549–1564 (2011).
- 28 Fava-Netto C. Estudos quantitativos sobre fixação de complemento na blastomicose sul americana, com antígeno polissacarídico. *Arg. Cir. Clin. Exp.* 18, 197–254 (1955).
- 29 Restrepo A, Jimenez BE. Growth of *Paracoccidioides brasiliensis* yeast phase in a chemically defined culture medium. *J. Clin. Microbiol.* 12(2), 279–281 (1980).
- 30 Vidakovics MLP, Paba J, Lamberti Y, Andre C, De Sousa MV, Rodriguez ME. Profiling the *Bordetella pertussis* proteome during iron starvation research. *J. Proteome Res.* 6, 2518–2528 (2006).
- Reports the methodology of membrane proteins extraction and their regulation by iron.
- 31 Da Fonseca CA, Jesuino RSA, Felipe MS, Cunha DA, Brito WA, Soares CMA. Two-dimensional electrophoresis and characterization of antigens from *Paracoccidioides brasiliensis*. *Microbes Infect.* 3(7), 535–542 (2001).
- 32 Barbosa SM, Bão SN, Andreotti PF *et al.* Glyceraldehyde-3-phosphate dehydrogenase of *Paracoccidioides brasiliensis* is a cell surface protein involved in fungal adhesion to extracellular matrix proteins and interaction with cells. *Infect. Immun.* 74(1), 382–389 (2006).
- 33 Bradford M. A rapid and sensitive method for the quantification of microgram quantities of protein utilizing the principle of protein-dye binding. *Anal. Biochem.* 72, 248–254 (1976).
- 34 Murad AM, Souza GHMF, Garcia JS, Rech EL. Detection and expression analysis of recombinant proteins in plant-derived complex mixtures using nanoUPLC-MSE. *J. Sep. Sci.* 34(19), 2618–2630 (2011).
- 35 Geromanos SJ, Vissers JPC, Silva JC *et al.* The detection, correlation, and comparison of peptide precursor and product ions from data independent LC-MS with data dependant LC-MS/MS. *Proteomics* 9(6), 1683–1695 (2009).
- 36 Curty N, Kubitschek-Barreira PH, Neves GW *et al.* Discovering the infectome of human endothelial cells challenged with *Aspergillus fumigatus* applying a mass spectrometry label-free approach. *J. Proteomics* 97, 126–140 (2014).
- 37 Silva JC. Absolute quantification of proteins by LCMS: a virtue of parallel MS acquisition. *Mol. Cell. Proteomics* 5(1), 144–156 (2006).
- 38 Silva JC, Denny R, Dorschel CA *et al.* Quantitative proteomic analysis by accurate mass retention time pairs. *Anal. Chem.* 77(7), 2187–2200 (2005).
- 39 Murad AM, Rech EL. NanoUPLC-MSE proteomic data assessment of soybean seeds using the Uniprot database. *BMC Biotechnol.* 12(1), 82 (2012).
- 40 Laird NM, Horvath S, Xu X. Implementing a unified approach to family-based tests of association. *Genet. Epidemiol.* 19(Suppl. 1), S36–S42 (2000).
- 41 Horton P, Park KJ, Obayashi T *et al.* WoLF PSORT: protein localization predictor. *Nucleic Acids Res.* 35(Suppl. 2), 585–587 (2007).
- 42 Frishman D, Mokrejs M, Kosykh D *et al.* The PEDANT genome database. *Nucleic Acids Res.* 31(1), 207–211 (2003).
- 43 Krogh A, Larsson B, von Heijne G, Sonnhammer ELL. Predicting transmembrane protein topology with a hidden Markov model: application to complete genomes. *J. Mol. Biol.* 305(3), 567–580 (2001).
- 44 Eisenhaber B, Schneider G, Wildpaner M, Eisenhaber F. A sensitive predictor for potential GPI lipid modification sites in fungal protein sequences and its application to genome-wide studies for *Aspergillus nidulans*, *Candida albicans*, *Neurospora crassa*, *Saccharomyces cerevisiae* and *Schizosaccharomyces*. *J. Mol. Biol.* 337(2), 243–253 (2004).
- 45 Bologna G, Yvon C, Duvaud S, Veuthey AL. N-terminal myristylation predictions by ensembles of neural networks. *Proteomics* 4(6), 1626–1632 (2004).
- 46 Maurer-Stroh S, Eisenhaber F. Refinement and prediction of protein prenylation motifs. *Genome Biol.* 6(6), R55 (2005).
- 47 Petersen TN, Brunak S, von Heijne G, Nielsen H. SignalP 4.0: discriminating signal peptides from transmembrane regions. *Nat. Methods* 8(10), 785–786 (2011).
- 48 Goldberg T, Hecht M, Hamp T *et al.* LocTree3 prediction of localization. *Nucleic Acids Res.* 42(W1), 1–6 (2014).
- 49 Zambuzzi-Carvalho PF, Tomazett PK, Santos SC *et al.* Transcriptional profile of *Paracoccidioides* induced by oenothein B, a potential antifungal agent from the Brazilian Cerrado plant Eugenia uniflora. *BMC Microbiol.* 13, 227 (2013).

- 50 Maizels RM, Blaxter ML, Robertson BD, Selkirk ME. *Parasite Antigens, Parasite Genes: A Laboratory Manual for Molecular Parasitology*. Cambridge University Press, Cambridge, UK (1992).
- 51 Sagaram US, Shaw BD, Shim WB. *Fusarium verticillioides GAP1*, a gene encoding a putative glycolipid-anchored surface protein, participates in conidiation and cell wall structure but not virulence. *Microbiology* 153(9), 2850–2861 (2007).
- 52 Renshaw H, Vargas-Muñiz JM, Richards AD, Asfaw YG, Juvvadi PR, Steinbach WJ. Distinct roles of myosins in *Aspergillus fumigatus* hyphal growth and pathogenesis. *Infect. Immun.* 84, IAI.01190–IAI.01115 (2016).
- 53 Knauer R, Lehle L. The oligosaccharyltransferase complex from yeast. *Biochim. Biophys. Acta* 1426(2), 259–273 (1999).
- 54 Ruiz-Canada C, Kelleher DJ, Gilmore R. Cotranslational and posttranslational N-glycosylation of polypeptides by distinct mammalian OST isoforms. *Clin. Lymphoma.* 9(1), 19–22 (2009).
- 55 Wang N, Seko A, Takeda Y, Kikuma T, Ito Y. Cooperative role of calnexin and TigA in *Aspergillus oryzae* glycoprotein folding. *Glycobiology* 25(10), 1090–1099 (2015).
- 56 Goto M. Protein O-glycosylation in fungi: diverse structures and multiple functions. *Biosci. Biotechnol. Biochem.* 71(6), 1415–1427 (2007).
- 57 Ouyang H, Luo Y, Zhang L, Li Y, Jin C. Proteome analysis of *Aspergillus fumigatus* total membrane proteins identifies proteins associated with the glycoconjugates and cell wall biosynthesis using 2D LC-MS/MS. *Mol. Biotechnol.* 44(3), 177–189 (2010).
- 58 Szopinska A, Degand H, Hochstenbach JF, Nader J, Morsomme P. Rapid response of the yeast plasma membrane proteome to salt stress. *Mol. Cell. Proteomics* 10(11), M111.009589 (2011).
- 59 Kanetsuna F, Carbonell LM. Cell wall glucans of the yeast and mycelial forms of *Paracoccidioides brasiliensis*. *J. Bacteriol.* 101(3), 675–680 (1970).
- 60 San-blas G. The cell wall of fungal human pathogens: its possible role in host-parasite relationships dermatophytes. *Young* 184(Ivic), 159–184 (1982).
- 61 Preechasuth K, Anderson JC, Peck SC, Brown AJP, Gow NAR, Lenardon MD. Cell wall protection by the *Candida albicans* class I chitin synthases. *Fungal Genet. Biol.* 82, 264–276 (2015).
- 62 Whitters EA, Cleves AE, McGee TP, Skinner HB, Bankaitis VA. SAC1p is an integral membrane protein that influences the cellular requirement for phospholipid transfer protein function and inositol in yeast. *J. Cell Biol.* 122(1), 79–94 (1993).
- 63 Longo LVG, Nakayasu ES, Gazos-Lopes F et al. Characterization of cell wall lipids from the pathogenic phase of *Paracoccidioides brasiliensis* cultivated in the presence or absence of human plasma. *PLoS ONE* 8(5), e63372 (2013).
- 64 Matthieu JM, Quarles RH. Quantitative scanning of glycoproteins on polyacrylamide gels stained with periodic acid-schiff reagent (PAS). *Anal. Biochem.* 55(1), 313–316 (1973).
- 65 Shaw BD, Hoch HC. The pycnidiospore of *Phyllosticta ampelicida*: surface properties involved in substratum attachment and germination. *Mycol. Res.* 103(7), 915–924 (1999).
- 66 Fujiki Y, Hubbard AL, Fowler S, Lazarow PB. Isolation of intracellular membranes by means of sodium carbonate treatment: application to endoplasmic reticulum. *J. Cell Biol.* 93(1), 97–102 (1982).
- 67 Molloy M, Herbert B, Slade M. Proteomic analysis of the *Escherichia coli* outer membrane. *Eur. J.* 2881, 1–11 (2000).
- 68 Cabezón V, Llama-Palacios A, Nombela C, Montoliva L, Gil C. Analysis of *Candida albicans* plasma membrane proteome. *Proteomics* 9(20), 4770–4786 (2009).
- 69 Parente AFA, Bailão AM, Borges CL et al. Proteomic analysis reveals that iron availability alters the metabolic status of the pathogenic fungus *Paracoccidioides brasiliensis*. *PLoS ONE* 6(7), e22810 (2011).
- 70 Carman GM, Han G-S. Regulation of phospholipid synthesis in *Saccharomyces cerevisiae* by zinc depletion. *Biochim. Biophys. Acta* 1771(3), 322–330 (2007).
- 71 Iwanyshyn WM, Han G-S, Carman GM. Regulation of phospholipid synthesis in *Saccharomyces cerevisiae* by zinc. *J. Biol. Chem.* 279(21), 21976–21983 (2004).
- 72 Zhang B, Yu Q, Jia C et al. The actin-related protein Sac1 is required for morphogenesis and cell wall integrity in *Candida albicans*. *Fungal Genet. Biol.* 81, 261–270 (2015).
- 73 MacDiarmid CW, Milanick MA, Eide DJ. Biochemical properties of vacuolar zinc transport systems of *Saccharomyces cerevisiae*. *J. Biol. Chem.* 277(42), 39187–39194 (2002).
- 74 Varki A. Biological roles of oligosaccharides: all of the theories are correct. *Glycobiology* 3(2), 97–130 (1993).
- 75 Albrecht A, Felk A, Pichova I et al. Glycosylphosphatidylinositol-anchored proteases of *Candida albicans* target proteins necessary for both cellular processes and host-pathogen interactions. *J. Biol. Chem.* 281(2), 688–694 (2006).
- 76 Mora-Montes HM, Bates S, Netea MG et al. Endoplasmic reticulum alpha-glycosidases of *Candida albicans* are required for N glycosylation, cell wall integrity, and normal host-fungus interaction. *Eukaryot. Cell* 6(12), 2184–2193 (2007).
- 77 Hall RA, Bates S, Lenardon MD et al. The Mnn2 mannosyltransferase family modulates mannoprotein fibril length, immune recognition and virulence of *Candida albicans*. *PLoS Pathog.* 9(4), 13–17 (2013).
- 78 Burda P, Aebi M. The dolichol pathway of N-linked glycosylation. *Biochim. Biophys. Acta* 1426(2), 239–257 (1999).
- 79 Willer T, Brandl M, Sipiczki M, Strahl S. Protein O-mannosylation is crucial for cell wall integrity, septation and viability in fission yeast. *Mol. Microbiol.* 57(1), 156–170 (2005).
- 80 Zhou H, Hu H, Zhang L et al. O-mannosyltransferase 1 in *Aspergillus fumigatus* (AfPmt1p) is crucial for cell wall integrity and conidium morphology, especially at an elevated temperature. *Eukaryot. Cell* 6(12), 2260–2268 (2007).

- 81 Zhang L, Feng D, Fang W *et al.* Comparative proteomic analysis of an *Aspergillus fumigatus* mutant deficient in glucosidase I (AfCwh41). *Microbiology* 155(7), 2157–2167 (2009).
- 82 Wu C, Bird AJ, Winge DR, Eide DJ. Regulation of the yeast TSA1 peroxiredoxin by ZAP1 is an adaptive response to the oxidative stress of zinc deficiency. *J. Biol. Chem.* 282(4), 2184–2195 (2007).
- 83 Li Q, Abrushev R, Harvey LM, McNeil B. Oxidative stress-associated impairment of glucose and ammonia metabolism in the filamentous fungus, *Aspergillus niger* B1-D. *Mycol. Res.* 112(9), 1049–1055 (2008).
- 84 Gupta SK, Maggon KK, Venkitasubramanian TA. Effect of Zinc on tricarboxylic acid cycle intermediates and enzymes in relation to aflatoxin biosynthesis. *J. Gen. Microbiol.* 99(1), 43–48 (1977).
- 85 Buchwald P, Krummeck G, Rödel G. Immunological identification of yeast SCO1 protein as a component of the inner mitochondrial membrane. *Mol. Gen. Genet.* 229(3), 413–420 (1991).
- 86 Glerum DM, Shtanko A, Tzagoloff A. SCO1 and SCO2 act as high copy suppressors of a mitochondrial copper recruitment defect in *Saccharomyces cerevisiae*. *J. Biol. Chem.* 271(34), 20531–20535 (1996).
- 87 Ignatev A, Kravchenko S, Rak A, Goody RS, Pylypenko O. A structural model of the GDP dissociation inhibitor Rab membrane extraction mechanism. *J. Biol. Chem.* 283(26), 18377–18384 (2008).
- 88 Garrett MD, Zahner JE, Cheney CM, Novick PJ. GDI1 encodes a GDP dissociation inhibitor that plays an essential role in the yeast secretory pathway. *EMBO J.* 13(7), 1718–1728 (1994).
- 89 Corbin BD, Seeley EH, Raab A *et al.* Metal chelation and inhibition of bacterial growth in tissue abscesses. *Science* 319(5865), 962–965 (2008).
- 90 Vignesh KS, Figueroa JAL, Porollo A, Caruso JA, Deepe GS Jr. Granulocyte macrophage-colony stimulating factor-induced Zn sequestration enhances macrophage superoxide and limits intracellular pathogen survival. *Immunity* 39(4), 697–710 (2013).
- 91 Laskaris P, Atrouni A, Calera JA, Enfert C. Administration of zinc chelators improves survival of mice infected with *Aspergillus fumigatus* both in monotherapy and in combination with caspofungin. *Antimicrob. Agents Chemother.* 60(10), 5631–5639 (2016).
- 92 Ibrahim AS, Gebremariam T, French SW, Edwards JE Jr, Spellberg B. The iron chelator deferasirox enhances liposomal amphotericin B efficacy in treating murine invasive pulmonary aspergillosis. *J. Antimicrob. Chemother.* 65(2), 289–292 (2009).
- 93 Leal SM, Roy S, Vareechon C *et al.* Targeting iron acquisition blocks infection with the fungal pathogens *Aspergillus fumigatus* and *Fusarium oxysporum*. *PLoS Pathog.* 9(7), 1–16 (2013).
- 94 Zaremba KA, Cruz AR, Yuang C-Y, Gallin JI. Antifungal activities of natural and synthetic iron chelators alone and in combination with azole and polyene antibiotics against *Aspergillus fumigatus*. *Antimicrob. Agents Chemother.* 53(6), 2654–2656 (2009).